Title
Lipolysis in Adipose Tissue: Roles of Desnutrin and Adipose-specific phospholipase A2

Author
Ahmadian, Maryam

Publication Date
2010

Peer reviewed|Thesis/dissertation

Lipolysis in Adipose Tissue: Roles of Desnutrin and Adipose-specific Phospholipase A_2

By

Maryam Ahmadian

A dissertation submitted in partial satisfaction of the

requirements for the degree of

Doctor of Philosophy

in

Molecular and Biochemical Nutrition

in the

Graduate Division

of the

University of California, Berkeley

Committee in Charge:

Professor Hei Sook Sul

Professor Marc K. Hellerstein

Professor Robert O. Ryan

Professor Gary L. Firestone

Spring 2010

ABSTRACT

Lipolysis in Adipose Tissue: Roles of Desnutrin and AdPLA

by

Maryam Ahmadian

Doctor of Philosophy in Molecular and Biochemical Nutrition

University of California, Berkeley

Professor Hei Sook Sul, Chair

Adipose tissue is the major energy storage depot in mammals, storing energy in the form triacylglycerol (TAG) during times of energy excess, and mobilizing TAG, via lipolysis, during times of energy need to generate fatty acids. Desnutrin (also known as ATGL) is a novel TAG hydrolase expressed highly only in white and brown adipose tissue (WAT and BAT). To investigate the role of desnutrin *in vivo*, transgenic mice that overexpress desnutrin predominantly in adipose tissue (aP2-desnutrin mice) were generated. aP2-desnutrin mice had increased lipolysis in adipose tissue and were resistant to diet-induced obesity. Surprisingly, this increased lipolysis in adipose tissue did not result in higher levels of serum non-esterified fatty acids (NEFA), but instead promoted fatty acid oxidation directly within adipocytes resulting in higher energy expenditure and a leaner phenotype. To further investigate the adipose-specific role of desnutrin, gene targeting by homologous recombination in embryonic stem cells was performed to generate adipose-specific conditional desnutrin knockout mice (desnutrin ASKO mice). In contrast to aP2-desnutrin mice, these mice had markedly decreased lipolysis in both WAT and BAT with massive accumulation of TAG in these tissues. These mice had impaired thermogenesis and decreased oxygen consumption. Notably, BAT in these mice was drastically enlarged, and resembled WAT, indicating that desnutrin may be important in the conversion of WAT to BAT.

While the classic model of the endocrine regulation of lipolysis by catecholamines and insulin has been extensively studied, the local regulation of lipolysis in adipose tissue by autocrine/paracrine factors is not well understood. Identification of adipose-specific phospholipase A_2 (AdPLA) revealed a surprisingly important and dominant role for adipocyte-derived PGE_2 in the autocrine/paracrine regulation of lipolysis. As a PLA_2, AdPLA catalyzes the release of fatty acids from the sn-2 position of phospholipids that is typically enriched in arachidonic acid, providing substrate for the initial, rate-limiting step in the synthesis of eicosanoids. To investigate the role of AdPLA *in vivo*, AdPLA null mice were generated. Through the PGE_2/EP3/cAMP pathway, AdPLA dominantly regulates lipolysis in adipose tissue in an autocrine/paracrine manner. The unrestrained adipocyte lipolysis in AdPLA null mice resulted in resistance to both diet-induced and genetic obesity. Consistent with results from aP2-desnutrin mice, despite elevated lipolysis in adipose tissue, serum NEFA levels were not elevated in AdPLA null mice

and fatty acid oxidation was increased in WAT, resulting in higher energy expenditure and resistance to obesity. Taken together, findings from aP2-desnutrin mice, desnutrin ASKO mice, and AdPLA null mice have led to the discovery of novel players in the lipolytic cascade, and revealed an unexpected link between lipolysis and the ability of adipose tissue to oxidize fatty acids and release heat, rather than to provide useful energy for work.

DEDICATION

I dedicate my thesis to my father, Jack Ahmadian, for always motivating me to do my best, supporting me in whatever I wanted to do, and instilling in me a love of learning.

ACKNOWLEDGEMENTS

I would like to express my sincerest appreciation to my PI, Dr. Hei Sook Sul, for giving me the opportunity to work on such an exciting thesis project and for her unwavering support and guidance, through every step of my dissertation work. She provided me with the training and skills necessary to pursue my research and confidence in my own ability to be an independent researcher. I will always remember the standards of excellence that she expected and will hold myself to them in the future.

I also thank my parents Jack and Suzanne Ahmadian and my brother Amir Ahmadian for their continued advice, support and encouragement.

TABLE OF CONTENTS

Chapter I: Overview of TAG Synthesis and Lipolysis

A) Triacylglycerol Metabolism in Adipose Tissue

ABSTRACT

Triacylglycerol (TAG) in adipose tissue serves as the major energy storage form in higher eukaryotes. Obesity, resulting from excess white adipose tissue, has increased dramatically in recent years resulting in a serious public health problem. Understanding of adipocyte-specific TAG synthesis and hydrolysis is critical to the development of strategies to treat and prevent obesity and its closely associated diseases, for example, Type 2 diabetes, hypertension and atherosclerosis. In this review, we present an overview of the major enzymes in TAG synthesis and lipolysis, including the recent discovery of a novel adipocyte TAG hydrolase.

INTRODUCTION

White adipose tissue (WAT) is the major energy reserve in higher eukaryotes. The primary purposes of WAT are synthesis and storage of triacylglycerol (TAG) in periods of energy excess, and hydrolysis of TAG to generate fatty acids for use by other organs during periods of energy deprivation [1]. Adipose tissue also secretes adipokines that regulate energy intake and metabolism. The prevalence of obesity resulting from excess WAT has increased dramatically in recent years resulting in a serious public health problem, since obesity is closely associated with a number of disorders including Type 2 diabetes, hypertension and atherosclerosis [2]. While adipocyte number has been shown to increase (hyperplasia) in morbid obesity, obesity is primarily attributed to adipocyte hypertrophy that occurs when TAG synthesis (esterification) exceeds TAG breakdown (lipolysis), resulting in elevated TAG storage [1]. Although it has been postulated that large adipocyte size may contribute to insulin resistance, the molecular mechanism is not clear.

Paradoxically, the metabolic abnormalities typically found in obesity are also associated with lipodystrophies that are characterized by selective loss of adipose tissue from particular regions of the body [3-6]. Although the underlying molecular mechanisms are not clear, metabolic complications may result from ectopic storage of TAG in tissues such as the liver and muscle [7-9]. A proper capacity for TAG storage in adipocytes is clearly important for normal metabolic regulation. In view of the wide range of health problems associated with improper fat storage and release, it is critical to understand adipocyte-specific regulation of TAG synthesis and hydrolysis.

BIOSYNTHESIS OF TRIACYLGLYCEROL

The synthesis of phosphatidic acid and its subsequent conversion to TAG was described more than 40 years ago by Kennedy and coworkers [10], and is summarized in Figure 1. The initial committal step in this pathway is the formation of lysophosphatidic acid (1-acylglycerol-3-phosphate) catalyzed by glycerol-3-phosphate acyltransferase (GPAT), which occurs in both the endoplasmic reticulum (ER) and mitochondria [11,12]. GPAT is believed to be the rate-limiting factor in glycerophospholipid synthesis. Lysophosphatidic

acid can also be formed by the acylation of dihydroxyacetone-phosphate (DHAP) by acylcoenzyme A (CoA):DHAP acyltransferase and the subsequent reduction of 1-acyl-DHAP by DHAP oxido-reductase. However, the contribution of the DHAP pathway to TAG synthesis remains unclear [13]. Lysophosphatidic acid is further esterified and converted into phosphatidic acid (1,2-diacylglycerol-3-phosphate) in the reaction catalyzed by 1-acylglycerol-3-phosphate acyltransferase (AGPAT), also named lysophosphatidate acyltransferase, an enzyme mainly present in the ER. Phosphatidic acid is then shunted into the synthesis of various phospholipids or into the synthesis of TAG, two separate branches of glycerolipid synthesis. Entry into TAG synthesis involves the conversion of phosphatidic acid to the intermediate 1,2-diacylglycerol (1,2-DAG) by the phosphatidic acid phosphatase (PAP) reaction. Diacylglycerol acyltransferase (DGAT) catalyzes the acylation of 1,2-DAG to form TAG.

In naturally occurring glycerophospholipids, saturated fatty acids are predominantly esterified at the sn-1 position and unsaturated fatty acids at the sn-2 position [14]. It is believed that the substrate selectivities of mitochondrial GPAT (mtGPAT) and AGPAT play key roles in this non-random distribution of fatty acids, but the mechanism(s) have not yet been elucidated[12]. Most enzymes in TAG synthesis are intrinsic membrane proteins and their substrates and products are hydrophobic, making purification and kinetic analysis difficult. Cloning and characterization of the enzymes mentioned previously has only been achieved during the last decade following advances in molecular biological techniques.

Our laboratory originally cloned mtGPAT, which was the first mammalian enzyme in TAG and phospholipid biosynthesis to be cloned [15-17]. While mammalian cells are known to have two GPATs, one in the ER (microsomal GPAT) and another in the mitochondria (mtGPAT), microsomal GPAT has not been cloned [13,18]. mtGPAT expression is regulated in a manner that is consistent with its role in energy storage. mtGPAT is not detectable in fasted animals but is transcriptionally induced, especially in liver and adipose tissue, when fasted animals are re-fed a high carbohydrate diet, or when diabetic animals are treated with insulin [19]. On the other hand, microsomal GPAT plays a housekeeping role, as it is not regulated by nutritional and hormonal signals. While mtGPAT preferentially uses saturated fatty acyl-CoA as a substrate, microsomal GPAT shows no preference [19]. Studies in mtGPAT-null mice have confirmed the importance of this enzyme in the synthesis of TAG. The absence of mtGPAT resulted in lower body weights, decreased fat-pad mass, lower liver and plasma triacylglycerol and a lower rate of very low-density lipoprotein (VLDL) secretion compared with wild-type controls [20]. Furthermore, examination of mtGPAT-null mice showed the potential presence of another mtGPAT isoform [17]. Additionally, a murine GPAT-like protein (xGPAT1) was identified [21]. It is unclear whether xGPAT1 is microsomal GPAT, the potential mtGPAT isoform mentioned above or whether it represents an entirely new isoform. It is also unclear how the product of mtGPAT (1-acylglycerol-3-phosphate) is transported out of the mitochondria to the ER where the final enzymes of TAG synthesis are located. In vitro studies have revealed that liver fatty-acid binding protein can transport 1-acyl glycerol-3-phosphate from the mitochondria to target microsomes [13]. However, whether fatty-acid binding protein serves as a transporter in vivo remains elusive.

Based on their known homology to mtGPAT, other acyltransferases for TAG synthesis in the Kennedy pathway were subsequently identified and studied, including AGPAT, DGAT and their isoforms [18,22-27]. To date, eight AGPAT genes have been identified, although the physiological functions of each are not well established [28,29]. Mutations in AGPAT2, the major isoform in adipose tissue, have been reported in patients with congenital generalized lipodystrophy, a rare autosomal recessive disorder characterized by a marked lack of body fat since birth [3]. The discovery of these AGPAT2 mutations suggested an important physiological function for these enzymes in TAG synthesis. Recent findings in AGPAT6-null mice further support this role [29]. AGPAT6 is normally expressed at high levels in WAT, brown adipose tissue and liver. AGPAT6-null mice exhibited a 25% reduction in body weight and resistance to both diet- and genetically-induced obesity. These results indicate that AGPAT6 may play a role in determining triglyceride content in adipose tissue, and its loss is not fully compensated by other members of the AGPAT family.

As described previously, the PAP reaction generates 1,2-DAG, which is utilized as an acylacceptor by DGAT during the synthesis of TAG. There are two types of PAPs, Mg2+-dependent (PAP1) and Mg2+-independent (PAP2) [30]. Until recently, only genes encoding PAP2s have been identified in yeast and mammalian systems. However, recent analysis has shown that phophatidic acid phosphohydrolase (PAH)1 (previously known as SMP2) from Saccharomyces cerevisiae is a PAP1 that functions in de novo lipid synthesis [31]. PAH1 has homology with lipin-1 (lipin) and, when expressed in Escherichia coli, lipin displays Mg2+-dependent PAP activity [31]. The Lpin1 gene is mutated in fatty liver dystrophy mice that display lipodystrophy with impaired TAG storage in adipose tissue [32]. Over-expression of lipin in adipose tissue results in increased adiposity and improved insulin sensitivity [32]. Recently, phosphorylation of lipin has been demonstrated to be affected by insulin or epinephrine, resulting in redistribution between the cytosol and ER [33]. Similar to the other enzymes in TAG synthesis, there are multiple isoforms of lipin. The synthesis of TAG catalyzed by DGAT is the final and unique step in TAG formation. It is believed that DGAT diverts 1,2-DAG from membrane phospholipid synthesis into TAG synthesis. Two mammalian DGATs have been identified, DGAT 1 and 2 [13]. Both enzymes are membrane-associated and share similar biochemical functions and tissue expression patterns. Both enzymes are also ubiquitously expressed with the highest expression in tissues involved in TAG metabolism, such as the liver, WAT, mammary gland and small intestine [22,25]. Despite these similarities, DGAT1 and 2 have significant differences. DGAT1 belongs to a family of enzymes that catalyze cholesterol ester biosynthesis and include the acyl-CoA:cholesterol acyltransferase enzymes, ACAT1 and 2 [22]. DGAT2 family members include wax synthases and acyl-CoA:monoacylglycerol acyltransferase [34]. Furthermore, in vitro studies have revealed that DGAT1, but not DGAT2, is a multifunctional acyltransferase able to catalyze the synthesis of DAG, retinyl esters and waxes, in addition to TAG [35]. The functional differences between these two enzymes are further emphasized by studies in mice lacking DGAT1 and 2 [34,36-39]. While mice lacking DGAT2 have a drastic reduction in whole body TAG and die shortly after birth, mice lacking DGAT1 are viable, have improved insulin sensitivity, demonstrate modest reductions in tissue TAG and are resistant to diet-induced obesity. The phenotypic

differences between these two mouse models indicate DGAT1 cannot compensate for the loss of DGAT2.

In addition to the previously described acyl-CoA-dependent reactions, acyl-CoA-independent pathways of TAG synthesis from DAG exist, including reactions catalyzed by phospholipid:diacylglycerol acyltransferase (PDAT) [40,41] and sn-1,2(2,3) diacylglycerol transacylase (DGTA) [42]. PDAT has been cloned and characterized in both yeast and plants but not in mammals [40,41]. The PDAT reaction is proposed to contribute to fatty-acid specificity in seed oils by transacylation reactions that enrich the oils in polyunsaturated fatty acids [40]. The DGTA reaction is believed to be important in TAG resynthesis during the lipolysis/re-esterification cycle [42]. Only partial purification and characterization of rodent microsomal DGTA has been reported [42]. Recently, in vitro acylglycerol transacylase activity has been reported for three mammalian enzymes, desnutrin (also named adipose triglyceride lipase [ATGL], iPLA2ζ, TTS2.2), adiponutrin (iPLA2ζ) and GS2 (iPLA2η) [43]. While desnutrin/ATGL has clearly been demonstrated to function as a lipase in vivo [44], further work will be required to understand the function of the other enzymes in acyl-CoA-independent TAG synthesis in mammals, particularly those enzymes that are specific to adipose tissue. In this regard, adiponutrin is highly and specifically expressed in adipose tissue where its expression is almost undetectable in fasted animals, but is dramatically upregulated upon refeeding [45].

HYDROLYSIS OF TRIACYLGLYCEROL

While TAG synthesis occurs in multiple tissues (e.g., in the liver for VLDL formation) lipolysis is quantitatively the most predominant in adipose tissue. During periods of energy demand, TAG synthesized in WAT is rapidly mobilized by the hydrolytic action of lipases, resulting in the release of free fatty acids that are taken up by other organs to meet the energy requirements of the organism [46,47]. Figure 1 contains an overview of this process. Until recently, the model of adipocyte lipolysis has been that hormone-sensitive lipase (HSL) catalyzes the hydrolysis of fatty acids from the sn-1 and sn-3 positions, generating 2-monoglycerol that is subsequently hydrolyzed by monoglyceride lipase to yield glycerol and fatty acids [48,49]. In times of energy need, such as fasting and exercise, adipocyte lipolysis is markedly increased by catecholamines that activate Gs-coupled receptors. These receptors, in turn, activate adenylyl cyclase to generate cyclic (c)AMP. Rising cellular concentrations of cAMP activate protein kinase A(PKA; cAMP-dependent protein kinase) that phosphorylates HSL at three serine residues (563,659 and 660) in a 150 amino acid stretch termed the regulatory module. This regulatory module is found within the C-terminal domain of HSL, which also contains the catalytic triad [50]. Phosphorylation results in increased hydrolytic activity [51], translocation of HSL from the cytosol to the lipid-droplet surface and enhanced TAG breakdown in the cell [49]. HSL can also be regulated by other kinases [49,52], including AMP-activated protein kinase [53]. The hydrolytic action of HSL, and possibly other non-HSL TAG lipases, is regulated by perilipin, a lipid droplet-associated protein [54]. Association of perilipin with lipid droplets may keep lipolysis at a basal level [55]. Under stimulated conditions, however, perilipin increases lipolysis [56-58]. Perilipin may translocate HSL to the lipid droplet and, presumably, allow access of this lipase to its substrate [56,59]. Perilipin is phosphorylated at multiple sites (Ser-81,Ser-223, Ser-277, Ser-434, Ser-492 and Ser-517) [57,60], and recently phosphorylation of Ser-517 was

found to play a global role in adipocytes for PKA-stimulated lipolysis [61]. While recent evidence suggests that perilipin phosphorylation, per se, may not be necessary for HSL translocation, it is required for increased activity by HSL under stimulated conditions [56]. In addition to perilipin, a number of PAT (perilipin/adipophilin/TIP47) family proteins have been identified on the lipid droplet and may contribute to the regulation of lipolysis [62]. Comparative gene identification (CGI)-58, another lipid droplet-associated protein, has been shown to colocalize with perilipin [63,64] and increase lipolysis by activating desnutrin/ATGL (discussed in the next section) [65]. HSL has broad substrate specificity, with hydrolytic activity against TAG, diacylglycerol [DAG] and monoacylglycerol, as well as cholesteryl and retinyl esters [51]. In vitro, HSL is 10-20-fold more active against DAG than TAG, and it may be the only, or at least the major, neutral cholesteryl ester (CE) hydrolase in vivo [51,66,67]. Until recently, HSL was believed to be the major regulatory enzyme in TAG hydrolysis. Studies in HSL-null mice, however, demonstrated normal WAT mass [68] and retained approximately 40% of TAG lipase activity [69-71]. While, HSL deficiency caused an accumulation of DAG in adipose tissue, no significant increase in TAG levels in WAT was observed [69]. Taken together, these findings suggested that HSL may be rate-limiting in DAG, but not TAG, hydrolysis and strongly suggested the presence in adipose tissue of additional distinct neutral lipase(s). Interestingly, absence of HSL in WAT causes a shift of the fatty-acid composition in TAG to higher levels of long-chain unsaturated fatty acids, an indication that in vivo HSL may prefer long-chain unsaturated fatty acids as a substrate [69] and, thereby, contribute to the observed preferential mobilization of some highly unsaturated fatty acids [72].

Recently, we identified and characterized a novel adipocyte TAG lipase that we called desnutrin [45]. Two other laboratories subsequently identified this same enzyme from database searches of proteins containing the conserved GXSXG pentapeptide motif and α/β-hydrolase fold, and named it ATGL or iPLA2ζ [43,73]. Murine desnutrin is a 54 kDa protein found predominantly in adipose tissue, but also at much lower levels in other tissues, notably cardiac and skeletal muscle and testis. In cells that contain fat stores, such as differentiated 3T3-L1cells [73] and HeLa cells grown in oleic acid-rich medium [74], desnutrin/ATGL is found tightly associated with the lipid droplet, as well as throughout the cytoplasm [45,73,74]. Desnutrin/ATGL contains an N-terminal patatin-like domain found in many plant acyl hydrolases, which is characterized by a conserved serine in the GXSXG motif, an α/β-hydrolase fold, a conserved aspartate belonging to the DX(G/A) motif and a glycine-rich region [45]. Desnutrin/ATGL is regulated by nutritional and hormonal signals. In mice, it is induced by fasting and suppressed by refeeding [45]. Glucocorticoids, which are elevated during fasting, increase desnutrin/ATGL expression [45], while insulin, which is increased during feeding,downregulates desnutrin/ATGL [75]. We have also found that desnutrin/ATGL is downregulated in ob/ob and db/db mice, further supporting a role for the enzyme in fat breakdown and contribution in the development of obesity [45].

Several lines of evidence indicate that desnutrin/ATGL is a TAG-specific lipase. Overexpression of desnutrin/ATGL in 293HEK cells [76] or COS-7 cells increases free fatty acid release to the medium, decreasing intracellular stores of TAG, without affecting intracellular phospholipid stores [45]. Desnutrin/ATGL has significantly higher TAG lipase activity (approximately six to tenfold higher) than DAG lipase activity, suggesting

a primary role for the enzyme in catalyzing the first, rate-limiting step in lipolysis [73]. Desnutrin/ATGL does not exhibit activity against CEs and retinyl esters [73]. The evolutionary conservation between the Drosophila TAG lipase, Brummer [77], the Saccharomyces cerevisiae TAG lipase, Tgl4 [78] and desnutrin/ATGL provide further support for desnutrin/ATGL's function as a lipase [73]. Mice lacking desnutrin/ATGL have provided further evidence supporting a role for desnutrin/ATGL in TAG hydrolysis in multiple tissues. Global loss of desnutrin/ATGL in mice resulted in increased body weight [44]. In these mice, WAT mass increased somewhat (twofold), while brown adipose tissue mass increased dramatically (8.5-fold). Compensatory increases in the hydrolytic activity of other adipocyte lipases, or decreases in the activity of enzymes involved in re-esterification, may explain the relatively small increase in WAT.

Desnutrin/ATGL also caused substantial ectopic storage of TAG in multiple other organs, which may also have influenced TAG accumulation in WAT. Studies in mice lacking desnutrin/ATGL, specifically in adipose tissue, are required to determine the effects of this enzyme on TAG metabolism in adipocytes. It has recently been reported that PKA-mediated phosphorylation of Ser-517 of perilipin A is important for desnutrin/ATGL-dependent lipolysis. In addition, CGI-58 has also been shown to stimulate ATGL activity [65] and mutations in CGI-58 in humans are associated with Chanarin-Dorfman Syndrome, a rare genetic disease where TAG accumulates excessively in multiple tissues [65]. Recent studies that utilized in vitro assays and organ cultures of murine WAT have shown that, together, desnutrin/ATGL and HSL are responsible for more than 95%of the TAG hydrolase activity in murine WAT [79]. However, additional TAG lipases,including triacylglycerol hydrolase (TGH) [80], TGH2 [81], as well as the patatin-domaincontaining proteins, GS2 and GS2-like [76], have been identified in adipocytes, but their role in adipocyte lipolysis requires further investigation.

CONCLUSION

Dysregulation of adipocyte TAG synthesis and lipolysis may contribute to the development of obesity, lipodystrophy and associated pathologies. Recently, many exciting advances have been made, including the discovery of a major TAG lipase that contributes to in vivo adipocyte lipolysis, as well as the identification of enzymes involved in TAG synthesis. Continued advances in our understanding of adipocyte-specific TAG metabolism are expected as new tools are developed.

FUTURE PERSPECTIVE

Major enzymes in adipocyte TAG metabolism have recently been identified. However, much remains to be elucidated regarding the in vivo function and properties of these enzymes and their isoforms, especially with regards to their relative roles in adipose-tissue metabolism. Studies involving differential regulation of various isoforms of enzymes in TAG synthesis by nutritional and hormonal factors are also lacking. Desnutrin/ATGL has been found to be the major adipocyte TAG lipase and thus plays a critical role in lipolysis. Generation of adiposespecific null and overexpressing mice will be required to clarify the adipose-specific role of desnutrin/ATGL as well as other enzymes in TAG metabolism. Further studies are needed to determine the function of lipid-droplet-associated proteins, such as caveolin-1, and their roles in lipid-droplet

formation and lipolysis. Fatty acids are utilized not only as fuels, but also as membrane components, precursors of eicosanoids and mediators of gene expression. Fattyacid composition of adipose tissue is not strictly correlated with dietary fatty acids, but may be regulated through selective incorporation and mobilization. Therefore, further studies need to be performed to characterize the fatty-acid specificity of enzymes in TAG metabolism and to determine whether different isoforms of these enzymes possess different fatty-acid specificities.

REFERENCES

1. Gregoire FM, Smas CM, Sul HS. Understanding adipocyte differentiation. Physiol. Rev 1998;78(3):783–809. [PubMed: 9674695]
2. Walley AJ, Blakemore AI, Froguel P. Genetics of obesity and the prediction of risk for health. Hum.Mol. Genet 2006;15(Suppl 2):R124–R130. [PubMed: 16987875]
3. Agarwal AK, Garg A. Congenital generalized lipodystrophy: significance of triglyceride biosyntheticpathways. Trends Endocrinol. Metab 2003;14(5):214–221. [PubMed: 12826327]
4. Bhayana S, Hegele RA. The molecular basis of genetic lipodystrophies. Clin. Biochem 2002;35(3):171–177. [PubMed: 12074822]
5. Reitman ML. Metabolic lessons from genetically lean mice. Annu. Rev. Nutr 2002;22:459–482.[PubMed: 12055354]
6. Shimomura I, Hammer RE, Richardson JA, et al. Insulin resistance and diabetes mellitus in transgenic mice expressing nuclear SREBP-1c in adipose tissue: model for congenital generalized lipodystrophy. Genes Dev 1998;12(20):3182–3194. [PubMed: 9784493]
7. Heilbronn L, Smith SR, Ravussin E. Failure of fat cell proliferation, mitochondrial function and fat oxidation results in ectopic fat storage, insulin resistance and Type II diabetes mellitus. Int. J. Obes.Relat. Metab. Disord 2004;28(Suppl 4):S12–S21. [PubMed: 15592481]
8. Perseghin G. Muscle lipid metabolism in the metabolic syndrome. Curr. Opin. Lipidol 2005;16(4):416–420. [PubMed: 15990590]
9. Raz I, Eldor R, Cernea S, et al. Diabetes: insulin resistance and derangements in lipid metabolism.Cure through intervention in fat transport and storage. Diabetes Metab. Res. Rev 2005;21(1):3–14.[PubMed: 15386813]
10. Weiss SB, Kennedy EP, Kiyasu JY. The enzymatic synthesis of triglycerides. J. Biol. Chem1960;235:40–44. [PubMed: 13843753]
11. Lehner R, Kuksis A. Biosynthesis of triacylglycerols. Prog. Lipid Res 1996;35(2):169–201. [PubMed:8944226]
12. Dircks L, Sul HS. Acyltransferases of de novo glycerophospholipid biosynthesis. Prog. Lipid Res1999;38(56):461–479. [PubMed: 10793891]
13. Coleman RA, Lee DP. Enzymes of triacylglycerol synthesis and their regulation. Prog. Lipid Res 2004;43(2):134–176. [PubMed: 14654091]
14. Soma MR, Mims MP, Chari MV, et al. Triglyceride metabolism in 3t3-L1 cells. An in vivo 13c Nmr study. J. Biol. Chem 1992;267(16):11168–11175. [PubMed: 1317859]
15. Dircks LK, Ke J, Sul HS. A conserved seven amino acid stretch important for murine mitochondrial glycerol-3-phosphate acyltransferase activity. Significance of arginine 318 in catalysis. J. Biol. Chem 1999;274(49):34728–34734. [PubMed: 10574940]
16. Yet SF, Lee S, Hahm YT, et al. Expression and identification of P90 as the murine mitochondrial glycerol-3-phosphate acyltransferase. Biochemistry 1993;32(36):9486–9491. [PubMed: 8369314]
17. Yet SF, Moon YK, Sul HS. Purification and reconstitution of murine mitochondrial glycerol-3-phosphate acyltransferase. Functional expression in baculovirus-infected insect cells. Biochemistry 1995;34(22):7303–7310. [PubMed: 7779773]

18. Lewin TM, Schwerbrock NM, Lee DP, et al. Identification of a new glycerol-3-phosphateacyltransferase isoenzyme, mtGPAT2, in mitochondria. J. Biol. Chem 2004;279(14):13488–13495.[PubMed: 14724270]
19. Shin DH, Paulauskis JD, Moustaid N, et al. Transcriptional regulation of P90 with sequence homology to Escherichia Coli glycerol-3-phosphate acyltransferase. J. Biol. Chem 1991;266(35):23834–23839. [PubMed: 1721057]
20. Hammond LE, Gallagher PA, Wang S, et al. Mitochondrial glycerol-3-phosphate acyltransferase deficient mice have reduced weight and liver triacylglycerol content and altered glycerolipid fatty acid composition. Mol. Cell Biol 2002;22(23):8204–8214. [PubMed: 12417724]
21. Harada N, Hara S, Yoshida M, et al. Molecular cloning of a murine glycerol-3-phosphate acyltransferase-like protein 1 (Xgpat1). Mol. Cell Biochem. 2007Epub ahead of print
22. Cases S, Smith SJ, Zheng YW, et al. Identification of a gene encoding an acyl coa:diacylglycerol acyltransferase, a key enzyme in triacylglycerol synthesis. Proc. Natl Acad. Sci. USA 1998;95(22):13018–13023. [PubMed: 9789033]
23. Buhman KK, Smith SJ, Stone SJ, et al. DGAT1 is not essential for intestinal triacylglycerol absorption or chylomicron synthesis. J. Biol. Chem 2002;277(28):25474–25479. [PubMed: 11959864]
24. Buhman KK, Chen HC, Farese RV Jr. The enzymes of neutral lipid synthesis. J. Biol. Chem 2001;276 (44):40369–40372. [PubMed: 11544264]
25. Cases S, Stone SJ, Zhou P, et al. Cloning of DGAT2, a second mammalian diacylglycerol acyltransferase, and related family members. J. Biol. Chem 2001;276(42):38870–38876. [PubMed:11481335]
26. Lu B, Jiang YJ, Zhou Y, et al. Cloning and characterization of murine 1-acyl-sn-glycerol 3-phosphate acyltransferases and their regulation by PPARα in murine heart. Biochem. J 2005;385(Pt 2):469–477. [PubMed: 15367102]
27. West J, Tompkins CK, Balantac N, et al. Cloning and expression of two human lysophosphatidic acid acyltransferase cDNAs that enhance cytokine-induced signaling responses in cells. DNA Cell Biol 1997;16(6):691–701. [PubMed: 9212163]
28. Agarwal AK, Barnes RI, Garg A. Functional characterization of human 1-acylglycerol-3-phosphateacyltransferase isoform 8: cloning, tissue distribution, gene structure, and enzymatic activity. Arch.Biochem. Biophys 2006;449(12):64–76. [PubMed: 16620771]
29. Vergnes L, Beigneux AP, Davis R, et al. AGPAT6 deficiency causes subdermal lipodystrophy and resistance to obesity. J. Lipid Res 2006;47(4):745–754. [PubMed: 16436371]
30. Carman GM, Han GS. Roles of phosphatidate phosphatase enzymes in lipid metabolism. TrendsBiochem. Sci 2006;31(12):694–699. [PubMed: 17079146]
31. Han GS, Wu WI, Carman GM. The Saccharomyces cerevisiae lipin homolog is a Mg2+-dependent phosphatidate phosphatase enzyme. J. Biol. Chem 2006;281(14):9210–9218. [PubMed: 16467296]
32. Phan J, Reue K. Lipin, a lipodystrophy and obesity gene. Cell Metab 2005;1(1):73–83. [PubMed:16054046]

33. Harris TE, Huffman TA, Chi A, et al. Insulin controls subcellular localization and multisite phosphorylation of the phosphatidiic acid phosphatase, lipin 1. J. Biol. Chem 2006;282(1):277–286.[PubMed: 17105729]
34. Stone SJ, Levin M, Farese RV Jr. Murine acyl coa:diacylglycerol acyltransferase-2 (DGAT2):membrane topology and identification of key functional amino acid residues. J. Biol. Chem. 2007Epub ahead of print
35. Yen CL, Brown CH 4th, Monetti M, et al. A human skin multifunctional O-acyltransferase that catalyzes the synthesis of acylglycerols, waxes, and retinyl esters. J. Lipid Res 2005;46(11):2388–2397. [PubMed: 16106050]
36. Chen HC. Enhancing energy and glucose metabolism by disrupting triglyceride synthesis: lessons from mice lacking DGAT1. Nutr. Metab. (Lond.) 2006;3(1):10. [PubMed: 16448557]
37. Chen HC, Farese RV Jr. Inhibition of triglyceride synthesis as a treatment strategy for obesity: lessons from DGAT1-deficient mice. Arterioscler. Thromb. Vasc. Biol 2005;25(3):482–486. [PubMed:15569818]
38. Smith SJ, Cases S, Jensen DR, et al. Obesity resistance and multiple mechanisms of triglyceride synthesis in mice lacking DGAT. Nat. Genet 2000;25(1):87–90. [PubMed: 10802663]
39. Chen HC, Smith SJ, Ladha Z, et al. increased insulin and leptin sensitivity in mice lacking acylCoa:diacylglycerol acyltransferase 1. J. Clin. Invest 2002;109(8):1049–1055. [PubMed: 11956242]
40. Stahl U, Carlsson AS, Lenman M, et al. Cloning and functional characterization of a phospholipid:diacylglycerol acyltransferase from arabidopsis. Plant Physiol 2004;135(3):1324–1335. [PubMed: 15247387]
41. Dahlqvist A, Stahl U, Lenman M, et al. Phospholipid:diacylglycerol acyltransferase: an enzyme that catalyzes the acyl-Coa-independent formation of triacylglycerol in yeast and plants. Proc. Natl Acad.Sci. USA 2000;97(12):6487–6492. [PubMed: 10829075]
42. Lehner R, Kuksis A. Triacylglycerol synthesis by an sn-1,2(2,3)-diacylglycerol transacylase from rat intestinalmicrosomes. J. Biol. Chem 1993;268(12):8781–8786. [PubMed: 8473321]
43. Jenkins CM, Mancuso DJ, Yan W, et al. Identification, cloning, expression, and purification of three novel human calcium-independent phospholipase A2 family members possessing triacylglycerol lipase and acylglycerol transacylase activities. J. Biol. Chem 2004;279(47):48968–48975. [PubMed:15364929]
44. Haemmerle G, Lass A, Zimmermann R, et al. Defective lipolysis and altered energy metabolism in mice lacking adipose triglyceride lipase. Science 2006;312(5774):734–737. [PubMed: 16675698]
45. Villena JA, Roy S, Sarkadi-Nagy E, et al. Desnutrin, an adipocyte gene encoding a novel patatin domain-containing protein, is induced by fasting and glucocorticoids: ectopic expression of desnutrin increases triglyceride hydrolysis. J. Biol. Chem 2004;279(45):47066–47075. [PubMed: 15337759]
46. Gibbons GF, Islam K, Pease RJ. Mobilisation of triacylglycerol stores. Biochim. Biophys. Acta 2000;1483(1):37–57. [PubMed: 10601694]
47. Gilham D, Lehner R. The physiological role of triacylglycerol hydrolase in lipid metabolism. Rev.Endocr. Metab. Disord 2004;5(4):303–309. [PubMed: 15486462]

48. Fredrikson G, Tornqvist H, Belfrage P. Hormone-sensitive lipase and monoacylglycerol lipase are both required for complete degradation of adipocyte triacylglycerol. Biochim. Biophys. Acta 1986;876(2):288–293. [PubMed: 3955067]
49. Holm C. Molecular mechanisms regulating hormone-sensitive lipase and lipolysis. Biochem. Soc.Trans 2003;31(Pt 6):1120–1124. [PubMed: 14641008]
50. Karlsson M, Contreras JA, Hellman U, et al. Cdna cloning, tissue distribution, and identification of the catalytic triad of monoglyceride lipase. Evolutionary relationship to esterases, lysophospholipases, and haloperoxidases. J. Biol. Chem 1997;272(43):27218–27223. [PubMed:9341166]
51. Fredrikson G, Strålfors P, Nilsson NÖ, et al. Hormone-sensitive lipase of rat apidose tissue. J. Biol.Chem 1981;256(12):6631–6320.
52. Greenberg AS, Shen WJ, Muliro K, et al. Stimulation of lipolysis and hormone-sensitive lipase via the extracellular signal-regulated kinase pathway. J. Biol. Chem 2001;276(48):45456–45461.[PubMed: 11581251]
53. Rossmeisl M, Flachs P, Brauner P, et al. Role of energy charge and AMP-activated protein kinase in adipocytes in the control of body fat stores. Int. J. Obes. Relat. Metab. Disord 2004;28(Suppl 4):S38–S44. [PubMed: 15592485]
54. Greenberg AS, Egan JJ, Wek SA, et al. Perilipin, a major hormonally regulated adipocyte-specific phosphoprotein associated with the periphery of lipid storage droplets. J. Biol. Chem 1991;266(17):11341–11346. [PubMed: 2040638]
55. Brasaemle DL, Rubin B, Harten IA, et al. Perilipin a increases triacylglycerol storage by decreasing the rate of triacylglycerol hydrolysis. J. Biol. Chem 2000;275(49):38486–38493. [PubMed:10948207]
56. Miyoshi H, Souza SC, Zhang HH, et al. Perilipin promotes hormone-sensitive lipase-mediatedadipocyte lipolysis via phosphorylation-dependent and -independent mechanisms. J. Biol. Chem 2006;281(23):15837–15844. [PubMed: 16595669]
57. Souza SC, Muliro KV, Liscum L, et al. Modulation of hormone-sensitive lipase and protein kinase A-mediated lipolysis by perilipin a in an adenoviral reconstituted system. J. Biol. Chem 2002;277(10):8267–8272. [PubMed: 11751901]
58. Tansey JT, Huml AM, Vogt R, et al. Functional studies on native and mutated forms of perilipins. Arole in protein kinase α-mediated lipolysis of triacylglycerols. J. Biol. Chem 2003;278(10):8401–8406. [PubMed: 12477720]
59. Sztalryd C, Xu G, Dorward H, et al. Perilipin a is essential for the translocation of hormone-sensitivelipase during lipolytic activation. J. Cell Biol 2003;161(6):1093–1103. [PubMed: 12810697]
60. Tansey JT, Sztalryd C, Hlavin EM, et al. The central role of perilipin a in lipid metabolism and adipocyte lipolysis. IUBMB Life 2004;56(7):379–385. [PubMed: 15545214]
61. Miyoshi H, Perfield JW 2nd, Souza SC, et al. Control of ATGL action by Serine 517 of perilipin a globally regulates PKA-stimulated lipolysis in adipocytes. J. Biol. Chem 2006;282(2):99–1002.
62. Brasaemle DL, Dolios G, Shapiro L, et al. Proteomic analysis of proteins associated with lipid droplets of basal and lipolytically stimulated 3t3-L1 adipocytes. J. Biol. Chem 2004;279(45):46835–46842.[PubMed: 15337753]

63. Subramanian V, Rothenberg A, Gomez C, et al. Perilipin a mediates the reversible binding of CGI-58 to lipid droplets in 3t3-L1 adipocytes. J. Biol. Chem 2004;279(40):42062–42071. [PubMed:15292255]
64. Yamaguchi T, Omatsu N, Matsushita S, et al. CGI-58 interacts with perilipin and is localized to lipid droplets. Possible involvement of CGI-58 mislocalization in Chanarin-Dorfman syndrome. J. Biol.Chem 2004;279(29):30490–30497. [PubMed: 15136565]
65. Lass A, Zimmermann R, Haemmerle G, et al. Adipose triglyceride lipase-mediated lipolysis of cellular fat stores is activated by CGI-58 and defective in Chanarin-Dorfman syndrome. Cell Metab 2006;3(5):309–319. [PubMed: 16679289]
66. Kraemer FB, Shen WJ. Hormone-sensitive lipase: control of intracellular tri-(di)acylglycerol and cholesteryl ester hydrolysis. J. Lipid Res 2002;43(10):1585–1594. [PubMed: 12364542]
67. Ben Ali Y, Chahinian H, Petry S, et al. Might the kinetic behavior of hormone-sensitive lipase reflect the absence of the lid domain? Biochemistry 2004;43(29):9298–9306. [PubMed: 15260473]
68. Harada K, Shen WJ, Patel S, et al. Resistance to high-fat diet-induced obesity and altered expression of adipose-specific genes in HSL-deficient mice. Am. J. Physiol. Endocrinol. Metab 2003;285 (6):E1182–E1195. [PubMed: 12954598]
69. Haemmerle G, Zimmermann R, Hayn M, et al. Hormone-sensitive lipase deficiency in mice causes diglyceride accumulation in adipose tissue, muscle, and testis. J. Biol. Chem 2002;277(7):4806–4815. [PubMed: 11717312]
70. Haemmerle G, Zimmermann R, Zechner R. Letting lipids go: hormone-sensitive lipase. Curr. Opin.Lipidol 2003;14(3):289–297. [PubMed: 12840660]
71. Osuga J, Ishibashi S, Oka T, et al. Targeted disruption of hormone-sensitive lipase results in male sterility and adipocyte hypertrophy, but not in obesity. Proc. Natl Acad. Sci. USA 2000;97(2):787–792. [PubMed: 10639158]
72. Raclot T, Leray C, Bach AC, et al. The selective mobilization of fatty acids is not based on their positional distribution in white-fat-cell triacylglycerols. Biochem. J 1995;311(Pt 3):911–916.[PubMed: 7487950]
73. Zimmermann R, Strauss JG, Haemmerle G, et al. Fat mobilization in adipose tissue is promoted by adipose triglyceride lipase. Science 2004;306(5700):1383–1386. [PubMed: 15550674]
74. Smirnova E, Goldberg EB, Makarova KS, et al. ATGL has a key role in lipid droplet/adiposome degradation in mammalian cells. EMBO Rep 2006;7(1):106–113. [PubMed: 16239926]
75. Kershaw EE, Hamm JK, Verhagen LA, et al. Adipose triglyceride lipase: function, regulation by insulin, and comparison with adiponutrin. Diabetes 2006;55(1):148–157. [PubMed: 16380488]
76. Lake AC, Sun Y, Li JL, et al. Expression, regulation, and triglyceride hydrolase activity of adiponutrin family members. J. Lipid Res 2005;46(11):2477–2487. [PubMed: 16150821]
77. Gronck S, Mildner A, Fellert S, et al. Brummer lipase is an evolutionary conserved fat storage regulator in Drosophila. Cell Metabolism 2005;1:323–329. [PubMed: 16054079]

78. Kurat CF, Natter K, Petschnigg J, et al. Obese yeast: triglyceride lipolysis is functionally conserved from mammals to yeast. J. Biol. Chem 2006;281(1):491–500. [PubMed: 16267052]
79. Schweiger M, Schreiber R, Haemmerle G, et al. Adipose triglyceride lipase and hormone-sensitive lipase are the major enzymes in adipose tissue triacylglycerol catabolism. J. Biol. Chem 2006;281(52):40236–40241. [PubMed: 17074755]
80. Soni KG, Lehner R, Metalnikov P, et al. Carboxylesterase 3 (Ec 3.1.1.1) is a major adipocyte lipase.J. Biol. Chem 2004;279(39):40683–40689. [PubMed: 15220344]
81. Okazaki H, Igarashi M, Nishi M, et al. Identification of a novel member of the carboxylesterase family that hydrolyzes triacylglycerol: a potential role in adipocyte lipolysis. Diabetes 2006;55(7):2091–2097. [PubMed: 16804080]

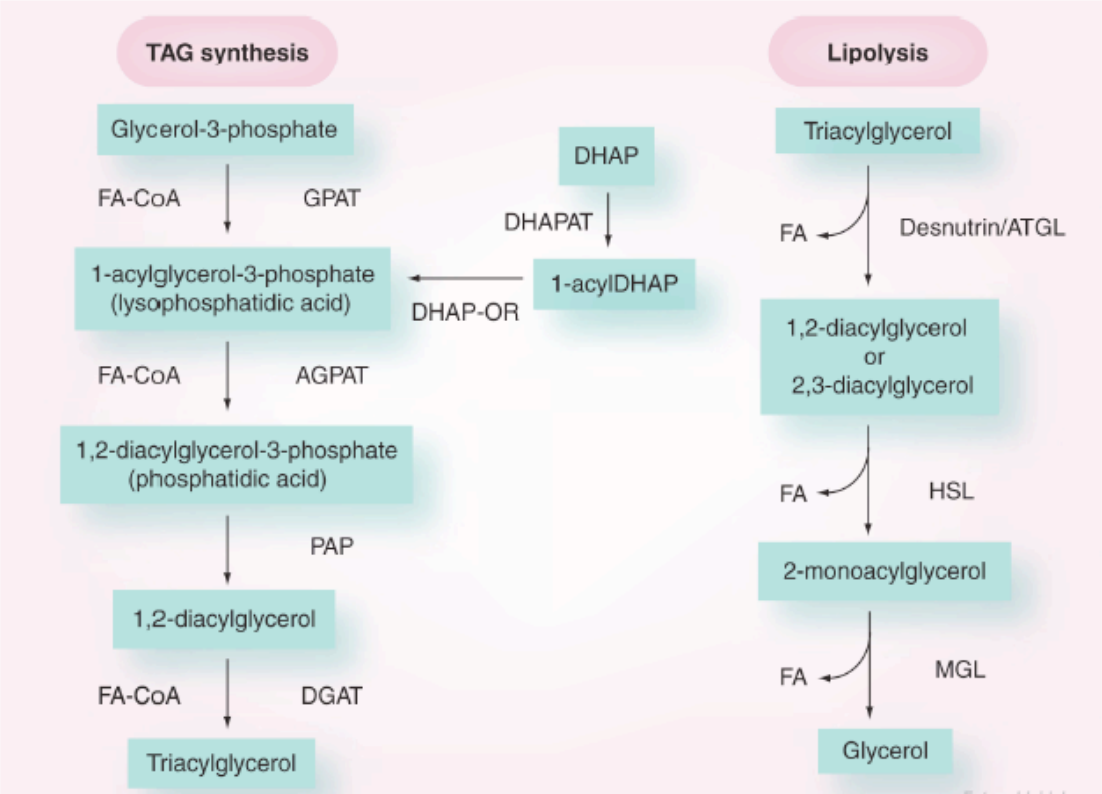

Figure I-1. The enzymes of triacylglycerol synthesis and hydrolysis AGPAT: 1-acylglycerol-3-phosphate acyltransferase; ATGL: Adipose triglyceride lipase; CoA: Coenzyme A; DGAT: Diacylglycerol acyltransferase; DHAP:Dihydroxyacetonephosphate;DHAPAT: Acyl-CoA:dihydroxyacetone-phosphate acyltransferase; DHAP-OR: Dihydroxyacetone-phosphate oxido-reductase; FA: Fatty acid; GPAT: Glycerol-3-phosphateacyltransferase; HSL: Hormone-sensitive lipase; MGL: Monoglyceride lipase; PAP:Phosphatidic acid phosphatase; TAG: Triacylglycerol.

B) Regulation of Lipolysis in Adipocytes

ABSTRACT

Lipolysis in adipocytes, the hydrolysis of triacylglycerol (TAG) to release fatty acids (FAs) and glycerol for use by other organs, is a unique function of white adipose tissue. Lipolysis in adipocytes occurs at the surface of cytosolic lipid droplets, which have recently gained much attention as dynamic organelles integral to lipid metabolism. Desnutrin/ATGL is now established as a bona fide TAG hydrolase and mutations in human desnutrin/ATGL/PNPLA2, as well as in its activator, comparative gene identification 58, are associated with Neutral Lipid Storage disease. Furthermore, recent identification of AdPLA as the major adipose phospholipase A_2, has led to the discovery of a dominant autocrine/paracrine regulation of lipolysis through PGE_2. Here, we review emerging concepts in the key players in lipolysis and the regulation of this process. We also examine recent findings in mouse models and humans with alterations/mutations in genes involved in lipolysis and discuss activation of lipolysis in adipocytes as a potential therapeutic target.

INTRODUCTION: LIPOLYSIS IN ADIPOCYTES

Triacylglycerol (TAG) stored in white adipose tissue is the major energy reserve in mammals. Excess TAG accumulation in adipose tissue results in obesity as well as related metabolic disorders such as type 2 diabetes, cardiovascular disease and hypertension (Ahmadian et al., 2007). TAG is synthesized and stored in cytosolic lipid droplets during times of energy excess, and is mobilized from lipid droplets, via lipolysis, during times of energy need to generate fatty acids (FAs) (Ahmadian et al., 2007, Walther and Farese, 2009). Whereas, TAG synthesis occurs in other organs, such as the liver for VLDL production, lipolysis for the provision of FAs as an energy source for other organs is a unique function of adipocytes (Ahmadian et al., 2007). Increasing lipolysis in adipocytes may be a potentially useful therapeutic target for treating obesity. However, chronically high levels of FAs in the blood, typically observed in obesity, are correlated with many detrimental metabolic consequences such as insulin resistance. Here, we discuss the key players of lipolysis within adipocytes, as well as the regulation of this process. We also highlight recent findings in mouse models and humans with alterations/mutations in genes involved in lipolysis and discuss manipulating adipocyte lipolysis as a potential therapeutic target.

LIPID DROPLETS

In adipocytes, TAG is stored in unilocular cytosolic lipid droplets. Although once considered to be inert storage sites, lipid droplets have recently become appreciated as dynamic organelles, central to lipid and energy metabolism. Lipid droplets are composed of a TAG and cholesterol ester core, surrounded by a phospholipid monolayer and coated

with many proteins. Several of these proteins are characterized by the presence of a conserved N-terminal motif defined as a PAT domain, named after perilipin, adipophilin (also called adipocyte differentiation-related protein, ADRP), and tail-interacting protein of 47kDa (TIP47) but also including OXPAT/MLDP and S3-12 (Brasaemle, 2007). Furthermore, these PAT proteins are expressed in different tissues, suggesting potential tissue-specific functions (Brasaemle, 2007). Additionally, other proteins that may be involved in lipid droplet formation, lipid synthesis, lipolysis and membrane-trafficking are also found on lipid droplets (Guo et al., 2009, Gubern et al., 2009, Gubern et al., 2008, Yu et al., 1998). Caveolin, an integral membrane protein associated with cell surface pits (caveolae), has also been shown to localize to lipid droplets and regulate lipolysis (Cohen et al., 2004). The relative abundance of lipid droplet associated proteins, their posttranslational modifications and interactions with other proteins help to regulate lipolytic activity in adipocytes.

Despite recent progress in lipid droplet biology, several fundamental questions remain. First, how are lipid droplets formed? While several theories on lipid droplet biogenesis exist, the most widely accepted model states that neutral lipids accumulate in the ER bilayer and subsequently bud from the cytosolic leaflet of the membrane (Walther and Farese, 2009). However, further research is required to understand lipid droplet biogenesis. Furthermore, how is TAG transported from the site of synthesis to the lipid droplet to increase its size? Lipids must either be transported to the lipid droplet, perhaps via vesicular transport, or synthesized locally, possibly by enzymes such as diacylglycerol acyltransferases (DGATs) that have been shown to be present on lipid droplets (Walther and Farese, 2009, Guo et al., 2009). It is also postulated that smaller lipid droplets from newly formed TAG could fuse together to form larger lipid droplets (Walther and Farese, 2009, Guo et al., 2009). In addition, to help adipocytes deal with large amounts of incoming FAs it has been suggested that both lipid droplet biogenesis and growth may occur at the plasma membrane (Ost et al., 2005). In support of this hypothesis, caveolins that are involved in plasma membrane organization and endocytosis have been detected on lipid droplets and caveolin knockout mice exhibit defects in lipolysis (Cohen et al., 2004). Further investigation will be required to fully understand the development, expansion as well as many other aspects of lipid droplet biology.

THE PLAYERS IN LIPOLYSIS IN ADIPOCYTES

During times of energy shortage, TAG stored in lipid droplets is hydrolyzed to FAs and glycerol via lipolysis. FAs released from adipose tissue can enter the circulation and be taken up by other organs as an energy source for β-oxidation and subsequent ATP generation. Additionally, liberated FAs and glycerol can also serve as substrates in the liver for ketogenesis and gluconeogenesis, respectively (Stipanuk, 2006)**.** Previously, hormone sensitive lipase (HSL) was considered to be the rate-limiting enzyme in TAG hydrolysis (Duncan et al., 2007). However, HSL knockout mice were not obese and accumulated diacylglycerol (DAG) in adipose tissue rather that TAG, implicating HSL as primarily a DAG lipase and suggesting the presence of additional novel lipase(s) in adipocytes (Haemmerle et al., 2002). In 2004, three laboratories independently identified the same novel TAG lipase named desnutrin, ATGL and phosphopholipase A_2 ζ, leading to re-evaluation of the classic model of lipolysis (Villena et al., 2004, Jenkins et al., 2004,

Zimmermann et al., 2004). Desnutrin/ATGL is predominantly expressed in adipose tissue and exhibits high substrate specificity for TAG (Villena et al., 2004, Zimmermann et al., 2004). Maximal activity of desnutrin/ATGL is dependent on its activator, comparative gene identification 58 (CGI-58), although the mechanism of this activation is not clear (Schweiger et al., 2009). Desnutrin/ATGL is now considered to be the major TAG lipase in adipose tissue, hydrolyzing TAG to DAG and a FA. DAG is subsequently hydrolyzed by HSL to generate monoacylglycerol (MAG) and a second FA. MAG lipase then hydrolyzes MAG producing glycerol and a third FA (Figure 1).

Mice lacking desnutrin/ATGL exhibit TAG accumulation in multiple organs, most notably the heart and die prematurely due to heart failure, preventing detailed characterization of lipolysis in adipocytes from these mice (Haemmerle et al., 2006). Transgenic mice overexpressing desnutrin/ATGL specifically in adipose tissue display elevated lipolysis and increased FA oxidation in white adipose tissue, resulting in higher energy expenditure and resistance to diet-induced obesity (Ahmadian et al., 2009). Interestingly, despite elevated lipolysis in these mice serum FA levels are not increased (Ahmadian et al., 2009). Generation of mice lacking desnutrin/ATGL specifically in adipose tissue will be crucial in fully characterizing the role of desnutrin/ATGL in lipolysis in adipocytes.

REGULATION OF LIPOLYSIS IN ADIPOCYTES

Lipolysis in adipocytes is strongly regulated by hormones. In the fasted state, elevated glucocorticoids upregulate desnutrin/ATGL transcription (Villena et al., 2004) (Figure 1 A). Furthermore, catecholamines, by binding to $G\alpha_s$-coupled β-adrenergic receptors, generate a signaling cascade that increases cAMP levels and activate protein kinase A (PKA). PKA phosphorylates HSL resulting in its translocation from the cytosol to the lipid droplet where it can hydrolyze DAG. PKA also phosphorylates the lipid droplet associated protein perilipin to provide lipases greater access to the lipid droplet (Brasaemle, 2007). In contrast, during the fed state insulin binds to its receptor in adipocytes and initiates a signaling event that, via phosphorylation and activation of phosphodiesterase 3B (PDE3B), decreases cAMP and ultimately inhibits lipolysis (Figure 1B). The importance of PDE3B in suppressing adipocyte lipolysis has been demonstrated in PDE3B null mice (Choi et al., 2006). In the fed state, insulin also suppresses the expression of desnutrin/ATGL, possibly through FoxO1 (Chakrabarti and Kandror, 2009). Although the C-terminal region of human desnutrin/ATGL contains two previously identified phosphoserine residues (S406 and S430), that are conserved in murine desnutrin/ATGL, phosphorylation of these sites does not appear to affect TAG hydrolysis or localization to lipid droplets (Duncan et al., 2009).

While the endocrine regulation of lipolysis by catecholamines and insulin has been well characterized, much remains to be investigated regarding the local regulation of lipolysis in adipocytes by autocrine/paracrine facors. Adipocytes secrete several factors that can regulate lipolysis locally, such as TNF-α which stimulates lipolysis and adenosine which inhibits lipolysis (Jaworski et al., 2007, Dhalla et al., 2009). Prostaglandins have also been shown to inhibit, stimulate, or have no effect on lipolysis depending on the concentration and species tested (Jaworski et al., 2007). However, recent identification of adipose-specific phospholipase A_2 (AdPLA) has shed new light on a dominant autocrine/paracrine regulation of lipolysis by adipocyte-derived PGE_2

(Duncan et al., 2008, Jaworski et al., 2009). AdPLA is a membrane-associated, calcium-dependent PLA_2 and represents a new group of PLA_2s, group XVI (Duncan et al., 2008). AdPLA is highly expressed exclusively in adipocytes and is the major PLA in adipocytes (Jaworski et al., 2009). As a PLA_2, AdPLA catalyzes the release of FAs from the *sn*-2 position of phospholipids that is typically enriched in arachidonic acid, a substrate for the synthesis of eicosanoids (Jaworski et al., 2009) (Figure 1B). PGE_2 is the predominant prostaglandin produced in white adipose tissue, and ablation of AdPLA in mice causes a >85% fall in PGE_2 levels in this tissue. While PGE_2 has 4 cognate receptors (EP1, EP2, EP3, and EP4), $G\alpha_i$-coupled EP3 is expressed at >10-fold higher levels than the other EP receptors in adipose tissue (Jaworski et al., 2009). Reduced PGE_2 levels induced by loss of AdPLA causes decreased EP3 signaling, which, in turn, elevates cAMP levels and activates lipolysis through PKA-mediated phosphorylation of HSL (Jaworski et al., 2009). The induction of AdPLA by feeding and insulin, suggests that it plays an important role in the suppression of lipolysis during the fed state (Jaworski et al., 2009). AdPLA null mice exhibit unrestrained adipocyte lipolysis and are resistant to both diet-induced and genetic obesity indicating that AdPLA is a critical factor in the development of obesity (Jaworski et al., 2009). Interestingly, similar to desnutrin/ATGL transgenic mice, increased lipolysis in these mice does not lead to elevated serum FA levels but instead promotes FA oxidation directly within adipocytes (Jaworski et al., 2009, Ahmadian et al., 2009).

In addition to the autocrine/paracrine regulation of lipolysis by PGE_2, other signaling pathways through cytokines, growth hormones, AMP-activated protein kinase and nicotinic acid have also been shown to regulate lipolysis (Lafontan, 2008, Jaworski et al., 2007). Furthermore, in primates but not rodents, regulation of lipolysis by naturietic peptides through a cGMP dependent protein kinase (PKG) has also been shown to exist (Lafontan, 2008). However, future investigation into these pathways will be required to establish their relative importance in regulating lipolysis.

HUMAN DISEASES WITH ALTERATIONS IN LIPOLYSIS IN ADIPOCYTES

Mutations in the human desnutrin/ATGL gene (PNPLA2) are associated with a rare inherited disorder called Neutral Lipid Storage Disease with Myopathy (NLSD-M), which results in systemic TAG accumulation, myopathy, cardiac abnormalities, and hepatomegaly (Schweiger et al., 2009). TAG accumulation in the heart causes cardiac defects reminiscent of the phenotype observed in mice lacking desnutrin/ATGL (Schweiger et al., 2009). Most of the identified mutations lead to the expression of C-terminally truncated versions of desnutrin/ATGL (Schweiger et al., 2009). Interestingly, these variants exhibit elevated enzyme activity *in vitro* compared to the full length form but fail to bind to lipid droplets in intact cells, suggesting that the lipolytic defect in these individuals is due to impaired localization of desnutrin/ATGL and that the C-terminus of desnutrin/ATGL likely contains a regulatory domain that affects hydrolase activity (Schweiger et al., 2009). In this regard, recent findings have shown that the N- and C-terminus of murine desnutrin/ATGL interact, suggesting that the negative regulatory role of the C-terminal domain *in vitro* likely results from masking of critical sites in the N-terminal patatin domain(Duncan et al., 2009). In humans, mutations in CGI-58, the activator of desnutrin/ATGL, have also been identified and, similar to individuals with mutated desnutrin/ATGL, they exhibit systemic TAG accumulation, mild myopathy and

hepatomegaly (Schweiger et al., 2009). However, these individuals also display ichthyosis. This disease is known as Chanarin-Dorfman Syndrome or NLSD with ichthyosis (NLSD-I). Affected individuals express mutant forms of CGI-58 that are unable to activate desnutrin/ATGL, indicating that the TAG accumulation in tissues is due to defective desnutrin/ATGL function. It is interesting to note that, although desnutrin/ATGL and CGI-58 are highly expressed in adipocytes where lipolysis is the major function, patients with NLSDL or NLSDM are not obese (Schweiger et al., 2009). Further investigation into the roles of desnutrin/ATGL and CGI-58, particularly in human adipose tissue will be necessary to better understand and treat these diseases. Additionally, identification of single nucleotide polymorphisms (SNPs) in other genes encoding proteins involved in lipolysis and characterization of their associated pathological syndromes will be crucial in helping to develop strategies to target lipolysis as a treatment for obesity or related diseases.

THERAPY

It might be predicted that increasing lipolysis in adipocytes would lead to chronically high levels of circulating FAs that are correlated with adverse metabolic effects such as insulin resistance. Therefore, inhibiting lipolysis to lower serum FA levels has been a therapeutic approach for the management of insulin resistance and type 2 diabetes. Nicotinic acid and its analog acipimox have been used as antilipolytic agents for the treatment of dyslipidemia (Dhalla et al., 2009). However, their therapeutic usefulness is limited since the initial decrease in serum FA levels is followed by a rebound effect resulting in increased serum FA levels and insulin resistance (Dhalla et al., 2009).

Interestingly, mouse models of increased lipolysis do not have elevated serum FA levels, revealing that increasing lipolysis in adipocytes does not alter serum FA levels. Rather, increasing lipolysis in mice results in leanness and promotes FA oxidation directly within adipocytes (Ahmadian et al., 2009, Jaworski et al., 2009, Saha et al., 2004, Tansey et al., 2001), suggesting that activation of lipolysis may be a promising therapeutic target for the treatment of obesity. In this regard, adipocytes from obese humans have reduced lipolytic capacity and desnutrin/ATGL expression is reduced in adipose tissue of *ob/ob* mice (Langin et al., 2005, Villena et al., 2004). It is important to note that when FAs are generated at a rate that exceeds the oxidative capacity of adipose tissue, ectopic TAG storage and insulin resistance may result, as seen in many lipodystrophy models (Jaworski et al., 2009). Therefore, partial activation of lipolysis in adipocytes may be a more promising therapeutic approach. However, since there are numerous genes involved in lipolysis including those that encode for lipolytic enzymes, regulatory proteins as well as lipid droplet associated proteins, it is important that the tissue specificity of the target is taken into account. As discussed above, mutations in desnutrin/ATGL as well as CGI-58 severely affect multiple tissues. In this regard, AdPLA may represent an ideal target for manipulating lipolysis since it is highly expressed only in adipose tissue and is therefore less likely to have off-target effects. Future investigation into the role AdPLA in human adipocytes as well as the pathological syndrome of humans with SNPs in the AdPLA (PLA2G16) gene will help answer some of these questions. Furthermore, as more lipid droplet associated proteins are identified

and characterized there will likely be more potential therapeutic targets for modulating lipolysis.

REFERENCES

Ahmadian, M., Duncan, R. E., Jaworski, K., Sarkadi-Nagy, E. & Sul, H. S. (2007). Triacylglycerol metabolism in adipose tissue. *Future Lipdol., 2*, 229-237.

Ahmadian, M., Duncan, R. E., Varady, K. A., Frasson, D., Hellerstein, M. K., Birkenfeld, A. L., Samuel, V. T., Shulman, G. I., Wang, Y., Kang, C. & Sul, H. S. (2009). Adipose overexpression of desnutrin promotes fatty acid use and attenuates diet-induced obesity. *Diabetes, 58*, 855-866.

Brasaemle, D. L. (2007). Thematic review series: adipocyte biology. The perilipin family of structural lipid droplet proteins: stabilization of lipid droplets and control of lipolysis. *J Lipid Res, 48*, 2547-2559.

Chakrabarti, P. & Kandror, K. V. (2009). FoxO1 controls insulin-dependent adipose triglyceride lipase (ATGL) expression and lipolysis in adipocytes. *J Biol Chem, 284*, 13296-13300.

Choi, Y. H., Park, S., Hockman, S., Zmuda-Trzebiatowska, E., Svennelid, F., Haluzik, M., Gavrilova, O., Ahmad, F., Pepin, L., Napolitano, M., Taira, M., Sundler, F., Stenson Holst, L., Degerman, E. & Manganiello, V. C. (2006). Alterations in regulation of energy homeostasis in cyclic nucleotide phosphodiesterase 3B-null mice. *J Clin Invest, 116*, 3240-3251.

Cohen, A. W., Razani, B., Schubert, W., Williams, T. M., Wang, X. B., Iyengar, P., Brasaemle, D. L., Scherer, P. E. & Lisanti, M. P. (2004). Role of caveolin-1 in the modulation of lipolysis and lipid droplet formation. *Diabetes, 53*, 1261-1270.

Dhalla, A. K., Chisholm, J. W., Reaven, G. M. & Belardinelli, L. (2009). A1 adenosine receptor: role in diabetes and obesity. *Handb Exp Pharmacol*, 271-295.

Duncan, R. E., Ahmadian, M., Jaworski, K., Sarkadi-Nagy, E. & Sul, H. S. (2007). Regulation of lipolysis in adipocytes. *Annu Rev Nutr, 27*, 79-101.

Duncan, R. E., Sarkadi-Nagy, E., Jaworski, K., Ahmadian, M. & Sul, H. S. (2008). Identification and functional characterization of adipose-specific phospholipase A2 (AdPLA). *J Biol Chem, 283*, 25428-25436.

Duncan, R. E., Wang, Y., Ahmadian, M., Lu, J., Sarkadi-Nagy, E. & Sul, H. S. (2009). Characterization of desnutrin functional domains:Critical residues for triacylglycerol hydrolysis in cultured cells. *J Lipid Res*.

Gubern, A., Barcelo-Torns, M., Casas, J., Barneda, D., Masgrau, R., Picatoste, F., Balsinde, J., Balboa, M. A. & Claro, E. (2009). Lipid droplet biogenesis induced by stress involves triacylglycerol synthesis that depends on group VIA phospholipase A2. *J Biol Chem, 284*, 5697-5708.

Gubern, A., Casas, J., Barcelo-Torns, M., Barneda, D., de la Rosa, X., Masgrau, R., Picatoste, F., Balsinde, J., Balboa, M. A. & Claro, E. (2008). Group IVA phospholipase A2 is necessary for the biogenesis of lipid droplets. *J Biol Chem, 283*, 27369-27382.

Guo, Y., Cordes, K. R., Farese, R. V., Jr. & Walther, T. C. (2009). Lipid droplets at a glance. *J Cell Sci, 122*, 749-752.

Haemmerle, G., Lass, A., Zimmermann, R., Gorkiewicz, G., Meyer, C., Rozman, J., Heldmaier, G., Maier, R., Theussl, C., Eder, S., Kratky, D., Wagner, E. F., Klingenspor, M., Hoefler, G. & Zechner, R. (2006). Defective lipolysis and

altered energy metabolism in mice lacking adipose triglyceride lipase. *Science, 312*, 734-737.

Haemmerle, G., Zimmermann, R., Hayn, M., Theussl, C., Waeg, G., Wagner, E., Sattler, W., Magin, T. M., Wagner, E. F. & Zechner, R. (2002). Hormone-sensitive lipase deficiency in mice causes diglyceride accumulation in adipose tissue, muscle, and testis. *J Biol Chem, 277*, 4806-4815.

Jaworski, K., Ahmadian, M., Duncan, R. E., Sarkadi-Nagy, E., Varady, K. A., Hellerstein, M. K., Lee, H.-Y., Samuel, V. T., Shulman, G. I., Kim, K.-H., de Val, S., Kang, C. & Sul, H. S. (2009). AdPLA ablation increases lipolysis and prevents obesity induced by high-fat feeding or leptin deficiency. *Nat Med, 15*, 159-168.

Jaworski, K., Sarkadi-Nagy, E., Duncan, R. E., Ahmadian, M. & Sul, H. S. (2007). Regulation of triglyceride metabolism. IV. Hormonal regulation of lipolysis in adipose tissue. *Am J Physiol Gastrointest Liver Physiol, 293*, G1-4.

Jenkins, C. M., Mancuso, D. J., Yan, W., Sims, H. F., Gibson, B. & Gross, R. W. (2004). Identification, cloning, expression, and purification of three novel human calcium-independent phospholipase A2 family members possessing triacylglycerol lipase and acylglycerol transacylase activities. *J Biol Chem, 279*, 48968-48975.

Lafontan, M. (2008). Advances in adipose tissue metabolism. *Int J Obes (Lond), 32 Suppl 7*, S39-51.

Langin, D., Dicker, A., Tavernier, G., Hoffstedt, J., Mairal, A., Ryden, M., Arner, E., Sicard, A., Jenkins, C. M., Viguerie, N., van Harmelen, V., Gross, R. W., Holm, C. & Arner, P. (2005). Adipocyte lipases and defect of lipolysis in human obesity. *Diabetes, 54*, 3190-3197.

Ost, A., Ortegren, U., Gustavsson, J., Nystrom, F. H. & Stralfors, P. (2005). Triacylglycerol is synthesized in a specific subclass of caveolae in primary adipocytes. *J Biol Chem, 280*, 5-8.

Saha, P. K., Kojima, H., Martinez-Botas, J., Sunehag, A. L. & Chan, L. (2004). Metabolic adaptations in the absence of perilipin: increased beta-oxidation and decreased hepatic glucose production associated with peripheral insulin resistance but normal glucose tolerance in perilipin-null mice. *J Biol Chem, 279*, 35150-35158.

Schweiger, M., Lass, A., Zimmermann, R., Eichmann, T. O. & Zechner, R. (2009). Neutral lipid storage disease: genetic disorders caused by mutations in adipose triglyceride lipase/PNPLA2 or CGI-58/ABHD5. *Am J Physiol Endocrinol Metab, 297*, E289-296.

Stipanuk, M. (2006). *Biochemical, Physiological, Molecular Aspects of Human Nutrition,* (Editor ed.). St. Louis: Elsevier.

Tansey, J. T., Sztalryd, C., Gruia-Gray, J., Roush, D. L., Zee, J. V., Gavrilova, O., Reitman, M. L., Deng, C. X., Li, C., Kimmel, A. R. & Londos, C. (2001). Perilipin ablation results in a lean mouse with aberrant adipocyte lipolysis, enhanced leptin production, and resistance to diet-induced obesity. *Proc Natl Acad Sci U S A, 98*, 6494-6499.

Villena, J. A., Roy, S., Sarkadi-Nagy, E., Kim, K. H. & Sul, H. S. (2004). Desnutrin, an adipocyte gene encoding a novel patatin domain-containing protein, is induced by

fasting and glucocorticoids: ectopic expression of desnutrin increases triglyceride hydrolysis. *J Biol Chem, 279***,** 47066-47075.

Walther, T. C. & Farese, R. V., Jr. (2009). The life of lipid droplets. *Biochim Biophys Acta, 1791***,** 459-466.

Yu, W., Bozza, P. T., Tzizik, D. M., Gray, J. P., Cassara, J., Dvorak, A. M. & Weller, P. F. (1998). Co-compartmentalization of MAP kinases and cytosolic phospholipase A2 at cytoplasmic arachidonate-rich lipid bodies. *Am J Pathol, 152***,** 759-769.

Zimmermann, R., Strauss, J. G., Haemmerle, G., Schoiswohl, G., Birner-Gruenberger, R., Riederer, M., Lass, A., Neuberger, G., Eisenhaber, F., Hermetter, A. & Zechner, R. (2004). Fat mobilization in adipose tissue is promoted by adipose triglyceride lipase. *Science, 306***,** 1383-1386.

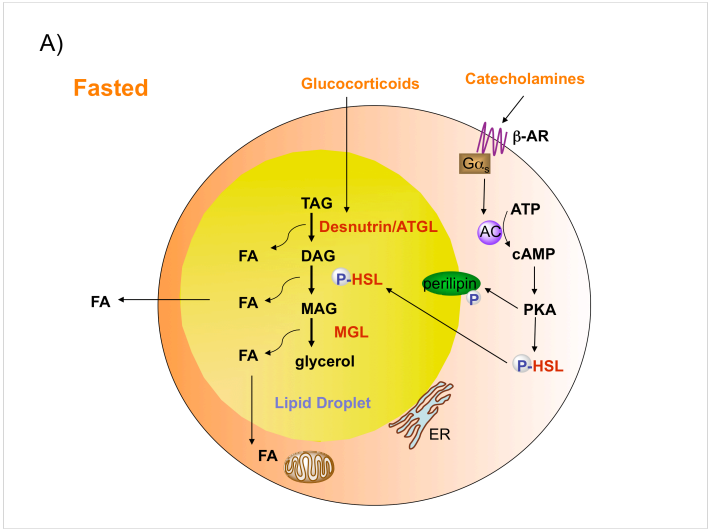

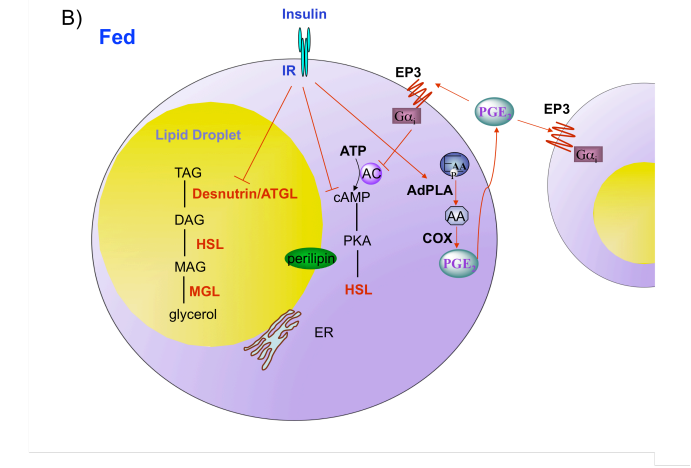

Figure I-2. Lipolysis in the fasted and fed state. A) Desnutrin/ATGL initiates lipolysis by hydrolyzing triacylglycerol (TAG) to diacylglycerol (DAG). Hormone-sensitive lipase (HSL) hydrolyzes DAG to monoacylglycerol (MAG), which is subsequently hydrolyzed by MAG lipase to generate glycerol and three fatty acids (FAs). The FAs generated during lipolysis can be released into the circulation for use by other organs or oxidized within adipocytes. During fasting, catecholamines, by binding to Gαs-coupled β-adrenergic receptors (β-AR), activate adenylate cyclase (AC) to increase cAMP and activate protein kinase A (PKA). PKA phosphorylates HSL, resulting in translocation of HSL from the cytosol to the lipid droplet. PKA also phosphorylates the lipid droplet associated protein perilipin. Additionally, during fasting, glucocorticoids increase the expression of desnutrin/ATGL. B) In the fed state, insulin binding to the insulin receptor (IR), results in decreased cAMP levels and decreased lipolysis. Insulin also suppresses expression of desnutrin/ATGL. Recent studies have revealed that lipolysis is dominantly regulated by prostaglandin E_2 (PGE_2) through adipose-specific phospholipase A_2 (AdPLA). AdPLA hydrolyzes the sn-2 position of phospholipids to generate arachidonic acid (AA), which via cyclooxygenase (COX) produces PGE_2, that acts locally by binding to Gαi-coupled EP3 present in adipocytes, resulting in inhibition of AC and decreased lipolys

C) Lipolysis and Fatty Acid Utilization in Adipocytes

ABSTRACT

Lipolysis for the provision of fatty acids (FA) as an energy source for other organs during times of energy demand occurs uniquely in white adipose tissue (WAT). Recent findings have identified a bona fide TAG hydrolase as well as the major adipose phospholipase A_2, AdPLA. By controlling PGE_2 levels, AdPLA dominantly regulates lipolysis in an autocrine/paracrine manner. Moreover, recent findings also demonstrate that, surprisingly, increasing lipolysis in adipose tissue does not necessarily increase serum FA levels, which are usually correlated with insulin resistance. Rather, it appears that increasing lipolysis in adipose tissue causes a shift within adipocytes towards increased FA utilization and energy expenditure and, thus, protects against obesity.

INTRODUCTION

Trialcylglycerol (TAG) is the major energy storage form in mammals. Excess TAG accumulation resulting in obesity is a major risk factor for metabolic disorders including type 2 diabetes and cardiovascular disease [1]. White adipose tissue (WAT) stores TAG during periods of energy excess and hydrolyzes TAG (lipolysis) to release fatty acids (FA) for use by other tissues during times of energy need [2]. While TAG synthesis occurs in other organs, such as the liver for VLDL production, lipolysis for the provision of FA for use by other organs is unique to adipocytes [3]. Strategies aimed at increasing lipolysis may therefore be useful in preventing obesity. However, elevated lipolysis may increase circulating FFA levels and ectopic TAG storage, which are associated with detrimental metabolic consequences, such as insulin resistance. New evidence, however, suggests that adipocytes have a capacity to increase FA utilization in response to increased lipolysis, which may make lipolysis a target for the prevention and treatment of obesity. Here, we focus on recent findings in understanding the regulation of lipolysis in adipose tissue and on changes in adipocyte FA metabolism and energy expenditure resulting from increased adipocyte lipolysis.

THE LIPOLYTIC CASCADE

TAG in adipose tissue is stored in unilocular cytosolic lipid droplets that are composed of a core of TAG and cholesterol esters, surrounded by a phospholipid monolayer, coated with lipid droplet associated proteins [4]. Many of these lipid droplet associated proteins are characterized by the presence a conserved amino acid sequence defined as a PAT (perilipin, adipophilin (also called adipocyte differentiation-related protein, ADRP), and tail-interacting protein of 47kDa (TIP47)) domain [5-7]. Several other lipid droplet associated proteins are also found on the lipid droplets, such as fat-specific protein of 27kDa (FSP27)/Cidec which has recently been shown to be required for the formation of unilocular lipid droplets of white adipocytes [7-10]. Although its role is unclear, caveolin, an integral membrane protein associated with cell surface pits, caveolae, has also been shown to localize to lipid droplets and regulate lipolysis [11-14]. The relative abundance of lipid droplet associated proteins, as well as their posttranslational modifications and interactions with other cytosolic proteins may control the accessibility of lipases to their TAG substrate and, therefore, affect lipolytic activity [7,15].

Adipocyte lipolysis proceeds in an orderly and regulated manner, with different enzymes acting at each step. Until recently, hormone-sensitive lipase (HSL) was thought to be the initial enzyme in TAG hydrolysis. However, mice lacking HSL were not obese and had substantial residual TAG hydrolase activity in WAT, accumulating diacylglycerol (DAG) rather than TAG [2]. These findings indicated that although HSL has TAG hydrolase activity *in vitro*, it functions primarily as a DAG hydrolase in adipose tissue, and suggested the presence of additional unidentified TAG hydrolase(s). Recently, we, and others, identified a novel TAG hydrolase called desnutrin (also called ATGL, TTS2.2, PNPLA2, or iPLA$_2\zeta$) [16-18]. Desnutrin/ATGL exhibits high substrate specificity for TAG, is predominantly expressed in adipose tissue, and is induced during fasting and by glucocorticoids, conditions that favor lipolysis [16,17]. Its function as a TAG hydrolase is evolutionarily conserved between humans, mice, *Drosophila, Saccharomyces cerevisiae,* and *Arabidopsis* highlighting the importance of this enzyme [17,19-23]. Although the mechanism is poorly understood, studies indicate that comparative gene identification 58 (CGI-58) serves as a coactivator of desnutrin/ATGL [7]. These findings have led to a new understanding of the lipolytic cascade: Desnutrin/ATGL initiates lipolysis by hydrolyzing a FA from TAG to produce DAG that is subsequently hydrolyzed by HSL to generate a second FA and monoacylglycerol (MAG). MAG lipase, then hydrolyzes MAG to yield the final FA and glycerol (Fig.1).

Together HSL and desnutrin/ATGL are responsible for over 95% of TAG hydrolase activity in murine WAT *in vitro* [24]. Desnutrin/ATGL null mice do not efficiently mobilize TAG stores and have massive TAG accumulation in multiple tissues, most notably the heart, causing cardiac failure and premature death [25]. The adipose-specific role of desnutrin/ATGL is therefore unclear in these mice. However, recent findings in transgenic mice overexpressing desnutrin in adipose tissue have provided further insight into the adipose-specific role of desnutrin/ATGL [26]. Interestingly, while overexpression of desnutrin/ATGL in adipose tissue increases lipolysis, it does not increase circulating FA levels. Overexpression of desnutrin/ATGL, however, promotes FA utilization within WAT, which is evidenced by increased cycling between DAG and TAG, increased expression of genes involved in FA oxidation and thermogenesis, and higher FA oxidation in WAT. As a result, desnutrin/ATGL mice have elevated energy expenditure and body temperatures, and are resistant to diet-induced obesity [26].

REGULATION OF LIPOLYSIS

Regulation of lipolysis that presumably occurs at the surface of lipid droplets is under tight hormonal regulation. During fasting, catecholamines by binding to Gα_s-coupled β-adernergic receptors activate adenylate cyclase, which in turn increases cAMP levels activating protein kinase A (PKA)[1]. PKA phosphorylates HSL, causing it to translocate from the cytosol to its site of action on the lipid droplet. PKA also phosphorylates the lipid droplet associated protein, perilipin, translocating it away from the lipid droplet, exposing a greater surface to hydrolytic attack by lipases [7,27]. Glucocorticoids, which are elevated during fasting, also upregulate desnutrin/ATGL transcription[17]. During the fed state, insulin by binding to its receptor in adipose tissue initiates a cascade of signaling events that inhibit lipolysis. The anti-lipolytic effect of insulin is mediated primarily through phosphorylation/activation of phosphodiesterase 3B, which decreases cAMP and thus PKA activity, causing reduced HSL/perilipin

phosphorylation, and decreased lipolysis [1] (Fig.1). Other signaling pathways also regulate lipolysis including regulation by cytokines, growth hormones, AMP-activated protein kinase, nicotinic acid, *etc*. Additionally, regulation of lipolysis by naturietic peptides through a cGMP dependent protein kinase (PKG) has been shown to also exist in humans. However, further investigations are required to establish the relative importance of these pathways in regulating lipolysis [28-34].

While the classic model of endocrine regulation of lipolysis by catecholamines and insulin has been extensively studied, the local regulation of lipolysis in adipose tissue by autocrine/paracrine factors is not well understood. Adipocytes secrete several factors that can regulate lipolysis locally, such as TNF-α which stimulates lipolysis [1,35-37]. Depending on the concentration and species tested, prostaglandins have also been shown to inhibit, stimulate, or have no effect on lipolysis [1]. Recently, however, identification of adipose-specific phospholipase A_2 (AdPLA) has revealed a surprisingly important and dominant role for adipocyte-derived PGE_2 in the autocrine/paracrine regulation of lipolysis [38,39]. AdPLA is a membrane-associated, calcium-dependent PLA_2, that represents a new group of PLA_2s, group XVI [39]. AdPLA is the major PLA in adipose tissue and is highly expressed only in adipocytes [39]. As a PLA_2, AdPLA catalyzes the release of fatty acids from the sn-2 position of phospholipids that is typically enriched in arachidonic acid, providing substrate for the initial, rate-limiting step in the synthesis of eicosanoids. In adipose tissue, PGE_2 is the predominant prostaglandin produced, and loss of AdPLA, in AdPLA null mice, causes a >85% fall in PGE_2 levels in WAT. PGE_2 has 4 cognate receptors (EP1, EP2, EP3, and EP4), although $G\alpha_i$-coupled EP3 is expressed at >10-fold higher levels than the other EP receptors in WAT [38]. A fall in PGE_2 levels induced by loss of AdPLA, therefore, causes a decreased EP3 signaling resulting in loss of inhibition of adenylate cyclase activity. This, in turn, elevates cAMP levels, activating lipolysis through PKA-mediated phosphorylation of HS (Fig.1). AdPLA is induced during feeding and by insulin, suggesting that autocrine/paracrine regulation by PGE_2 through AdPLA is an integral part of the coordinated suppression of lipolysis that occurs in response to anabolic stimuli [38]. The physiological importance of AdPLA/ PGE_2 in WAT is highlighted by the unrestrained adipocyte lipolysis and extremely lean phenotype of AdPLA null mice [38]. Importantly, these observations raise the notion that regulation of adipocyte lipolysis may alter FA metabolism and energy expenditure and thus be a critical factor in the development of obesity.

ENERGY METABOLISM AND FATTY ACID UTILIZATION IN WAT

AdPLA null mice exhibit unrestrained lipolysis and are resistant both diet-induced and genetic obesity induced by leptin deficiency [38]. Notably, similar to desnutrin/ATGL transgenic mice, despite drastically increased WAT lipolysis, serum FA levels are not elevated in AdPLA null mice. Two main factors appear to have contributed to this phenomenon. First, since WAT mass is substantially reduced, net liberation of FA from WAT is likely lower than would be expected from these mice with elevated lipolytic rates. Second, increased lipolysis in WAT, accompanied by increased energy expenditure, suggests increased oxidation of fatty acids. However, hepatic and skeletal muscle FA oxidation are not increased in these mice. Instead, similar to desnutrin/ATGL transgenic mice, there is a substantial upregulation of genes encoding proteins involved in oxidation and thermogenesis in WAT such as peroxisome proliferator-activated

receptor delta (PPARδ) and uncoupling protein 1 (UCP-1). Moreover, FA oxidation in adipocytes is, in fact, significantly higher. In this regard, several other mouse models including perilipin null mice and FSP27 null mice have been reported to be lean with elevated lipolysis, no change in serum FA levels, and increased FA oxidation in WAT [10,40-43]. Although FA oxidation has not been considered to be a major metabolic pathway in adipocytes, these findings discussed above demonstrate that increased adipocyte FA oxidation may play a significant role in energy metabolism and adiposity [36]. Furthermore, higher UCP-1 expression in WAT is a striking effect observed in models of increased lipolysis [26,38]. In addition, several recently generated mouse models including corepressor receptor interacting protein 140 (RIP 140) null mice, translation initiation factor elF4E null mice, as well as adipose-specific knockout mice of an essential component of mammalian TOR complex 1 (mTORC1), *raptor*, all exhibit higher UCP-1 expression in WAT resulting in an enhanced metabolic rate and leanness, evidence that increased mitochondrial uncoupling in WAT can protect against obesity [44,50]. In this regard, overexpression of UCP-1 in WAT of mice has previously been shown to increase mitochondrial respiratory uncoupling specifically in WAT, resulting in a drastically leaner phenotype [51-53]. Taken together, these findings suggest that increased lipolysis may cause a shift within adipocytes towards increased FA utilization and energy expenditure resulting in resistance to obesity.

INSULIN RESISTANCE IN ADIPOSE TISSUE

The effects of increasing lipolysis in WAT on whole body insulin sensitivity still remain unclear. It is presumed that elevated lipolysis in WAT increases circulating FA levels and promotes insulin resistance. However, as discussed above, several recent mouse models with elevated lipolysis have shown that increasing lipolysis in WAT promotes energy dissipation and FA oxidation in WAT and does not necessarily increase circulating FA levels. Notably, these mouse models all have higher FA oxidation in WAT with elevated lipolysis, but have varying phenotypes in regards to insulin resistance. Desnutrin/ATGL transgenic mice and FSP27-null mice have improved insulin sensitivity while AdPLA null mice and perilipin null mice are insulin resistant [10,26,38,40]. The differences in these models can be partially explained by differences in TAG storage capacity of WAT. Notably, glucose uptake in WAT of AdPLA null mice was actually higher on a per gram basis compared to wild type mice, however, since the total mass of adipose tissue was drastically reduced, total glucose uptake by adipose tissue was lower than in wildtype mice, highlighting the importance of an appropriate amount of WAT in maintaining glycemic control [38]. By sequestering FA in the form of TAG, adipose tissue is thought to protect against insulin resistance. Moreover, when FAs are generated at a rate that exceeds the oxidative capacity of adipocytes, this can result in the deposition of FAs in other organs and may promote insulin resistance, as seen in lipodystrophy models. Therefore, the total mass as well as the oxidative capacity of WAT could contribute to insulin resistance. In this regard, the relative contribution of WAT to whole body insulin-stimulated glucose uptake is controversial. While WAT has been shown to account for less than 10% of whole-body glucose uptake in mice, adipose tissue specific ablation of Glut4 results in impaired glucose homeostasis indicating an importance for adipose tissue in glucose homeostasis [54]. However, adipose tissue specific ablation of the insulin receptor causes selective insulin resistance in only adipose tissue but does not

impair whole-body glucose metabolism [55]. Secretion of adipokines, macrophage infiltration, as well as other unknown factors, may contribute to the different phenotypes in these models with altered insulin sensitivity [56-58]. However, it is clear that increased lipolysis resulting in elevated FA utilization within adipocytes can be a factor affecting insulin sensitivity.

CONCLUSION

Recently, many exciting advances have been made in understanding lipolysis and FA utilization in adipose tissue. Identification/characterization of the TAG hydrolase, desnutrin/ATGL has firmly established the lipolytic cascade. While the endocrine regulation of lipolysis by catecholamines and insulin has been extensively studied, the local regulation of lipolysis in adipose tissue by autocrine/paracrine may also be critical. Recent identification of AdPLA has revealed a new autocrine/paracrine regulation of lipolysis in adipose tissue. By controlling PGE_2 levels, AdPLA dominantly inhibits lipolysis and plays a critical role in the development of obesity. Moreover, recent findings also demonstrate that, surprisingly, increasing lipolyisis in adipose tissue does not necessarily increase serum FA levels, which are usually correlated with insulin resistance. Rather, it appears that increasing lipolysis in adipose tissue causes a shift within adipocytes towards increased FA utilization and energy expenditure and, thus, protect against obesity.

Important questions still remain. Increasing lipolysis in WAT promotes FA utilization in WAT. Conversely, what are the metabolic consequences when lipolysis is decreased in WAT? How does increasing lipolysis promotes FA oxidation in adipose tissue; do FAs resulting from lipolysis act as ligands for peroxisome proliferators-activated receptors (PPARs) or HNF4 and promote expression of genes in oxidative metabolism [59,60]? Can increasing lipolysis in human WAT prevent obesity without causing significant adverse effects on other organs or on insulin sensitivity? What is the pathological syndrome of humans with single nucleotide polymorphisms detected in genes encoding for proteins involved in lipolysis, such as the AdPLA (PLA2G16) gene? Answers to these questions will help to develop strategies to target lipolysis as a treatment for obesity and its related pathologies.

REFERENCES

1. Jaworski, K., *et al.* (2007) Regulation of triglyceride metabolism. IV. Hormonal regulation of lipolysis in adipose tissue. *Am J Physiol Gastrointest Liver Physiol* 293, G1-4
2. Duncan, R.E., *et al.* (2007) Regulation of lipolysis in adipocytes. *Annu Rev Nutr* 27, 79-101
3. Ahmadian, M., *et al.* (2007) Triacylglycerol metabolism in adipose tissue. *Future Lipidol* 2, 229-237
4. Martin, S., and Parton, R.G. (2006) Lipid droplets: a unified view of a dynamic organelle. *Nat Rev Mol Cell Biol* 7, 373-378
5. Wolins, N.E., *et al.* (2001) TIP47 associates with lipid droplets. *J Biol Chem* 276, 5101-5108
6. Brasaemle, D.L., *et al.* (1997) Adipose differentiation-related protein is an ubiquitously expressed lipid storage droplet-associated protein. *J Lipid Res* 38, 2249-2263
7. Brasaemle, D.L. (2007) Thematic review series: adipocyte biology. The perilipin family of structural lipid droplet proteins: stabilization of lipid droplets and control of lipolysis. *J Lipid Res* 48, 2547-2559
8. Brasaemle, D.L., *et al.* (2004) Proteomic analysis of proteins associated with lipid droplets of basal and lipolytically stimulated 3T3-L1 adipocytes. *J Biol Chem* 279, 46835-46842
9. Guo, Y., *et al.* (2008) Functional genomic screen reveals genes involved in lipid-droplet formation and utilization. *Nature* 453, 657-661
10. Nishino, N., *et al.* (2008) FSP27 contributes to efficient energy storage in murine white adipocytes by promoting the formation of unilocular lipid droplets. *J Clin Invest* 118, 2808-2821
11. Cohen, A.W., *et al.* (2004) Role of caveolin-1 in the modulation of lipolysis and lipid droplet formation. *Diabetes* 53, 1261-1270
12. Fujimoto, T., *et al.* (2001) Caveolin-2 is targeted to lipid droplets, a new "membrane domain" in the cell. *J Cell Biol* 152, 1079-1085
13. Pol, A., *et al.* (2004) Dynamic and regulated association of caveolin with lipid bodies: modulation of lipid body motility and function by a dominant negative mutant. *Mol Biol Cell* 15, 99-110
14. Ortegren, U., *et al.* (2007) A new role for caveolae as metabolic platforms. *Trends Endocrinol Metab* 18, 344-349
15. Wolins, N.E., *et al.* (2006) A proposed model of fat packaging by exchangeable lipid droplet proteins. *FEBS Lett* 580, 5484-5491
16. Zimmermann, R., *et al.* (2004) Fat mobilization in adipose tissue is promoted by adipose triglyceride lipase. *Science* 306, 1383-1386
17. Villena, J.A., *et al.* (2004) Desnutrin, an adipocyte gene encoding a novel patatin domain-containing protein, is induced by fasting and glucocorticoids: ectopic expression of desnutrin increases triglyceride hydrolysis. *J Biol Chem* 279, 47066-47075
18. Jenkins, C.M., *et al.* (2004) Identification, cloning, expression, and purification of three novel human calcium-independent phospholipase A2 family members

possessing triacylglycerol lipase and acylglycerol transacylase activities. *J Biol Chem* 279, 48968-48975
19. Fischer, J.*, et al.* (2007) The gene encoding adipose triglyceride lipase (PNPLA2) is mutated in neutral lipid storage disease with myopathy. *Nat Genet* 39, 28-30
20. Gronke, S.*, et al.* (2005) Brummer lipase is an evolutionary conserved fat storage regulator in Drosophila. *Cell Metab* 1, 323-330
21. Kurat, C.F.*, et al.* (2006) Obese yeast: triglyceride lipolysis is functionally conserved from mammals to yeast. *J Biol Chem* 281, 491-500
22. Kurat, C.F.*, et al.* (2009) Cdk1/Cdc28-dependent activation of the major triacylglycerol lipase Tgl4 in yeast links lipolysis to cell-cycle progression. *Mol Cell* 33, 53-63
23. Eastmond, P.J. (2006) SUGAR-DEPENDENT1 encodes a patatin domain triacylglycerol lipase that initiates storage oil breakdown in germinating Arabidopsis seeds. *Plant Cell* 18, 665-675
24. Schweiger, M.*, et al.* (2006) Adipose triglyceride lipase and hormone-sensitive lipase are the major enzymes in adipose tissue triacylglycerol catabolism. *J Biol Chem* 281, 40236-40241
25. Haemmerle, G.*, et al.* (2006) Defective lipolysis and altered energy metabolism in mice lacking adipose triglyceride lipase. *Science* 312, 734-737
26. Ahmadian, M.*, et al.* (2009) Adipose overexpression of desnutrin promotes fatty acid use and attenuates diet-induced obesity. *Diabetes* 58, 855-866
27. Granneman, J.G., and Moore, H.P. (2008) Location, location: protein trafficking and lipolysis in adipocytes. *Trends Endocrinol Metab* 19, 3-9
28. Tunaru, S.*, et al.* (2003) PUMA-G and HM74 are receptors for nicotinic acid and mediate its anti-lipolytic effect. *Nat Med* 9, 352-355
29. Birkenfeld, A.L.*, et al.* (2005) Lipid mobilization with physiological atrial natriuretic peptide concentrations in humans. *J Clin Endocrinol Metab* 90, 3622-3628
30. Langin, D. (2006) Adipose tissue lipolysis as a metabolic pathway to define pharmacological strategies against obesity and the metabolic syndrome. *Pharmacol Res* 53, 482-491
31. Arner, P.*, et al.* (2008) FGF21 attenuates lipolysis in human adipocytes - a possible link to improved insulin sensitivity. *FEBS Lett* 582, 1725-1730
32. Daval, M.*, et al.* (2005) Anti-lipolytic action of AMP-activated protein kinase in rodent adipocytes. *J Biol Chem* 280, 25250-25257
33. Taggart, A.K.*, et al.* (2005) (D)-beta-Hydroxybutyrate inhibits adipocyte lipolysis via the nicotinic acid receptor PUMA-G. *J Biol Chem* 280, 26649-26652
34. Lafontan, M.*, et al.* (2008) Control of lipolysis by natriuretic peptides and cyclic GMP. *Trends Endocrinol Metab* 19, 130-137
35. Wang, S.*, et al.* (2008) Lipolysis and the integrated physiology of lipid energy metabolism. *Mol Genet Metab* 95, 117-126
36. Lafontan, M. (2008) Advances in adipose tissue metabolism. *Int J Obes (Lond)* 32 Suppl 7, S39-51
37. Langin, D., and Arner, P. (2006) Importance of TNFalpha and neutral lipases in human adipose tissue lipolysis. *Trends Endocrinol Metab* 17, 314-320

38. Jaworski, K., *et al.* (2009) AdPLA ablation increases lipolysis and prevents obesity induced by high-fat feeding or leptin deficiency. *Nat Med* 15, 159-168
39. Duncan, R.E., *et al.* (2008) Identification and functional characterization of adipose-specific phospholipase A2 (AdPLA). *J Biol Chem* 283, 25428-25436
40. Saha, P.K., *et al.* (2004) Metabolic adaptations in the absence of perilipin: increased beta-oxidation and decreased hepatic glucose production associated with peripheral insulin resistance but normal glucose tolerance in perilipin-null mice. *J Biol Chem* 279, 35150-35158
41. Puri, V., *et al.* (2007) Fat-specific protein 27, a novel lipid droplet protein that enhances triglyceride storage. *J Biol Chem* 282, 34213-34218
42. Martinez-Botas, J., *et al.* (2000) Absence of perilipin results in leanness and reverses obesity in Lepr(db/db) mice. *Nat Genet* 26, 474-479
43. Tansey, J.T., *et al.* (2001) Perilipin ablation results in a lean mouse with aberrant adipocyte lipolysis, enhanced leptin production, and resistance to diet-induced obesity. *Proc Natl Acad Sci U S A* 98, 6494-6499
44. Tiraby, C., and Langin, D. (2003) Conversion from white to brown adipocytes: a strategy for the control of fat mass? *Trends Endocrinol Metab* 14, 439-441
45. Polak, P., *et al.* (2008) Adipose-specific knockout of raptor results in lean mice with enhanced mitochondrial respiration. *Cell Metab* 8, 399-410
46. Christian, M., *et al.* (2006) Metabolic regulation by the nuclear receptor corepressor RIP140. *Trends Endocrinol Metab* 17, 243-250
47. Christian, M., *et al.* (2005) RIP140-targeted repression of gene expression in adipocytes. *Mol Cell Biol* 25, 9383-9391
48. Parker, M.G., *et al.* (2006) The nuclear receptor co-repressor RIP140 controls the expression of metabolic gene networks. *Biochem Soc Trans* 34, 1103-1106
49. Tsukiyama-Kohara, K., *et al.* (2001) Adipose tissue reduction in mice lacking the translational inhibitor 4E-BP1. *Nat Med* 7, 1128-1132
50. Rosen, E.D., and Spiegelman, B.M. (2006) Adipocytes as regulators of energy balance and glucose homeostasis. *Nature* 444, 847-853
51. Kopecky, J., *et al.* (1995) Expression of the mitochondrial uncoupling protein gene from the aP2 gene promoter prevents genetic obesity. *J Clin Invest* 96, 2914-2923
52. Orci, L., *et al.* (2004) Rapid transformation of white adipocytes into fat-oxidizing machines. *PNAS* 101, 2058-2063
53. Yamada, T., *et al.* (2006) Signals from intra-abdominal fat modulate insulin and leptin sensitivity through different mechanisms: neuronal involvement in food-intake regulation. *Cell Metab* 3, 223-229
54. Herman, M.A., and Kahn, B.B. (2006) Glucose transport and sensing in the maintenance of glucose homeostasis and metabolic harmony. *J Clin Invest* 116, 1767-1775
55. Bluher, M., *et al.* (2002) Adipose tissue selective insulin receptor knockout protects against obesity and obesity-related glucose intolerance. *Dev Cell* 3, 25-38
56. Cinti, S., *et al.* (2005) Adipocyte death defines macrophage localization and function in adipose tissue of obese mice and humans. *J Lipid Res* 46, 2347-2355
57. Schenk, S., *et al.* (2008) Insulin sensitivity: modulation by nutrients and inflammation. *J Clin Invest* 118, 2992-3002

58. Guilherme, A.*, et al.* (2008) Adipocyte dysfunctions linking obesity to insulin resistance and type 2 diabetes. *Nat Rev Mol Cell Biol* 9, 367-377
59. Michalik, L.*, et al.* (2006) International Union of Pharmacology. LXI. Peroxisome proliferator-activated receptors. *Pharmacol Rev* 58, 726-741
60. Palanker, L.*, et al.* (2009) Drosophila HNF4 regulates lipid mobilization and beta-oxidation. *Cell Metab* 9, 228-239

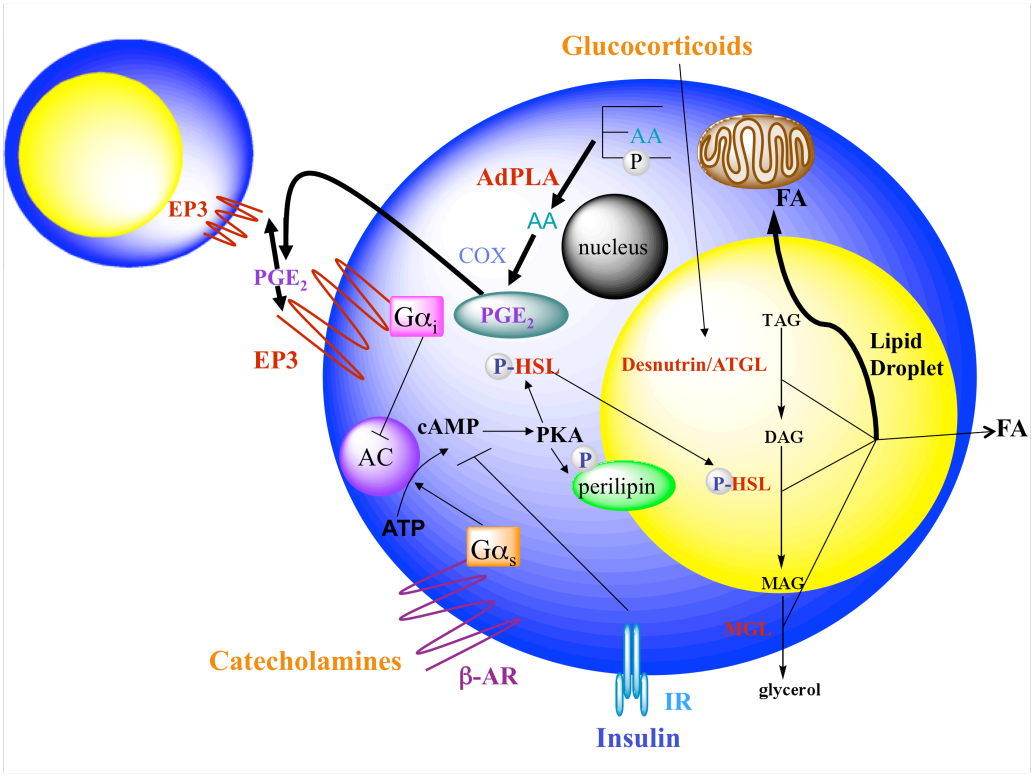

Figure I-3. Regulation of lipolysis in adipocytes. (i) Desnutrin/ATGL performs the initial step of triacylglycerol (TAG) hydrolysis, resulting in diacylglycerol (DAG). (ii) DAG is hydrolyzed by hormone sensitive lipase (HSL) to monoacylglycerol (MAG), which is subsequently hydrolyzed by (iii) MAG lipase to generate glycerol and three FA. (iv) The FA generated during lipolysis can be released into the circulation for use by other organs or re-esterified to TAG. Glycerol 3-phosphate (G-3-P) can be used as a backbone for TAG synthesis. FA released from lipolysis can also be oxidized within the adipocyte. Lipolysis is under tight endocrine regulation. (v) During fasting, catecholamines by binding to Gas-coupled b-adrenergic receptors (b-AR), activate adenylate cyclase (AC) to increase cAMP and thus activate protein kinase A (PKA). PKA phosphorylates HSL, resulting in translocation of HSL from the cytosol to the lipid droplet and increased lipolysis. PKA also phosphorylates the lipid droplet associated protein perilipin. (vi) Additionally, during fasting, glucocorticoids increase the expression of desnutrin/ATGL. (vii) In the fed state, insulin binding to the insulin receptor (IR) results in decreased cAMP levels and decreased lipolysis. Additionally, during the fed state, insulin increases the expression of adipose-specific phospholipase A2 (AdPLA). Recent findings revealed that lipolysis is dominantly regulated by prostaglandin E2 (PGE2) through AdPLA. (viii) AdPLA hydrolyzes the sn-2 position of phospholipids to generate arachidonic acid (AA), which via cyclooxygenase (COX) produces PGE2. (ix) PGE2 secreted by adipocytes can act locally by binding to the Gai-coupled EP3 present in adipocytes, resulting in inhibition of AC and decreased lipolysis.

Chapter II: Adipose Overexpression of Desnutrin Promotes Fatty Acid Use and Attenuates Diet-Induced Obesity

ABSRACT
To investigate the role of desnutrin in adipose tissue triacylglycerol (TAG) and fatty acid metabolism,we generated transgenic mice overexpressing desnutrin (also called adipose triglyceride lipase [ATGL]) in adipocytes (aP2-desnutrin) and also performed adenoviral-mediated overexpression of desnutrin in 3T3-L1CARΔ1 adipocytes. aP2-desnutrin mice were leaner with decreased adipose tissue TAG content and smaller adipocyte size. Overexpression of desnutrin increased lipolysis but did not result in increased serum nonesterified fatty acid levels or ectopic TAG storage. We found increased cycling between diacylglycerol (DAG) and TAG and increased fatty acid oxidation in adipocytes from these mice, as well as improved insulin sensitivity.We show that by increasing lipolysis, desnutrin overexpression causes reduced adipocyte TAG content and attenuation of diet-induced obesity. Desnutrin-mediated lipolysis promotes fatty acid oxidation and re-esterification within adipocytes.

INTRODUCTION

In mammals, white adipose tissue (WAT) is the primary energy storage depot, accumulating fuel reserves in the form of triacylglycerol (TAG) during times of energy excess (1). However, unlike TAG synthesis that also occurs at high levels in liver for VLDL production, lipolysis for the provision of fatty acids (FAs) as an energy source for use by other organs is unique to adipocytes. The release of FA from TAG proceeds in an orderly and regulated manner. TAG is hydrolyzed first to form diacylglycerol (DAG) and then monoacylglycerol(MAG) that is hydrolyzed to liberate the final FA and glycerol (1–4).

We and others have recently identified a TAG lipase that belongs to the patatin-like domain-containing family of proteins (5–7). We named this enzyme desnutrin (also called PNPLA2, adipose triglyceride lipase, TTS2.2, and iPLA2) because it is induced during a low nutritional state in mice (i.e., fasting) and it belongs to the same patatin-like domain-containing family as another nutritionally regulated protein, adiponutrin. Desnutrin is highly expressed in adipose tissue but is also found at low levels in other tissues (6). Understanding the role of desnutrin in fat metabolism, specifically in adipose tissue, is of critical importance, because dysregulated adipocyte TAG lipolysis may cause elevated circulating FA concentrations that are associated with severe metabolic derangements, including the development of insulin resistance and type 2 diabetes (8). Central to this understanding is the question of the metabolic fate of FAs derived from desnutrin-mediated TAG lipolysis, particularly when the release of these FAs is dissociated from the energy requirements of other organs.

FAs liberated from adipocyte TAG can enter several possible metabolic pathways. Primarily, they are released to the systemic circulation, providing oxidative substrates for use by other tissues during energy deprivation and therefore maintaining whole-body energy homeostasis (1,9). Alternatively, however, FAs hydrolyzed from TAG can also be used directly within the adipocyte in reesterification reactions producing TAG or other lipid species or in oxidative metabolism. FA oxidation occurs in the mitochondria and peroxisomes. Although mitochondrial FA oxidation is normally tightly coupled to ATP synthesis, uncoupling of this process can result in energy wasting and

heat production. Peroxisomal FA oxidation is always poorly coupled, generating heat instead of ATP.

To investigate the adipocyte-specific function of desnutrin and the metabolic fate of FAs released from lipolysis, we generated transgenic mice constitutively overexpressing desnutrin in adipose tissue and also used adenoviralmediated overexpression of desnutrin in differentiated 3T3-L1CAR1 adipocytes. We report that desnutrin-mediated lipolysis attenuates diet-induced obesity and, surprisingly, does not result in ectopic TAG storage or increased serum nonesterified FA (NEFA) levels. Rather, desnutrin overexpression increases apparent cycling between TAG and DAG (and/or MAG) in adipose tissue and promotes FA oxidation specifically within adipocytes. As a result, aP2-desnutrin mice are leaner and resistant to diet-induced obesity with improved insulin sensitivity.

RESEARCH DESIGN AND METHODS

Transgene construct and generation and maintenance of transgenic mice. The 1.7 kb coding sequence for hemagluttinin (HA)-tagged desnutrin, including a bovine growth hormone polyadenylation sequence, was subcloned under control of the 5.4-kb adipocyte FA-binding protein (aP2) promoter and microinjected into the pronucleus of fertilized eggs of C57BL/6 X CBA mice. aP2-desnutrin mice and their wild-type littermates were fed a high-fat diet (HFD) (45 kcal% fat, 35 kcal% carbohydrate, and 20 kcal% protein; Research Diets) ad libitum at weaning. Experiments were performed in 20-week-old transgenic mice and compared with sex-matched littermates.

RNA extraction and real-time RT-PCR. Total RNA was prepared using Trizol Reagent (Invitrogen), and cDNA was synthesized from 2.5 g of total RNA by Superscript II reverse transcriptase (Invitrogen). Desnutrin-HA transgene expression was determined by RT-PCR (forward primer: 5-CTACTGAACCAACCCAACCCT-3; reverse primer: 5-TTAGTAATCTGGAACATCGTATGGGTA-3). Tissue gene expression was determined by RT-qPCR performed with an ABI PRISM 7700 sequence fast detection system (Applied Biosystems) and was quantified by measuring the threshold cycle normalized to glyceraldehyde-3-phosphate dehydrogenase (GAPDH) or -actin and then expressed relative to wild-type controls.

Immunoblotting. Total lysates were subjected to 8% SDS-PAGE, transferred to PVDF membranes, and probed with rabbit anti-desnutrin antibody or rabbit anti-GAPDH antibody followed by peroxidase conjugated goat anti-rabbit antibody.Blots were visualized using enhanced chemiluminescence (PerkinElmer),and images were captured using a Kodak Image Station 4000MM.

Adipocyte size determination. Gonadal fat samples were fixed in 10% buffered formalin, embedded in paraffin, cut into 6-m-thick sections, and stained with hematoxylin and eosin. Five separate fields from four different mice were quantified using a LEICA DM IRB microscope.

Ex vivo lipolysis. Gonadal fat pads from overnight-fasted mice were cut into 50-mg samples and incubated at 37°C in 500l of Krebs-Ringer medium buffered with bicarbonate plus HEPES containing 2% FA-free BSA and 0.1% glucose with or without 0.5 mmol/l dibutyryl cAMP (Sigma). FA and glycerol release were measured in aliquots from incubation buffer using the NEFA C Kit (Wako) and Free Glycerol Reagent (Sigma), respectively.
In vitro triolein lipase assay. TAG hydrolase activity of WAT extracts was performed essentially as described (10). Briefly, WAT was homogenized in lysis buffer (0.25 mol/l sucrose, 1 mmol/l EDTA, pH 7.0, 1 mmol/l DTT) and then centrifuged at 4°C for 20 min at 10,000g. Triolein lipase activity was assayed in 100g of supernatants. The reaction was initiated by addition of 100 l of substrate that was prepared by sonicating 100 mmol/l potassium phosphate, 2 mmol/l EDTA, pH 7.4, with 200 mol/l [3H]triolein (40,000 cpm/reaction), 25 mol/l lecithin, 10 mol/l taurocholate, 1% BSA, and 1 mmol/l DTT. Reaction mixtures were incubated at 37°C for 30 min, terminated by addition of 3.25 ml of methanol/chloroform/heptane (10:9:7), and extracted with 1 ml of 0.1 mol/l potassium carbonate and 0.1 mol/l boric acid, pH 10.5. Liberated FAs were quantified in 700 l of the upper phase by liquid scintillation counting.

Tissue analysis. Total neutral lipids were extracted by the method of Folch (11). Lipids were solubilized in 1% Triton X-100, and TAG was measured using Infinity Reagent (Thermo). Fat-free mass was estimated by subtracting total adipose tissue mass from body weights.

Cell culture. 3T3-CAR preadipocytes, provided by Dr. D. Orlicky (University of Colorado), were maintained and differentiated as previously described (12). These cells stably express the coxsackievirus and adenovirus receptor allowing for 100-fold greater transduction efficiency with adenovirus (13) but are otherwise indistinguishable from the parental 3T3-L1 cell line (14). For radiolipid studies, day 8 differentiated 3T3-CAR adipocytes grown in 12-well plates were pulse-labeled for 4 h with 0.05 Ci per well of [U-14C]palmitic acid, washed with cold media, and infected at the start of the chase period at an MOI of 100 with adenovirus expressing green fluorescent protein (GFP) or GFP-desnutrin. 14C-FA was measured in the medium 30 h later by liquid scintillation. For studies on endogenous TAG content and lipolysis, adipocytes were infected as described at time point 0. Three days later, medium was changed to serum-free medium, with or without dibutyryl cAMP, 6 h before measurement of FA and glycerol release. For imaging studies, 3T3-L1CAR adipocytes grown and differentiated on coverslips were stained with Nile Red and DAPI to visualize neutral lipids and nuclei, respectively, and were fixed for image capture using a Zeiss Axiophot LSM 510Meta confocal microscope. Total lipids were extracted from 3T3-L1CAR adipocytes by the method of Bligh and Dyer (15) and resolved by TLC in hexane:diethylether:acetic acid (80:20:2). For determination of endogenous lipids, the band corresponding to

TAG was scraped and solubilized in 1% Triton X-100 and measured as described. Radiolabeled TAG was scraped and quantified by liquid scintillation counting.

Indirect calorimetry and body temperature. Oxygen consumption (VO2) was measured using the Comprehensive Laboratory Animal Monitoring System (Columbus Instruments). Data were normalized to body weights. Body temperatures were assessed in 25-week-old male mice using a RET-3 rectal probe for mice (Physitemp).

Hyperinsulinemic-euglycemic clamp. We implanted jugular venous catheters 7 days before the study. After an overnight fast, we infused [3-3H]glucose (Perkin Elmer) at a rate of 0.05 Ci min1 for 2 h to assess basal glucose turnover followed by the hyperinsulinemic-euglycemic clamp for 140 min with a primed/continuous infusion of human insulin (154 pmol/kg prime [21 mU/kg]) over 3 min followed by 17 pmol kg1 min–1 (3 mU /kg /min) infusion (Novo Nordisk, Princeton, NJ), a continuous infusion of [3-3H]glucose (0.1 Ci/min), and a variable infusion of 20% dextrose to maintain euglycemia (100–120 mg/dl). We obtained plasma samples from the tail and measured tissue-specific glucose uptake after injection of a bolus of 10 Ci of 2-deoxy-D-[1-^{14}C]glucose (Perkin Elmer) at 85 min (16). We analyzed our results as previously described (17).

$^{2}H_2O$ labeling and GCMS analysis of TAG-glycerol and TAG-FA. The heavy water ($^{2}H_2O$) labeling protocol and GCMS analyses of TAG-glycerol and TAG-FA from adipose tissue have been described previously in detail (18). Mice were administered $^{2}H_2O$ in drinking water starting at 20 weeks of age for a 2-week period after which lipids were extracted from gonadal fat pads by the method of Folch (11) for subsequent analysis.

Calculation of all-source TAG-glycerol synthesis. Fractional TAG-glycerol synthesized from -glycerol phosphate during the period of $^{2}H_2O$ administration was measured as described (18):

$$f\text{TAG} = \text{EM1}_{\text{TAG-glycerol}}/\text{A1}_{\text{TAG-glycerol}}.$$

EM1 is the measured excess mass isotopomer abundance for M1-glycerol at time t and A1 is the asymptotic mass isotopomer abundance for M1-glycerol, assuming that four of five C-H bonds of glycerol phosphate are replaced by H-atoms from tissue water (18):

Net lipolysis was estimated from fTAG synthesis and adipose mass as follows:

*f*TAG X (adipose mass/labeling time) –(change in adipose mass/labeling time)/fat pad mass.

Values with net lipolysis equivalent to zero were excluded from analysis.

Calculation of de novo lipogenesis. Fractional contributions from de novo lipogenesis (DNL) are calculated using a combinatorial model as previously described (18):fDNL EM1FA/A1FAwhere f DNL represents the fraction of total TAG-palmitate in the depot that derived from DNL during the labeling period. The fraction of newly synthesized TAG-palmitate that came from DNL is also calculated by correcting the measured fractional contribution from DNL (fDNL) for the degree of replacement of adipose TAG during the labeling period:DNL contribution to newly synthesized TAG fDNL/fTAG

FA oxidation. Gonadal fat pads were digested for 1 h at 37°C with collagenase in Krebs-Ringer medium buffered with bicarbonate plus HEPES supplemented with 3 mmol/l glucose and 1% BSA, filtered through nylon mesh, and centrifuged, and adipocytes were collected from the upper phase. FA oxidation was determined by measuring $^{14}CO2$ production from [^{14}C]palmitic acid (0.2 Ci/ml) after incubation for 1 h at 37°C with gentle shaking. The buffer was acidified with 0.25 ml of H_2SO_4 (5N) and maintained sealed at 37°C for an additional 30 min. Trapped radioactivity was quantified by liquid scintillation.

Serum parameters. Fasting serum triglycerides and FAs were analyzed in the morning after an overnight fast with Infinity Triglyceride reagent (Thermo Trace) and NEFA C kit (Wako), respectively. Serum insulin, leptin, and adiponectin levels were determined using ELISA kits (Crystal Chem and B-Bridge).

Statistical Analysis. The results are expressed as means SEM. Statistically significant differences between two groups were assessed by Student's t test. Differences between multiple groups were assessed by one-way ANOVA with Bonferroni's post hoc test.

RESULTS

Desnutrin overexpression in adipose tissue attenuates diet-induced obesity

We generated transgenic mice overexpressing HA-tagged desnutrin under control of the aP2 promoter to investigate the adipocyte-specific role of desnutrin. Results reported here are a comparison between mice from the founder line with the highest desnutrin transgene expression and their littermates. Similar results were obtained from an additional founder line (data not shown). RT-PCR analysis indicated that expression of the transgene was limited to WAT and brown adipose tissue (BAT) and was not detected in any other tissues examined (Fig. 1A). Desnutrin was expressed 4.8-fold and 3.4-fold above endogenous levels in gonadal WAT and BAT, respectively, as analyzed by RT-qPCR (Fig.1B). We also detected a 3.5-fold increase in expression of CGI-58, a putative activator of desnutrin, in WAT of aP2-desnutrin mice (Fig. 1C). Using a

desnutrin-specific antibody, we detected a band for desnutrin-HA protein in WAT and BAT of aP2-desnutrin mice but not in wild-type mice (Fig. 1D). We quantified desnutrin protein levels and found that although there was no difference in endogenous protein levels in both WAT and BAT in wild-type and aP2-desnutrin mice, total desnutrin levels (endogenous transgene) were increased by approximately twofold in transgenic mice (Fig. 1D). To confirm the presence of a functional enzyme, we assayed homogenates of WAT from aP2-desnutrin mice and found a 40% increase in total triolein lipase activity (Fig. 1E). This represents a substantial increase in total triglyceride lipase activity over controls, because baseline TAG lipase activity is already considerable in WAT extracts as a result of the presence of additional triglyceride lipases, including hormone-sensitive lipase (1).

aP2-desnutrin mice and wild-type littermates were fed a standard chow diet or an HFD at weaning. On a chow diet, there was no difference in body weight (Fig. 2B, inset), fat pad weight, or organ weight between wild-type and aP2-desnutrin mice at 20 weeks of age (Fig. 2C, left panels).However, on an HFD, aP2-desnutrin mice were leaner(Fig. 2A, upper panel) and gained weight at a slower rate than wild-type littermates (Fig. 2B) despite similar food intakes (Fig. 2A, lower panel). Although there was no difference in kidney, lung, or heart weights, liver weights in aP2-desnutrin mice were 15% lower compared with wildtype (Fig. 2D, left panel). Inguinal, gonadal, renal, and subcutaneous depots weighed 56, 59, 47, and 52% less, respectively, compared with depots from wild-type littermates(Fig. 2D, right panel). BAT depots from aP2-desnutrin mice weighed 20% less than depots from wildtype mice. We conclude that aP2-desnutrin mice are protected from HFD-induced obesity. To understand the mechanism underlying desnutrin-mediated protection from diet-induced obesity, we compared HFD-fed aP2-desnutrin mice and their wild-type littermates.

Decreased adipose tissue mass can result from a reduction in adipocyte size and/or a reduction in adipocyte number due to impaired differentiation (9,19 –21). The expression level of adipocyte marker genes, including CCAAT/enhancer binding protein (C/EBP), preadipocyte factor (Pref)-1, peroxisome proliferator–activated receptor (PPAR)-, and aP2/a-FABP (adipocyte FA binding protein), was similar in aP2-desnutrin mice and their wild-type littermates on an HFD, suggesting normal adipocyte differentiation (Fig. 2E). Histological analysis, however, revealed a greater frequency of smaller adipocytes in gonadal fat pads from aP2-desnutrin mice when compared with wild-type littermates (Fig. 2F). We found a 55% reduction in adipose tissue TAG content in aP2-desnutrin mice relative to wild-type littermates (Fig. 3A), indicating that decreased adipocyte size and TAG content explains protection from diet-induced obesity. Because the effect of desnutrin on TAG stores has been shown only in nonadipocytes, which do not contain large lipid droplets (22), we also performed adenovirus-mediated overexpression of GFP-desnutrin in adipocytes (Fig. 3B). As previously shown (7), desnutrin localized strongly to lipid droplets in contrast to control GFP (Fig. 3C). Overexpression of desnutrin decreased endogenous TAG levels by 23% under basal conditions and by 25% after 6 h of stimulation with dibutyryl cAMP (Fig. 3D). Similarly, radiolabeled TAG was depleted more rapidly in cells overexpressing desnutrin-GFP than in cells expressing control GFP (Fig. 3E). Taken together, these results indicate that desnutrin overexpression results in smaller adipocytes with lower TAG content but does not affect differentiation.

Desnutrin overexpression increases lipolysis and apparent cycling between TAG and DAG

We next measured in vivo TAG metabolism over a 2-week period using a recently developed heavy water labeling technique (18,23). The fractional contribution of TAG synthesis to adipose tissue TAG (fTAG) was not different (Fig. 4A), although the net in vivo lipolytic rate, calculated from the absolute rate of new TAG synthesis and the change in adipose mass, was significantly higher per gram of adipose tissue in aP2-desnutrin mice compared with wild-type littermates (Fig. 4B). Interestingly, there was an increase (P 0.07) in the fractional contribution from DNL (fDNL) to adipose tissue palmitate in aP2-desnutrin mice compared with wild-type littermates (Fig. 4C). The ratio of de novo synthesized palmitate to new TAG synthesis (Fig.4D), which represents the contribution from DNL to newly formed adipose TAG-palmitate (18,24), was greater than unity in aP2-desnutrin mice (1.10 0.25) but less than unity in wild-type littermates (0.67 0.12). This change in the ratio of DNL to TAG synthesis, particularly to values greater than 100%, in the absence of an increase in absolute DNL (data not shown), likely reflects recycling between TAG and DAG and/or MAG. This also suggests that re-esterification of DAG/MAG occurs predominantly with FA originating from DNL rather than from preexisting unlabeled FA. In support of our findings of increased re-esterification, we found no change in WAT DAG levels between wild-type and aP2-desnutrin mice (3.18+/- 0.32g/mg versus 3.26+/- 0.34 g/mg, respectively). These results are consistent with increased TAG lipolysis in aP2-desnutrin mice, beyond that which was apparent from measures of the complete hydrolysis of TAG to free glycerol.

In agreement with our findings from in vivo lipolysis, we found that glycerol release from adipocytes isolated from fed aP2-desnutrin mice was significantly higher under basal and adenosine deaminase or isoproterenol-stimulated conditions (Fig. 5A, left panel). FA release was also significantly higher from adenosine deaminase or isoproterenol-treated adipocytes from aP2-desnutrin mice (Fig. 5A, right panel). We also found that FA release from explants of gonadal WAT incubated in the presence or absence of dibutyryl cAMP was 55% higher under basal conditions and 42% higher under dibutyryl cAMP-stimulated conditions after 4 h (Fig. 5B). Under basal conditions, glycerol release tended to be higher in explants from aP2-desnutrin mice compared with wild-type mice, although this difference did not reach significance (Fig. 5C).Under stimulated conditions, glycerol release was signifi (65% higher) and 4 h (95% higher). Cultured 3T3-L1 adipocytes overexpressing desnutrin-GFP had a significantly increased release of FA (Fig. 5D) as well as glycerol (Fig. 5E), and the proportionate increase in the release of glycerol was greater under dibutyryl cAMP-stimulated conditions than under basal conditions (28% versus 12% higher, respectively).

aP2-desnutrin mice have improved insulin sensitivity

Because aP2-desnutrin mice have increased lipolysis and are protected from diet-induced obesity, we postulated there may be alterations in insulin sensitivity. To investigate insulin action on whole-body and tissue-specific glucose metabolism, we performed hyperinsulinemic–euglycemic clamps with radioisotope-labeled glucose infusion in HFD-fed wild-type and aP2-desnutrin mice. The steady-state glucose infusion rate during the clamps was higher in aP2-desnutrin mice, reflecting increased insulin responsiveness (Fig. 6A–B), and whole-body glucose uptake was increased by 20% (P

0.08) (Fig. 6C). Skeletal muscle 2-deoxyglucose uptake was 38% higher in aP2-desnutrin versus wild-type mice (Fig. 6D), whereas adiposetissue glucose uptake did not differ (Fig. 6E). The ability of insulin to suppress hepatic glucose production during the clamp was improved by 36% in aP2-desnutrinmice (Fig. 6F). Corresponding to increased hepatic insulin sensitivity, Oil red O staining of liver sections revealed smaller lipid droplets in aP2-desnutrin mice (Fig. 6G). We examined TAG levels in various nonadipose tissues and found significantly lower TAG levels in the livers of aP2-desnutrin mice and, although not statistically significant, a tendency toward lower TAG levels in other tissues, including skeletal muscle (Fig. 6H). Despite increased lipolysis in aP2-desnutrin mice, we found no significant differences in most serum metabolites measured including NEFA and glycerol as well as TAG, adiponectin, and leptin (wild-type mice 5.77 1.79 ng/ml versus aP2-desnutrin mice 3.73 0.36 ng/ml, n 6) (Table 1), although serum insulin levels were significantly lower in HFD-fed aP2-desnutrin mice (3.44 0.27 ng/ml for wild-type versus 2.38 0.16 ng/ml for aP2-desnutrin, P 0.01).

Desnutrin overexpression increases thermogenesis, energy expenditure, and FA oxidation within adipose tissue

Because aP2-desnutrin mice had decreased adipose tissue mass but an equivalent intake of food and an absence of ectopic TAG storage compared with wild-type mice, we hypothesized that these mice may have increased energy expenditure. Average body temperatures measuredover the course of a day were 0.28°C higher in aP2- desnutrin compared with wild-type mice (Fig. 7A). To investigate the source of the increased thermogenesis, mice were housed in metabolic chambers for 24 h, where oxygen consumption and locomotor activity were assessed. Total oxygen consumption was 30% higher in aP2-desnutrin mice over a 24-h period (Fig. 7B). Activity levels, however, were not different between aP2-desnutrin and wild-type mice (data not shown). Thus, aP2-desnutrin mice have increased energy expenditure without changes in food intake or physical activity.

To further investigate potential mechanisms underlying the increased thermogenesis and oxygen consumption in aP2-desnutrin mice, we examined genes involved in oxidative metabolism. In skeletal muscle and liver, two tissues that play an important role in the use and regulation of energy substrates, there were no significant differences in the expression of acyl CoA oxidase or PPAR between wild-type and aP2-desnutrin mice (Fig. 8C and D). In BAT of aP2 desnutrin mice, uncoupling protein (UCP)-1 was upregulated by 2.9-fold (Fig. 8B). PPARcoactivator (PGC)-1 was also upregulated by 4.2-fold in BAT of aP2-desnutrin mice. However, the significance of the changes in expression of these genes in BAT is unclear because we observed no difference in cold tolerance when mice were housed at an ambient temperature of 4°C (datanot shown). However, there was a significant upregulation in aP2-desnutrin WAT of genes involved in thermogenesis and in both mitochondrial and peroxisomal FA oxidation (Fig. 8A), including UCP-1 (7.1-fold), carnitine palmitoyltransferase (CPT)-1(3.7-fold), PPARα(3.4-fold), PPARδ(2.4-fold), PGC-1(3.3-fold), fatty acyl coA oxidase (AOx)(4.4-fold), phytanoyl-CoA hydroxylase (PhyH) (2.4-fold), and catalase (4.4-fold). When we measured the production of $^{14}CO2$ from [^{14}C]palmitate in isolated adipocytes, we found that it was almost 2.5-fold higher in WAT of aP2-desnutrin mice compared with their wild-type littermates (Fig. 8E), clearly demonstrating

increased FA oxidation within adipocytes from aP2-desnutrin mice. Therefore, in agreement with our observation that serum NEFA is unchanged in aP2-desnutrin mice, we report that desnutrin overexpression increases expression of oxidative genes and promotes FA oxidation in adipocytes.

DISCUSSION

Dysregulation of adipocyte lipolysis, resulting in elevated circulating NEFA, is associated with obesity and comorbidities, including the development of type 2 diabetes (8). Understanding the effects of desnutrin overexpression on adipose tissue TAG hydrolysis and TAG stores, as well as subsequent FA metabolism is therefore fundamental to the investigation of obesity and obesity-related diseases. Using transgenic mice constitutively overexpressing desnutrin in adipose tissue as well as adenoviral-mediated overexpression of desnutrin in differentiated 3T3-L1CAR1 adipocytes, we investigated the metabolic fate of FA derived from desnutrin-mediated TAG lipolysis.

Mice lacking desnutrin showed accumulation of TAG in a variety of tissues with a relatively small (approximately twofold) increase in WAT mass and premature mortality with massive TAG accumulation in the heart (25). We show that desnutrin overexpression in adipose tissue of mice attenuated diet-induced obesity by reducing fat pad TAG content and adipocyte size. Desnutrin overexpression in differentiated 3T3-L1CAR1 adipocytes also resulted in accelerated TAG breakdown, causing depletion of TAG stores. Our results from aP2-desnutrin mice are in contrast to results from a previous study in which adipose tissue overexpression of hormone-sensitive lipase did not result in a leaner phenotype in mice fed an HFD (26). New insights into the metabolic fate of FA generated from TAG were provided by the in vivo heavy water labeling study. The net in vivo lipolytic rate over 2 weeks, which represents the complete turnover of TAG to glycerol and FA, was elevated in adipose tissue from aP2-desnutrin mice. Findings were also consistent with increased re-esterification of DAG (and/or MAG) to TAG predominantly with newly synthesized FAs and suggested that although desnutrin overexpression increased the hydrolysis of TAG to DAG, a major fate of that DAG was retention within adipocytes. This finding also suggests that TAG lipolysis to DAG occurred at an even greater rate than that which is apparent from measures of the complete hydrolysis of TAG to free glycerol.

Despite the marked increase in lipolysis in adipose tissue of aP2-desnutrin mice, serum NEFA levels were not increased. FA levels in the blood represent a balance between liberation from adipose tissue and uptake by peripheral tissues, and therefore a number of factors may play a role in regulating serum NEFA concentrations. Net FA liberation is likely lower than expected in aP2-desnutrin mice, because adipose tissue mass is substantially reduced compared with wild-type mice. Increased removal of FA from the bloodstream by other organs may also have contributed, although TAG content was not increased in any tissues measured and was, in fact, significantly decreased in livers of aP2-desnutrin mice. Results from our heavy water labeling study suggest that, at least in part, increased re-esterification may have limited the release of FAs from adipose tissue in vivo. However, because reesterification appeared to involve the incorporation ofnewly synthesized FAs to a greater extent than preexisting fatty acids, and because aP2-desnutrin mice had reduced adipose TAG content, increased loss of the hydrolyzed FA from adipose tissue was also indicated. Although there was no change in oxidative

gene expression in skeletal muscle or liver, there was a substantial upregulation in aP2-desnutrin WAT of genes involved in mitochondrial -oxidation such as CPT-1; in peroxisomal-oxidation such as AOx, PhyH, and catalase; and in thermogenesis such as PPAR, PPAR, and PGC-1. The most striking change was a 7.1-fold upregulation of UCP-1 expression. Measurement of FA oxidation by adipocytes isolated from aP2-desnutrin mice indicated a marked increase compared with their wild-type littermates and confirmed increased use of FAs directly within adipose tissue. Notably, UCP-1 induction results in increased heat production at the expense of ATP synthesis, as does peroxisomal FA -oxidation, and aP2-desnutrin mice had significantly higher body temperatures over the course of the day, corresponding to a significantly higher rate of oxygen consumption. Taken together, our findings indicate that increased thermogenesis resulting from oxidation of hydrolyzed FAs within adipose tissue of aP2-desnutrin mice contributed to the leaner phenotype and, at least in part, to the absence of a rise in serum NEFA in these mice.

Although the present study is the first to demonstrate regulation of FA oxidation after overexpression of a TAG lipase, others have suggested that increased oxidation in adipocytes may contribute to protection against the development of diet-induced obesity (27–29). For example, overexpression of UCP-1 in WAT of mice has been shown to increase respiratory uncoupling specifically in WAT,resulting in a leaner phenotype (27), and hyperleptinemia in rats was found to increase WAT UCP-1 and adipocyte FA oxidation, resulting in dramatic fat loss (28). Perilipin null mice also have elevated adipocyte FA oxidation and a leaner phenotype (27–29). These studies support our findingof leanness in aP2-desnutrin mice that have increased UCP-1 expression and adipocyte FA oxidation.

In association with their leaner phenotype, aP2-desnutrin mice demonstrate improved insulin sensitivity in hyperinsulinemic-euglycemic clamping studies attributable primarily to increased insulin-stimulated skeletal muscle glucose uptake and suppression of hepatic glucose production. Decreased liver TAG content may have contributed to the improved hepatic insulin sensitivity in these mice. Despite abundant evidence of increased lipolysis in aP2-desnutrin mice, circulating NEFA levels were unchanged and therefore cannot be a factor in mediating changes in insulin sensitivity. Adiponectin and leptin levels, which are associated with insulin sensitivity, were also unchanged in these mice. Thus, our aP2-desnutrin mice represent a new model in which a long-term increase in adipocyte lipolysis results in metabolic adaptations, including increased FA oxidation, leanness, and improved insulin sensitivity. In this regard, mice overexpressing UCP-1 in adipose tissue also exhibit leanness and increased adipocyte FA oxidation (27), as well as an unexplained improvement in insulin sensitivity (30). Given the similarities of the two models, it is possible that investigation of yet to be identified factors linking increased energy use in WAT to insulin sensitivity may provide new insight into understanding obesity/diabetes.

In conclusion, we show that, by increasing lipolysis, overexpression of desnutrin in adipose tissue causes reduced adipocyte TAG content and attenuation of diet-induced obesity, at least in part, by promoting FA oxidation and re-esterification within adipocytes. Overexpression of desnutrin in adipocytes also causes improved insulin responsiveness resulting from increased peripheral and hepatic insulin sensitivity that occurs independent of changes in circulating NEFA levels.

REFERENCES

1. Duncan RE, Ahmadian M, Jaworski K, Sarkadi-Nagy E, Sul HS: Regulation of lipolysis in adipocytes. Annu Rev Nutr 27:79 –101, 2007
2. Chon S-H, Zhou YX, Dixon JL, Storch J: Developmental and nutritional regulation of monoacylglycerol lipase and monoacylglycerol acyltransferase. J Biol Chem 282:33346 –33357, 2007
3. Jaworski K, Sarkadi-Nagy E, Duncan RE, Ahmadian M, Sul HS: Regulation of triglyceride metabolism. IV. Hormonal regulation of lipolysis in adipose tissue. Am J Physiol Gastrointest Liver Physiol 293:G1–G4, 2007
4. Tornqvist H, Belfrage P: Purification and some properties of a monoacylglycerol-hydrolyzing enzyme of rat adipose tissue. J Biol Chem 251:813–819, 1976
5. Jenkins CM, Mancuso DJ, Yan W, Sims HF, Gibson B, Gross RW: Identification, cloning, expression, and purification of three novel human calcium-independent phospholipase A2 family members possessing triacylglycerol lipase and acylglycerol transacylase activities. J Biol Chem 279:48968–48975, 2004
6. Villena JA, Roy S, Sarkadi-Nagy E, Kim KH, Sul HS: Desnutrin, an adipocyte gene encoding a novel patatin domain-containing protein, is induced by fasting and glucocorticoids: ectopic expression of desnutrin increases triglyceride hydrolysis. J Biol Chem 279:47066–47075, 2004
7. Zimmermann R, Strauss JG, Haemmerle G, Schoiswohl G, Birner-Gruenberger R, Riederer M, Lass A, Neuberger G, Eisenhaber F, Hermetter A, Zechner R: Fat mobilization in adipose tissue is promoted by adipose triglyceride lipase. Science 306:1383–1386, 2004
8. Unger RH: Lipotoxic diseases. Annu Rev Med 53:319 –336, 2002
9. Gregoire FM, Smas CM, Sul HS: Understanding adipocyte differentiation. Physiol Rev 78:783– 809, 1998
10. Soni KG, Lehner R, Metalnikov P, O'Donnell P, Semache M, Gao W, Ashman K, Pshezhetsky AV, Mitchell GA: Carboxylesterase 3 (EC 3.1.1.1) is a major adipocyte lipase. J Biol Chem 279:40683– 40689, 2004
11. Folch J, Lees M, Sloane Stanley GH: A simple method for the isolation and purification of total lipides from animal tissues. J Biol Chem 226:497–509, 1957
12. Kim KH, Lee K, Moon YS, Sul HS: A cysteine-rich adipose tissue-specific secretory factor inhibits adipocyte differentiation. J Biol Chem 276:11252–11256, 2001
13. Orlicky DJ, DeGregori J, Schaack J: Construction of stable coxsackievirus and adenovirus receptor-expressing 3T3–L1 cells. J Lipid Res 42:910 –915, 2001
14. Ross SA, Song X, Burney MW, Kasai Y, Orlicky DJ: Efficient adenovirus transduction of 3T3–L1 adipocytes stably expressing coxsackie-adenovirus receptor. Biochem Biophys Res Commun 302:354 –358, 2003

15. Bligh EG, Dyer WJ: A rapid method of total lipid extraction and purification. Can J Biochem Physiol 37:911–917, 1959
16. Youn JH, Buchanan TA: Fasting does not impair insulin-stimulated glucose uptake but alters intracellular glucose metabolism in conscious rats. Diabetes 42:757–763, 1993
17. Samuel VT, Choi CS, Phillips TG, Romanelli AJ, Geisler JG, Bhanot S, McKay R, Monia B, Shutter JR, Lindberg RA, Shulman GI, Veniant MM: Targeting foxo1 in mice using antisense oligonucleotides improves hepatic and peripheral insulin action. Diabetes 55:2042–2050, 2006
18. Turner SM, Murphy EJ, Neese RA, Antelo F, Thomas T, Agarwal A, Go C, Hellerstein MK: Measurement of TG synthesis and turnover in vivo by 2H2O incorporation into the glycerol moiety and application of MIDA. Am J Physiol Endocrinol Metab 285:E790–E803, 2003
19. Lee K, Villena JA, Moon YS, Kim K-H, Lee S, Kang C, Sul HS: Inhibition of adipogenesis and development of glucose intolerance by soluble preadipocyte factor-1 (Pref-1). J Clin Invest 111:453– 461, 2003
20. Smas CM, Sul HS: Pref-1, a protein containing EGF-like repeats, inhibits adipocyte differentiation. Cell 73:725–734, 1993 21. Villena JA, Kim K-H, Sul HS: Pref-1 and ADSF/resistin: two secreted factors inhibiting adipose tissue development. Horm Metab Res 34:1–7, 2002
22. Smirnova E, Goldberg EB, Makarova KS, Lin L, Brown WJ, Jackson CL: ATGL has a key role in lipid droplet/adiposome degradation in mammalian cells. EMBO Rep 7:106 –113, 2006
23. Turner SM, Roy S, Sul HS, Neese RA, Murphy EJ, Samandi W, Roohk DJ, Hellerstein MK: Dissociation between adipose tissue fluxes and lipogenic gene expression in ob/ob mice. Am J Physiol Endocrinol Metab 292: E1101–E1109, 2007
24. Strawford A, Antelo F, Christiansen M, Hellerstein MK: Adipose tissue triglyceride turnover, de novo lipogenesis, and cell proliferation in humans measured with 2H20. Am J Physiol Endocrinol Metab 286:E577–E588, 2003
25. Haemmerle G, Lass A, Zimmermann R, Gorkiewicz G, Meyer C, Rozman J, Heldmaier G, Maier R, Theussl C, Eder S, Kratky D, Wagner EF, Klingenspor M, Hoefler G, Zechner R: Defective lipolysis and altered energy metabolism in mice lacking adipose triglyceride lipase. Science 312:734–737, 2006 26. Lucas S, Tavernier G, Tiraby C, Mairal A, Langin D: Expression of human hormone-sensitive lipase in white adipose tissue of transgenic mice increases lipase activity but does not enhance in vitro lipolysis. J Lipid Res 44:154 –163, 2003
27. Kopecky J, Clarke G, Enerback S, Spiegelman B, Kozak LP: Expression of the mitochondrial uncoupling protein gene from the aP2 gene promoter prevents genetic obesity. J Clin Invest 96:2914 –923, 1995
28. Orci L, Cook WS, Ravazzola M, Wang M, Park BH, Montesano R, Unger RH: Rapid transformation of white adipocytes into fat-oxidizing machines. Proc Natl Acad Sci U S A 101:2058 –2063, 2004
29. Saha PK, Kojima H, Martinez-Botas J, Sunehag AL, Chan L: Metabolic

adaptations in the absence of perilipin. J Biol Chem 279:35150 –35158, 2004
30. Yamada T, Katagiri H, Ishigaki Y, Ogihara T, Imai J, Uno K, Hasegawa Y, Gao J, Ishihara H, Niijima A, Mano H, Aburatani H, Asano T, Oka Y: Signals from intra-abdominal fat modulate insulin and leptin sensitivity through different mechanisms: neuronal involvement in food-intake regulation. Cell Metab 3:223–229, 2006

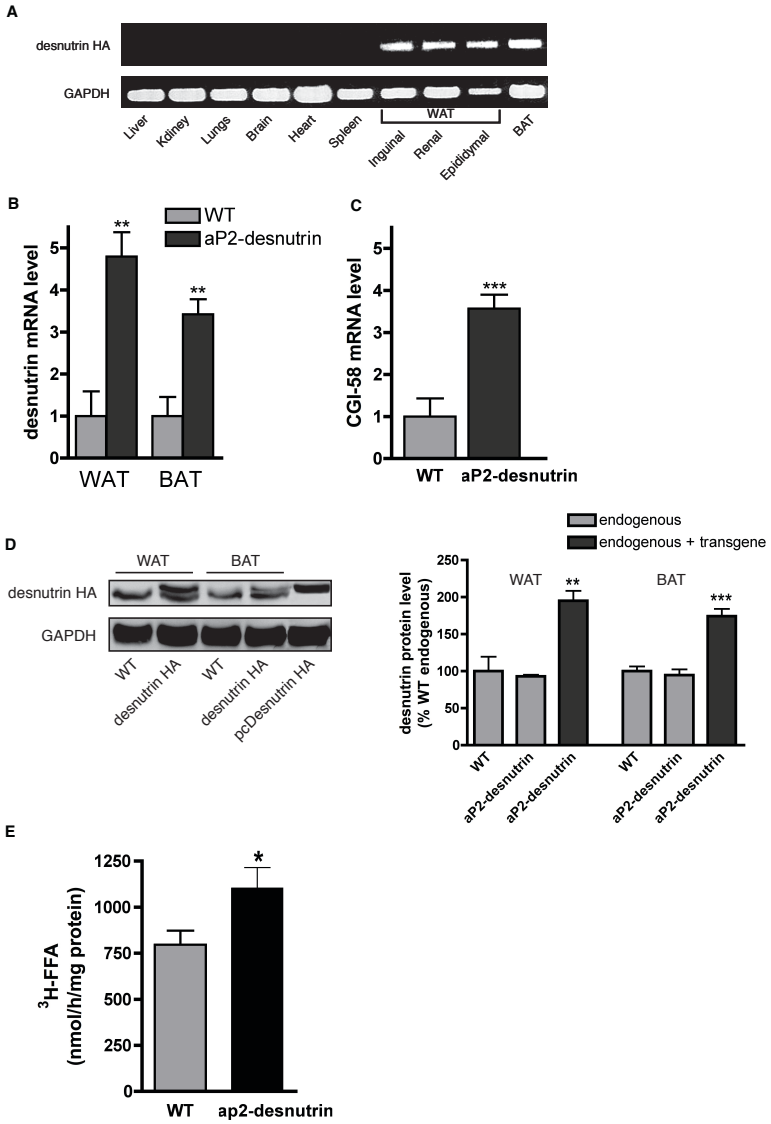

Fig.1

Figure II-1. Desnutrin overexpression in adipose tissue of mice. *A*: Transgene expression was verified by RT-PCR in tissues from aP2-desnutrinmice. GAPDH, glyceraldehyde-3-phosphate dehydrogenase. *B*: DesnutrinmRNA level in gonadal WAT and BAT as determined by RT-qPCR(n =5–6), wild type; f, aP2-desnutrin. *C*: CGI-58 mRNA level in gonadal WAT as determined by RT-qPCR (n =6–7). *D*: Immunoblotand quantification of desnutrin-HA fusion protein in gonadal WAT andBAT. _, endogenous; f, endogenous _ transgene. *E*: TAG lipase activity in WAT homogenates from wild-type and aP2-desnutrin mice.*$P < 0.05$, **$P < 0.01$, ***$P < 0.001$. All data are from female mice. WT,wild type.

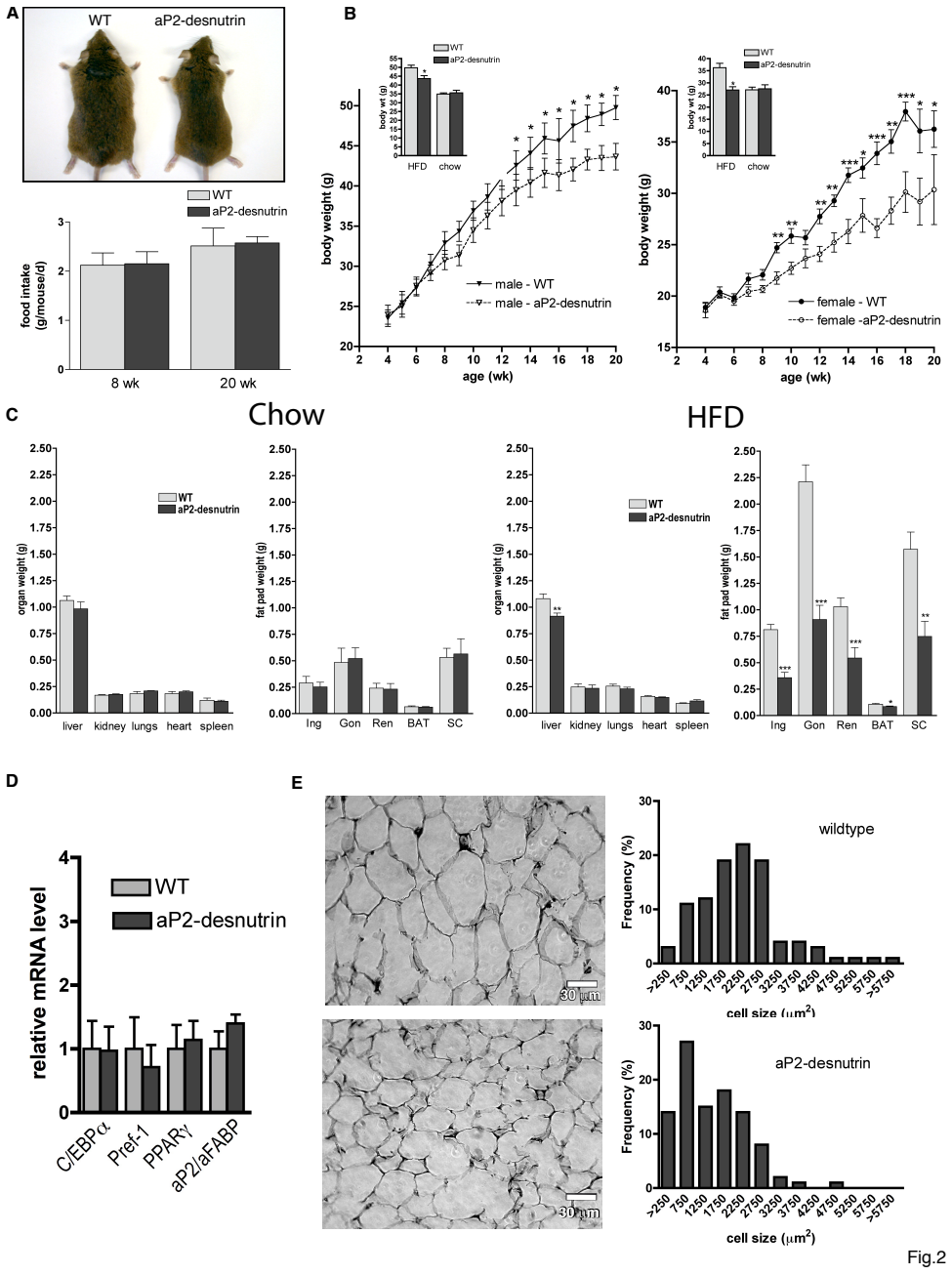

Fig.2

Figure II-2. Weight gain, fat pad weight, and adipocyte size in aP2-desnutrin mice. *A*: Gross appearance of female wild-type and aP2-desnutrin littermates (*upper panel*). Food intakes of female mice at 8 and 20 weeks (Wk) (*lower panel*). *B*: Time course of body weights over 20 weeks inmice fed an HFD. *Inset*: Average body weights at 20 weeks in mice fed a chow diet or an HFD (n _ 9–11). *C* and *D*: Organ and fat pad weights infemale mice fed a chow diet (*C*) or an HFD (*D*) (n _ 9–11). Gon, gonadal fat pad; Ing, inguinal fat pad; Ren, renal fat pad; SC, subcutaneous fatpad. *E*: RT-qPCR for C/EBP_, Pref-1, PPAR_, and aP2/aFABP from WAT of female wild-type and aP2-desutrin mice fed an HFD (n _ 4–6). *F*:Representative images of hematoxylin and eosin–stained sections of gonadal WAT and frequency distribution of adipocyte cell size in gonadal WAT. *$P < 0.05$, **$P < 0.01$, ***$P < 0.001$. (A high-quality digital representation of this figure is available in the online issue.)

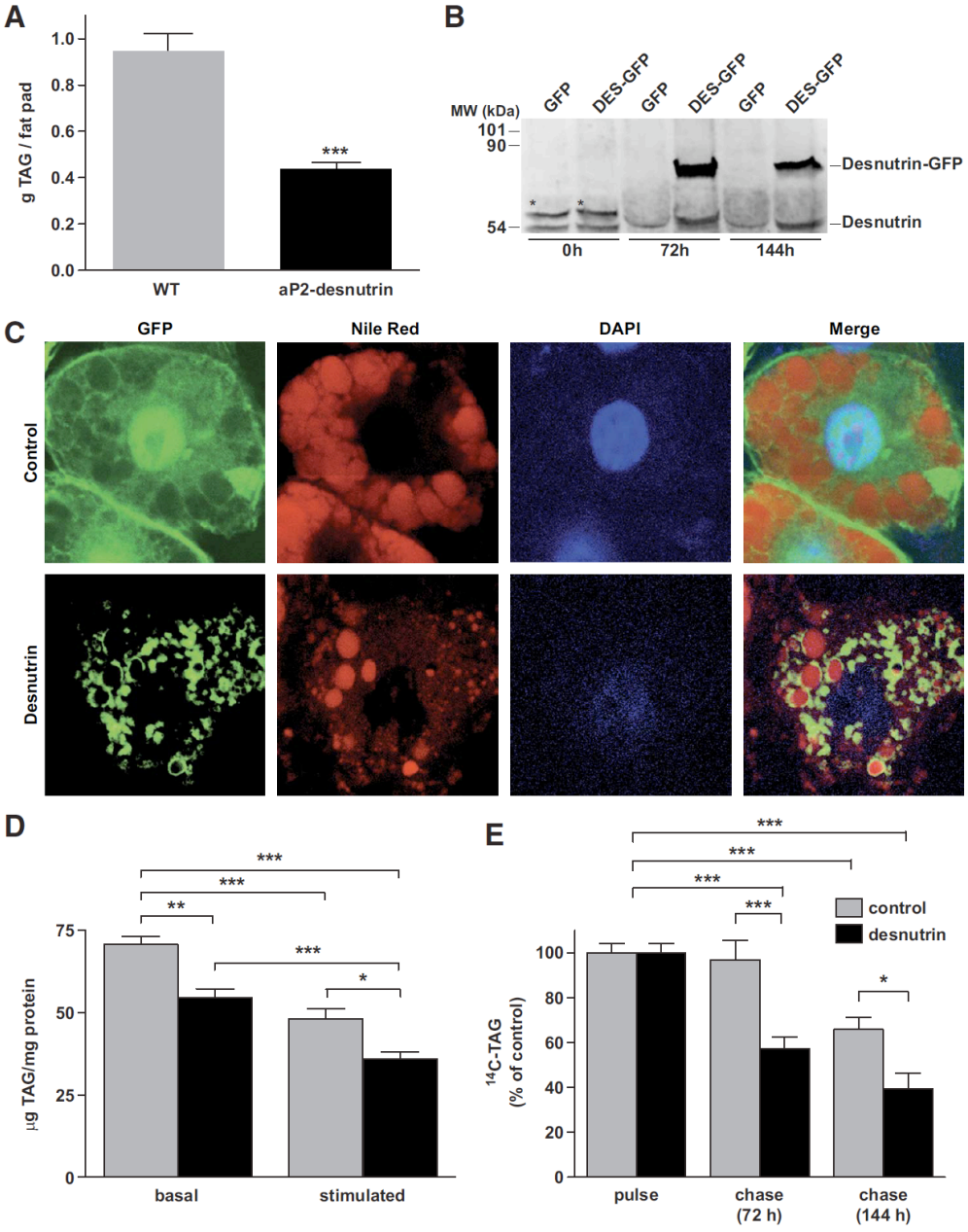

Figure II-3. Overexpression of desnutrin in adipocytes decreases TAG content. *A*: TAG content of gonadal fat pads (*n* _ 6–9). WT, wild type. *B*: Immunoblot of endogenous desnutrin and desnutrin-GFP in differentiated 3T3-L1CAR_1 adipocytes. *Nonspecific band. DES, desnutrin. *C*: Confocal microscopy images showing localization of desnutrin-GFP to TAG-rich lipid droplets in contrast to the diffuse localization of GFP alone. *D*: Endogenous TAG content from 3T3-L1CAR_1 adipocytes. Three days after infection with GFP or desnutrin-GFP, medium was replaced with serum-free medium and cells were maintained for an additional 6 h either with dibutyryl cAMP (stimulated) or without (basal) before analysis of TAG content. *E*: Time course of TAG breakdown in 3T3-L1CAR_1 adipocytes labeled with [14C]palmitate before infection with GFP or desnutrin-GFP and chase with cold medium. $*P < 0.05$, $**P < 0.01$, $***P < 0.001$. (A high-quality digital representation of this figure is available in the online issue.)

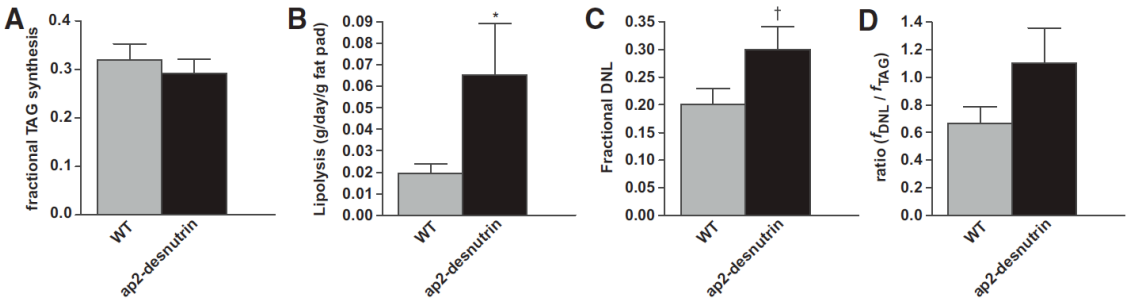

Figure II-4. In vivo measures of TAG metabolism in WAT. *A*: Fractional in vivo synthesis of TAG-glycerol in gonadal WAT (*n* _ 6). *B*: In vivo lipolysis in gonadal WAT (*n* _ 3–6). *C*: Fractional in vivo DNL in gonadal WAT (*n* _ 6). *D*: Ratio of fractional in vivo DNL/fractional in vivo synthesis of TAG-glycerol in gonadal WAT (*n* _ 6). **P* < 0.05, †*P* _ 0.07. WT, wild type.

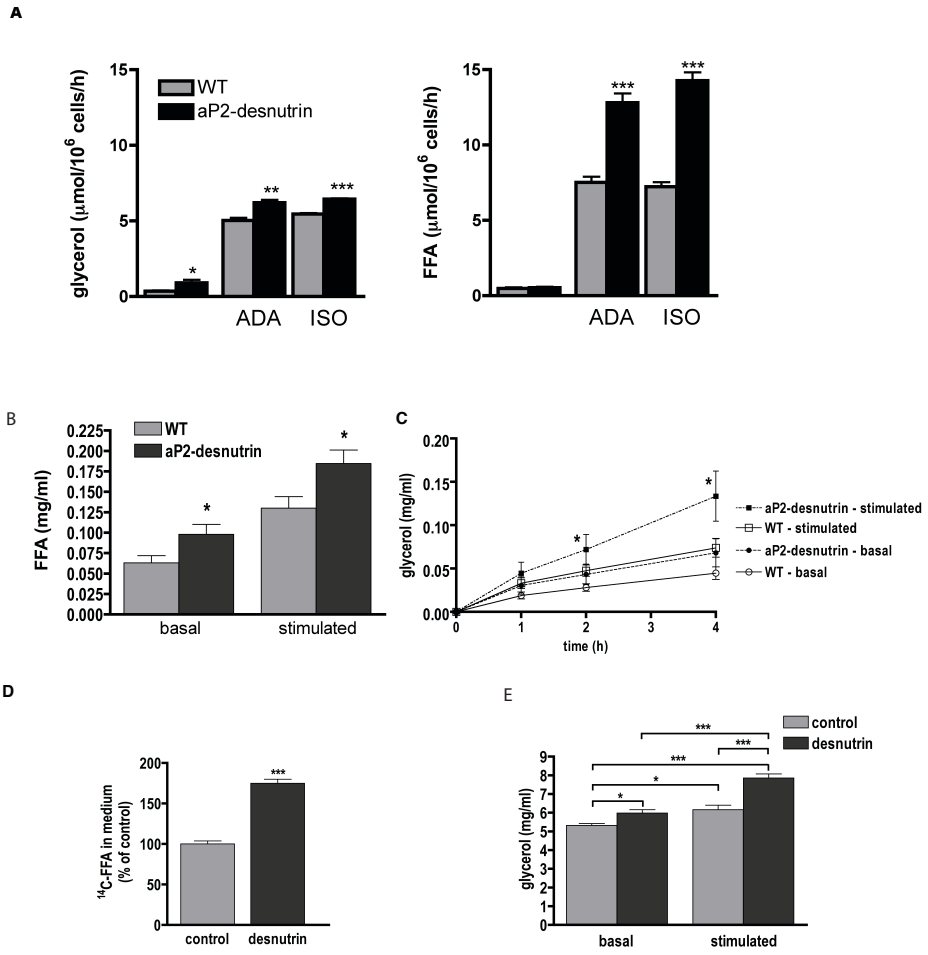

Fig5

Figure II-5. Desnutrin overexpression increases lipolysis. *A*: Glycerol and FA release from isolated adipocytes of fed female wild-type or aP2-desnutrin mice under basal conditions or stimulated with adenosine deaminase (ADA) or isoproterenol (iso). FA (*B*) and glycerol (*C*) release from 50 mg explants of fresh gonadal WAT incubated under basal conditions or stimulated with 0.5 mmol/l dibutyryl cAMP (*n* _ 9–12). *D*: Radiolabeled-FA release from 3T3-L1CAR_1 adipocytes. Cells were labeled with [14C]palmitate and then infected with adenoviral desnutrin-GFP or GFP (control) and chased with cold medium. [14C]FA in the medium were quantified 30 h after infection. *E*: Glycerol release from 3T3-L1CAR_1 adipocytes after infection with GFP or desnutrin-GFP for 3 days. Six hours before assessment of glycerol concentrations, medium was replaced with serum-free medium either with dibutyryl cAMP (stimulated) or without (basal). _, control; f, desnutrin. **P* < 0.05, ***P* < 0.01, ****P* < 0.001.

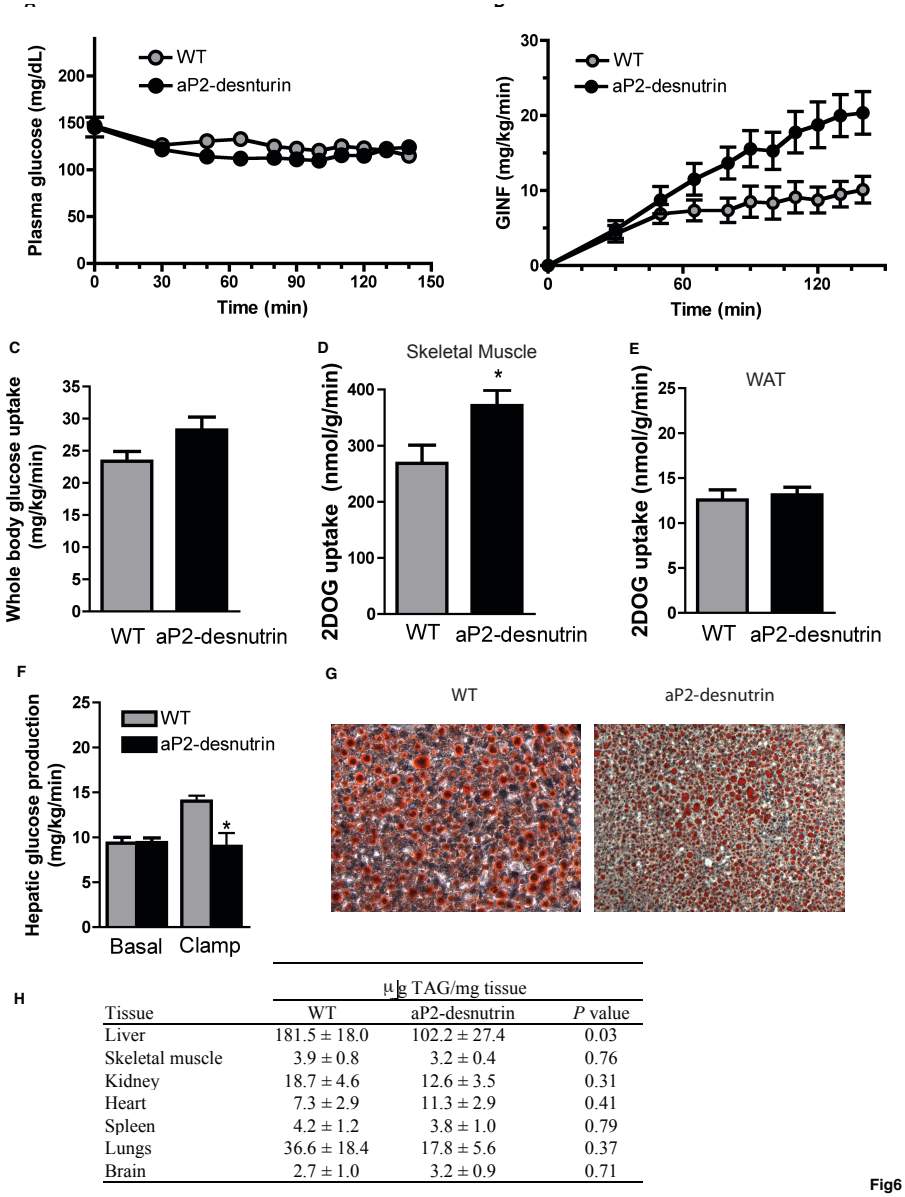

H

	μg TAG/mg tissue		
Tissue	WT	aP2-desnutrin	*P* value
Liver	181.5 ± 18.0	102.2 ± 27.4	0.03
Skeletal muscle	3.9 ± 0.8	3.2 ± 0.4	0.76
Kidney	18.7 ± 4.6	12.6 ± 3.5	0.31
Heart	7.3 ± 2.9	11.3 ± 2.9	0.41
Spleen	4.2 ± 1.2	3.8 ± 1.0	0.79
Lungs	36.6 ± 18.4	17.8 ± 5.6	0.37
Brain	2.7 ± 1.0	3.2 ± 0.9	0.71

Fig6

Figure II-6. Improved insulin sensitivity in aP2-desnutrin mice. *A* and *B*: Plasma glucose (*A*) and glucose infusion (GINF) (*B*) rates (n=7–8) *C*: Whole-body glucose uptake (n =7–8). *D*: Skeletal muscle (gastrocnemius) glucose uptake (n =7–8). *E*: Epididymal WAT glucose uptake (n =7–8). *F*: Hepatic glucose production during hyperinsulinemic-euglycemic clamps (n =7–8). *G*: Cryosections of frozen livers stained with Oil red O. *H*: Tissue TAG content in indicated organs (n=3–9). *P < 0.05. (A high-quality digital representation of this figure is available in the online issue.)

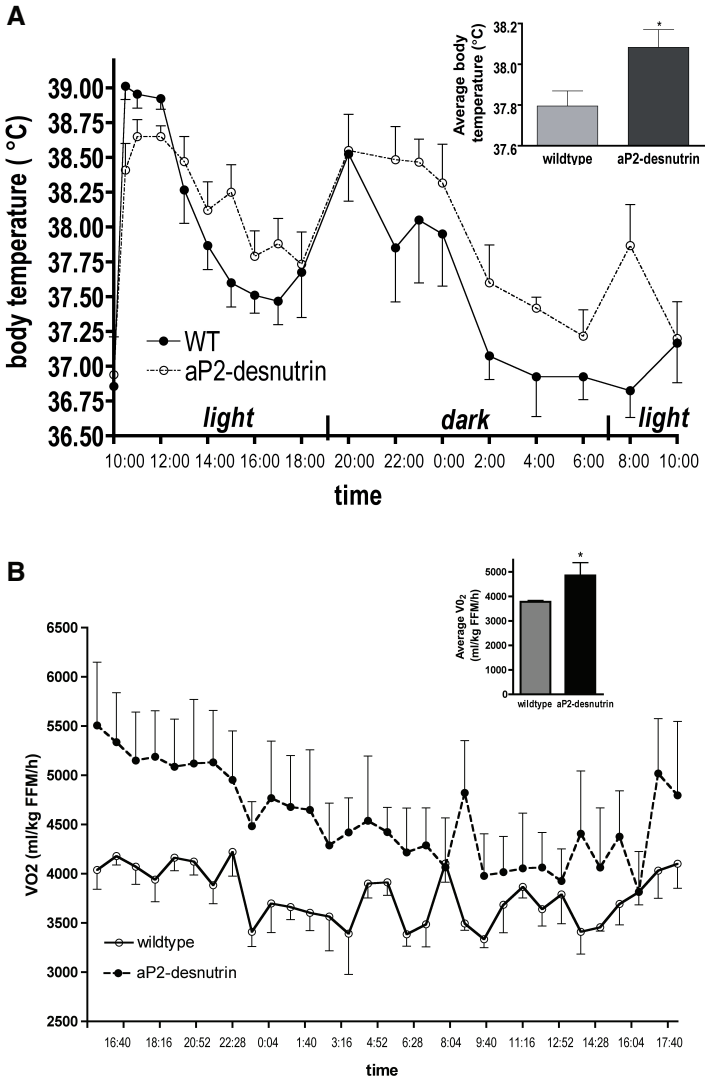

Fig7

Figure II-7. Increased thermogenesis and energy expenditure in aP2-desnutrin mice. *A*: Body temperatures of 20-week-old male mice. Temperatures were measured beginning at 10 AM following a 17-h overnight fast and before resumption of feeding and were monitored for 24 h (n =4–6). *Inset*: Average body temperature (°C) over the day. *B*: Oxygen consumption rate (VO2) measured through indirect calorimetry and the average VO2 over 24 h (*inset*) (n =4). *$P < 0.05$. FFM, fat-free mass.

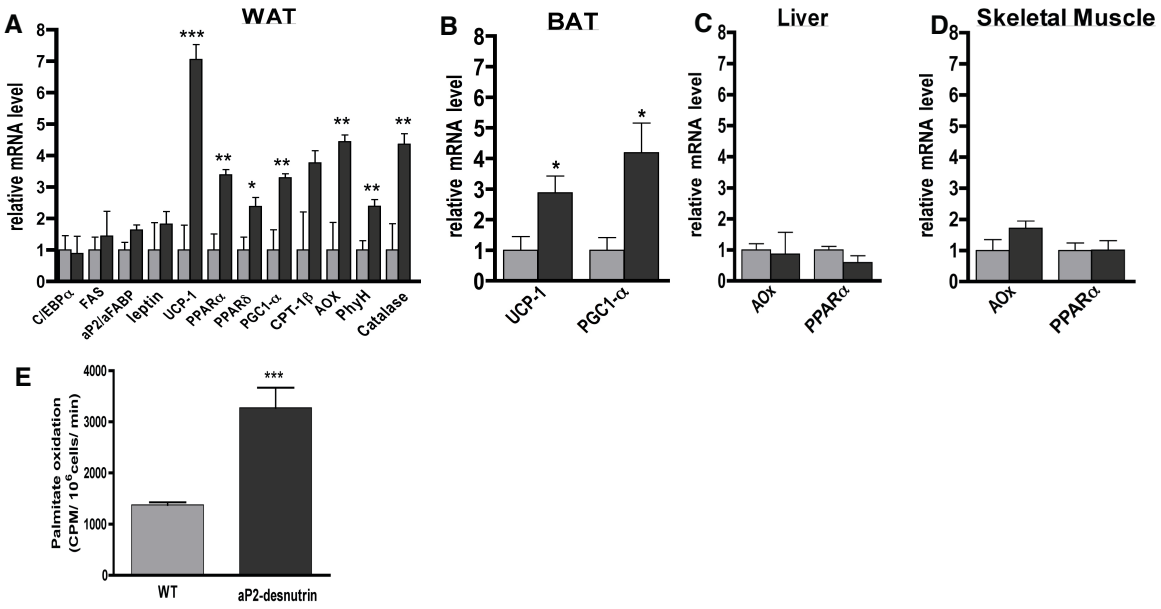

Figure II-8 Gene expression in WAT, BAT, liver, and skeletal muscle and increased FA oxidation in adipocytes. Relative mRNA levels were measured by RT-qPCR for the indicated genes from WAT (*A*), BAT (*B*), liver (*C*), and skeletal muscle (*D*) (*n* =5–6). *E*: Oxidation of [14C]palmitate to 14CO2 by adipocytes isolated from aP2-desnutrin mice or wild-type (WT) controls. WT, light gray bars; aP2-desnutrin, black bars. **P* < 0.05, ***P* < 0.0****P* < 0.001. AOx, _-oxidation.

TABLE 1
Serum parameters of chow- or HFD-fed and fasted male mice

	Chow				HFD			
	Wild-type fasted	aP2-des fasted	Wild-type fed	aP2-des fed	Wild-type fasted	aP2-des fasted	Wild-type fed	aP2-des fed
FA (mmol/l)	1.57 ± 0.09	1.86 ± 0.10	0.84 ± 0.06	1.00 ± 0.07	1.39 ± 0.06	1.46 ± 0.11	0.84 ± 0.07	1.00 ± 0.07
Glycerol (mmol/l)	0.76 ± 0.02	0.82 ± 0.04	0.65 ± 0.04	0.66 ± 0.02	0.76 ± 0.03	0.72 ± 0.03	0.66 ± 0.02	0.76 ± 0.05
Triglyceride (mg/dl)	69.81 ± 1.50	67.55 ± 3.63	74.46 ± 4.17	76.33 ± 3.30	70.65 ± 3.06	65.34 ± 1.68	61.21 ± 2.46	65.71 ± 5.07
Adiponectin (µg/ml)	14.75 ± 1.08	15.10 ± 0.83	—	—	17.05 ± 0.79	17.35 ± 0.80	—	—

Chapter III: Adipose-specific Ablation of Desnutrin Converts Brown to White Adipose Tissue and Promotes Diet-Induced Obesity

ABSTRACT

Two types of adipose tissue exist, white (WAT) and brown adipose tissue (BAT). WAT stores energy in the form of triacylglycerol (TAG) to hydrolyze (lipolysis) and release fatty acids into the circulation during times of energy shortage. BAT, on the other hand, hydrolyzes TAG to use fatty acids to activate UCP-1 and generate heat (thermogenesis). Here, to investigate the role of desnutrin/ATGL in WAT and BAT, we generated adipose-specific knockout mice of desnutrin/ATGL (desnutrin-ASKO). We found that desnturin-ASKO mice have massive TAG accumulation exclusively in WAT and BAT and are prone to diet-induced obesity, and yet are more insulin sensitive. Furthermore, the phenotype of BAT in desnutrin-ASKO resembles WAT. Decreased expression of UCP-1, CPT-1β and increased expression of RIP140, as well as decreased number and altered morphology of mitochondria clearly showed a conversion of BAT to WAT. As a result, desnutrin-ASKO mice are cold intolerant, have lower energy expenditure and are unresponsive to the β3 agonist, CL31624. Overall, ablation of desnutrin/ATGL promotes diet-induced obesity and the conversion of BAT to WAT.

INTRODUCTION

Lipolysis for the provision of fatty acids (FAs) as an energy source takes place at the surface of lipid droplets where triacylglycerol (TAG) is rapidly mobilized by the hydrolytic action of lipases (1). TAG is hydrolyzed first to form diacylglycerol (DAG) then monoacylglycerol (MAG) that is hydrolyzed to liberate the final FA and glycerol. We, and others, identified desnutrin/ATGL (also called PNPLA2, TTS2.2 and $iPLA_2\zeta$) as a TAG lipase, expressed at the highest levels white (WAT) and brown (BAT) adipose tissue, but also found in other organs (2-4). Total knockout mice of desnutrin/ATGL have massive TAG accumulation in multiple organs, most notably the heart and die prematurely making true characterization of the adipose-specific role of desnutrin difficult (5). Transgenic mice overexpressing desnutrin/ATGL in WAT and BAT exhibit increased FA oxidation and expression of thermogenic genes in both WAT and BAT making them resistant to diet-induced obesity and raising the notion that desnutrin may play an important role in promoting oxidation and thermogenesis in both WAT and BAT (6).

WAT and BAT play a critical role in controlling energy balance. As the primary energy reserve in mammals, WAT stores energy in the form of TAG during times of energy surplus and hydrolyzes TAG via lipolysis during times of energy deprivation to generate FAs (7). These FAs can be taken up by other organs and used as an energy source to produce ATP. In contrast to WAT, BAT is specialized in thermogenesis, using energy to produce heat rather than to generate ATP (8). BAT activity is mediated by uncoupling protein 1 (UCP-1), which increases in expression in response to cold, activation of the sympathetic nervous system (SNS), and administration of β-agonists (8). FAs generated through lipolysis in BAT activate UCP-1 and, therefore, are critical for thermogenesis.

Recently, it has been established that even adults possess metabolically active BAT (9). Furthermore, so-called “transdifferentiation”, the conversion between BAT and WAT has been detected at least in rodents, allowing physiological reprogramming of the adipocyte genome and considerable organ plasticity (10). These observations have generated intense research interest in BAT. White-brown adipocyte transdifferentiation

could offer new therapeutic avenues for treating obesity and related disorders, however what triggers this transformation is not known. Since FAs are required to activate UCP-1 and therefore, thermogenesis, inhibition of lipolysis may evoke the conversion of BAT to WAT. To investigate the role of desnutrin/ATGL and the physiological consequence of lack desnutrin/ATGL-mediated lipolysis specifically in WAT and BAT we generated adipose-specific knockout mice of desnutrin/ATGL. Here, we report that ablation of desnutrin/ATGL promotes diet induced obesity and the conversion of BAT to WAT.

METHODS

Generation of Desnutrin Floxed Mice- A desnturin targeting vector was constructed that introduced loxP sites upstream and downstream of exon1 which contains its translation start site and catalytic domain. The pFlexible plasmid containing the puromycin resistance gene (pFlex) (provided by Allan Bradley) was used for construction of the desnutrin targeting vector. FRT sites flanking the puromycin resistance gene facilitates its removal by Flp Recombinase and loxP sites facilitate removal of the targeted exon1 by Cre recombinase. The desnutrin sequence, amplified by PCR from 129/SV genomic DNA was cloned into pFlex. For the 5' homology arm, a 1.92 kb fragment containing the desnutrin promoter was amplified by PCR introducing Asc1 restriction sites at both the 5' and 3' ends and cloned into the Asc1 site of pFlex. For the conditional arm, a 1.56 kb fragment containing part of the desnutrin promoter and exon1 was amplified by PCR introducing and HindIII site at the 5' end a PacI site at the 3' end and cloned into HindIII-PacI digested pFlex with the inserted 5' homology arm. For the 3' homology arm, a 3.6 kb fragment containing intron 1 through exon 7 was amplified by PCR introducing NotI sites at both the 5' and 3' end and cloned into the NotI site of pFlex with 5' homology and conditional arms. The resulting targeting vector was digested with PmeI and electroporated into 129/SvJ E14 ES cells. The cells were selected by maintaining them in puromycin-containing media. ES cell clones with the desired homologous recombination event were identified by PCR, microinjected into 3.5-day blastocysts derived from C57BL/6 females, and transferred to pseudopregnant C57BL/6 recipients. Chimeric mice were then bred with C57BL/6 mice for germline transmission. The presence of the targeted allele in the agouti-colored offspring was confirmed by PCR. These mice were then mated with mice expressing FLP recombinase driven by the human ACTB promoter m (Jackson laboratory) to excise the puromycin resistance gene to generate desnutrin flox/+ mice that were identified by PCR using primer sequences flanking the puromycin resistance gene and FRT sites. Homozygous desnutrin flox/flox mice were crossed with transgenic mice expressing Cre recombinase under the control of the aP2 promoter b (Jackson Laboratory). Offspring inheriting both the targeted allele and the Cre trangene (aP2-Cre-desnutrin flox/+) were crossed with desnutrinflox/flox mice to yield desnutrin flox/flox Cre adipose-specific knockout mice (desnutrin-ASKO). Adipose tissue specific knockout for the desnutrin gene, removal of exon 1, was verified by PCR with primer sequences flanking exon 1 and loxP sites using DNA extracted from adipose tissue with a DNeasy kit (Qiagen).

Mouse maintenance. All studies received approval from the University of California at Berkeley Animal Care and Use Committee. We compared desnutrin-ASKO and flox/flox

littermates on a mixed genetic background (C57BL/6J and 129SVJ), but we also confirmed the results in a C57BL/6J background. We provided either a standard chow or a HFD (45% of kcal from fat, 35% of kcal from carbohydrate and 20% of kcal from protein, Research Diets) ad libitum.

Indirect calorimetry and body temperature. Oxygen consumption (VO2) was measured using the Comprehensive Laboratory Animal Monitoring System (CLAMS; Columbus Instruments). Data were normalized to body weights. Body temperatures were assessed in 25 wk-old male mice using a RET-3 rectal probe for mice (Physitemp). CL31624 was injected into mice intraperitoneally a 1mg/kg body weight.

Glucose and Insulin Tolerance Tests. Glucose and insulin tolerance tests. For the GTT, we injected mice intraperitoneally with D-glucose (2 mg per g body weight) after an overnight fast and monitored the tail blood glucose levels. For ITT, mice were injected with insulin (humulin, Eli Lilly) (0.75 mU per g body weight) after a 5-h fast.

Adipocyte size determination. Gonadal fat samples and intrascapular BAT were fixed in 10% buffered formalin, embedded in paraffin, cut into 8μm-thick sections, and stained with hemotoxylin and eosin. Adipocyte size was determined with Image J software (US National Institutes of Health), measuring at least 300 cells from each sample.

Lipolysis. Gonadal fat pads or BAT from overnight fasted mice were cut into 50mg samples and incubated at 37 degrees without shaking in 500ul of Krebs-Ringer media (12 mM HEPES, 121mM NaCl, 4.9 mM KCl, 1.2 mM MgSO4 and 0.33 mM CaCl2) containing 2% fatty acid free BSA and 0.1% glucose with or without 10uM isoproterenol. FA and glycerol release were measured in aliquots from incubation buffer using the NEFA C Kit (Wako) and Free Glycerol Reagent (Sigma), respectively.

RNA extraction and real time RT-PCR. Total RNA was prepared using Trizol Reagent (Invitrogen) and cDNA was synthesized from 2.5 μg of total RNA by Superscript II reverse transcriptase (Invitrogen). Gene expression was determined by RT-qPCR performed with an ABI PRISM7700 sequence fast detection system (Applied Biosystems), and was quantified by measuring the threshold cycle normalized to GAPDH then expressed relative to flox/flox controls.

Immunoblotting. Total lysates were subjected to 8% SDS-PAGE, transferred to PVDF membranes, and probed with rabbit anti-desnutrin antibody or rabbit anti-GAPDH antibody followed by peroxidase conjugated goat anti-rabbit antibody. Blots were visualized using enhanced chemiluminescence (PerkinElmer) and images were captured using a Kodak Image Station 4000MM.

Transmission electron microscopy. BAT and WAT were fixed in a 2% glutaraldehyde in 0.1 M PB (phosphate buffer), pH 7.3 at 4°C overnight; then postfixed in 1% OsO4 and embedded in an Epon-Araldite mixture. Ultrathin sections (0.2um) mounted on 150-mesh copper grids were stained with leadcytrate and observed under a FEI Tecnai 12 transmission electron microscope.

Indirect calorimetry and body temperature. Oxygen consumption (VO2) was measured using the Comprehensive Laboratory Animal Monitoring Sysfm (CLAMS: Columbus Instruments). Data were normalized to body weights. Body temperatures were assessed using a RET-3 rectal probe for mice (Physitemp).

Blood and Tissue Metabolites- Serum Parameters. Fasting serum triglycerides and free fatty acids were analyzed with Infinity Triglyceride reagent (Thermo Trace) and NEFA C kit (Wako), respectively. Serum insulin, were determined using enzyme–linked immunosorbent assay kits (Alpco).

Statistical Analyses. The results are expressed as means +/- SEM. Statistically significant differences between two groups were assessed by Student's *t* test.

RESULTS

Adipose-specific ablation of desnutrin prevents diet-induced obesity and increases lipolysis

To determine the role of desnutrin/ATGL and the physiological consequence of lack of desnutrin/ATGL-mediated lipoysis, specifically in adipose tissue, we used gene targeting to generate floxed mice, that have the first exon of desnutrin/ATGL, containing the translational start site as well as the conserved lipase consensus motif (GXSXG) flanked by lox P sites (flox/flox mice) (Fig. S1). Flox/flox mice were subsequently crossed with aP2-Cre mice to generate desnutrin/ATGL adipose-specific knockout (desnutrin-ASKO mice) and compared to flox/flox mice for all experiments (Fig. S1). Desnutrin-ASKO mice were born at the expected Mendelian frequency and have a normal life expectancy. Using a desnutrin-specific antibody, western blot analysis verified that the desnutrin/ATGL protein was not detected in WAT and BAT of desnutrin-ASKO mice, but was still present in flox/flox mice (Fig. S2). However, in other organs such as heart, liver and skeletal muscle, desnutrin/ATGL protein levels were unchanged in desnutrin-ASKO compared to flox/flox mice (Fig. S2).

To investigate the effects of diminished desnutrin/ATGL on adiposity, mice were placed on a high fat diet (HFD) at weaning. Although total body weights did not differ at weaning, by 11 weeks of age, desnutrin-ASKO mice fed a HFD began to gain weight at a higher rate than wild type littermates (Fig. S-3A, left and Fig. 1A). Increased weight gain was also observed in chow-fed desnutrin-ASKO mice, albeit to a lesser extent (Fig. S-3A, right). This increased body weight was not due to increased food intake as desnutrin-ASKO and flox/flox mice showed no difference in food intake (Fig. S-3B). Liver, kidney and heart weights were not increased in desnutrin-ASKO mice fed a HFD and, therefore, could not account for the decreased body weights in desnutrin-ASKO mice (Fig.S-3C). However, WAT and BAT depot sizes were markedly enlarged in desnutrin-ASKO mice (Fig. 1A). Gonadal, subcutaneous and renal WAT depot weights were 1.4, 1.7 and 1.9-fold higher, respectively, after 20 weeks on a HFD in desnutrin-ASKO mice compared flox/flox mice (Fig. 1B). BAT was drastically transformed, weighing 5.3-fold more than flox/flox mice, and resembling WAT in terms of its pale color (Fig.1B and C). Increased

adipose tissue mass can result from an increase in adipocyte size an/or an increase in adipocyte number due to enhanced differentiation. To test if adipocyte differentiation was enhanced in desnutrin-ASKO mice, we measured the expression levels of early and late markers of adipocyte differentiation (11; 12). The expression levels of early adipocyte marker genes, including, CCAAT/enhancer binding proteinδ (C/EBPδ) and preadipocyte factor-1 (Pref-1) as well as late markers such as CCAAT/enhancer binding protein α (C/EBPα), peroxisome proliferator-activated receptor-γ (PPARγ) and fatty acid binding protein (aP2/FABP4) were not increased in desnutrin-ASKO WAT, indicating normal white adipocyte differentiation (Fig. 3A). Similar to WAT, in desnutrin-ASKO BAT there were also no increases in the expression of Pref-1, C/EBPα, C/EBPδ, PPARγ as well as in PRD1-BF1-RIZ1 homologous domain containing 16 (PRDM16), which has been shown to be important for brown adipocyte differentiation (Fig. 3A)(13). Histological analysis, however, revealed a greater frequency of larger adipocytes in gonadal fat pads from desnutrin-ASKO mice when compared to flox/flox mice indicating increased adipocyte size (Fig. 1C). Similarly, brown adipocyte size was also markedly increased in desnutrin-ASKO mice. Whereas BAT from flox/flox mice contained characteristic small adipocytes with multilocular lipid droplets, desnutrin-ASKO BAT mice was full of large adipocytes with unilocular lipid droplets (Fig.1C). Furthermore, while interscapular fat in flox/flox mice had distinct regions of WAT and BAT, this area in desnutrin/ASKO mice was homogenous, containing only large adipocytes with unilocular lipid droplets and looked like WAT (Fig.1C). Taken together, these findings indicate that the increased adiposity in desnutrin-ASKO mice was due to increased adipocyte TAG storage in both WAT and BAT, rather than enhanced adipocyte differentiation.

Given that desnutrin/ATGL is the major TAG hydrolase in adipose tissue, we predicted that the increased TAG storage observed in desnutrin-ASKO WAT and BAT was due to impaired lipolysis. We therefore determined lipolysis by measuring glycerol and FA release from explants of WAT from desnutrin-ASKO mice and flox/flox littermates. Indeed, glycerol release over 4 hours was drastically decreased in desnutrin-ASKO mice compared to flox/flox mice under both basal and isoproterenol-stimulated conditions (Fig. 2A, left). Although FA release was not changed under basal conditions in WAT, it was decreased by 22% after 2 hours and 41% after 4 hours under isoproterenol-stimulated conditions (Fig. 2A, right). In BAT of desnturin-ASKO mice lipolysis, determined by FA release, was also severely blunted, being decreased by 60% under basal conditions (Fig. 2C). Therefore, other lipases in adipose tissue cannot compensate for lack of desnutrin/ATGL.

Desnutrin/ATGL ablation promotes the conversion of BAT to WAT

To elucidate the molecular mechanisms underlying the drastic transformation of desnutrin-ASKO BAT, we performed a detailed gene expression profile of this tissue and in parallel also examined WAT. In BAT, we found that the expression of genes involved in thermogenesis, mitochondrial FA oxidation as well as peroxisomal FA oxidation were decreased compared to flox/flox mice. UCP-1 expression was markedly decreased at both the mRNA and protein level (Fig. 3B, left panel and inset). Additionally, ATP5B, cytochrome C oxidase IV (COXIV), carnitine palmitoyltransferase 1β (CPT1β), cell death-inducing DFFA-like effector A (CIDEA) and phytanoyl-CoA hydroxylase (PhyH)

were decreased by 38%, 39%, 33%, 44% and 49%, respectively. We predicted that other thermogenic pathways, may be upregulated to compensate for decreased UCP-1 activity. Indeed, we found that type 2 iodothyronine deiodinase (D2) was upregulated by 9.7-fold in BAT of desnutrin-ASKO mice compared to flox/flox mice (1.0+/- 0.18 versus 9.7+/- 0.82, n=6-9, p=.002). Consistent with our findings in BAT, we also found that UCP-1 and UCP-2 expression were decreased by 46% and 44% in WAT. Additionally, we found no change in lipoprotein lipase (LPL), fatty acid synthase (FAS) or forkhead box C2 (FOXC2) in WAT. However, diacylglycerol acyltransferase1 (DGAT1) expression was decreased in WAT, likely a compensatory mechanism to prevent re-esterification. To gain further insight into the upstream signaling events mediating the repression of oxidative and thermogenic genes in desnutrin-ASKO BAT, we measured the expression levels of receptor interacting protein 140 (RIP140) and c-terminal binding peptide 1 (CTPB1), transcriptional co-repressors found to play a crucial role in suppressing oxidative and thermogenic genes in adipose tissue (14-16). Indeed, RIP140 and CTBP1 were upregulated by 2.8 and 3.5-fold, respectively in BAT of desnutrin-ASKO mice. Taken together, impaired desnutrin/ATGL-mediated lipolysis has transformed the gene expression profile of desnutrin-ASKO BAT to a less oxidative and thermogenic state.

Desnutrin-ASKO mice are cold intolerant and have decreased energy expenditure

To obtain a more detailed observation of the morphology of BAT in desnutrin-ASKO mice, we used transmission electron microscopy to examine BAT from desnutrin-ASKO and flox/flox mice. Whereas BAT from flox/flox mice, was full of characteristic small multilocular lipid dropets, BAT from desnutrin-ASKO mice contained large, less numerous lipid droplets (Fig 3B, upper). We also observed more numerous mitochondria in BAT from desnutrin-ASKO mice and closer examination revealed that mitochondria from desnutrin-ASKO BAT were composed of randomly oriented cristae, characteristic of WAT, compared to the classic laminar cristae found in flox/flox BAT (Fig 3A, lower).

In order to determine the physiological consequence of impaired desnutrin/ATGL-mediated lipolysis, we subjected desnutrin-ASKO mice and flox/flox littermates to cold stress by housing them at 4°C. While flox/flox mice were able to maintain body temperature well into 5 hours after cold exposure, desnutrin-ASKO were unable to maintain body temperature, reaching life-threatening hypothermia after just 90 min (Fig. 4A). Given these observations, combined with severely blunted lipolysis and increased adiposity, we hypothesized that desnutrin-ASKO mice may have a decreased metabolic rate, particularly during the fasted state when lipolysis derived FAs become crucial as an energy source. To test this, mice were housed in metabolic chambers overnight, in the fasted state, where oxygen consumption and locomoter activity were assessed. While there was no change in activity levels between desnutrin-ASKO and flox/flox mice (data not shown), total oxygen consumption was decreased in desnutrin-ASKO mice (Fig. 4B). Cold exposure leads to increased SNS signaling through β3 adrenergic receptors, which increase energy expenditure through stimulation lipolysis and activation of UCP-1. Since desnutrin-ASKO mice have impaired lipolysis and thermogenesis we hypothesized that administration of a β3 agonist should no longer exert its thermogenic effects in desnutrin-ASKO mice (17). To test this, we injected a β3 agonist (CL31624) to desnutrin-ASKO and flox/flox mice and monitored oxygen consumption. In response to CL31624 injection, flox/flox mice exhibited a drastic

increase in their metabolic rate, as indicated by oxygen consumption, however, desnutrin-ASKO mice showed no change in oxygen consumption, revealing a blunted β3 adrenergic response (Fig. 4C). Taken together, these results indicate that BAT in desnutrin-ASKO mice is unresponsive both physiological and pharmacological thermogenic stimulation, revealing the requirement of desnutrin/ATGL for eliciting a β3 thermogenic response.

Desnutrin-ASKO mice have improved insulin sensitivity and decreased ectopic TAG storage

Alterations in FA metabolism often result in changes in insulin sensitivity. Consistent with the blunted lipolysis in desnutrin-ASKO mice, serum FA levels were decreased by 39% (Fig. 5A). According to the Randle hypothesis, a reciprocal relationship between glucose and FAs as substrates exists (18). We predicted that due to impaired adiopcyte lipolysis and decreased serum FA levels, desnutrin-ASKO mice may preferentially utilize glucose as an energy source and therefore have improved insulin sensitivity. Indeed, fasting levels of glucose and insulin were both decreased in flox/flox and desnutrin-ASKO mice fed a HFD. To further investigate insulin sensitivity in desnutrin-ASKO mice, we performed glucose and insulin tolerance tests (GTT and ITT) in flox/flox and desnutrin-ASKO mice. Desnutrin-ASKO mice showed improved glucose clearance during a GTT (Fig.5B). During an ITT, desnutrin-ASKO mice exhibited a prolonged response to insulin compared to flox/flox mice (Fig.5B). In support of the improved insulin sensitivity in desnurtrin-ASKO, ectopic storage in the liver was also decreased. By 20 weeks of age, liver weight was decreased by 32% in desnutrin-ASKO mice fed a HFD (Fig1B). Closer examination of the liver and staining with Oil Red O revealed decreased lipid accumulation (Fig. 5C). These results indicate that despite accumulation of TAG in adipose tissue, desnutrin/ATGL ablation in adipose tissue reduces TAG storage. Impaired adipocyte lipolysis in desnutrin-ASKO mice likely leads to energy deprivation in organs such as the liver resulting in increased utilization of internal TAG stores thus preventing ectopic TAG storage and improving insulin sensitivity.

DISCUSSION

Lipolysis for the provision of FAs as a substrate for other tissues is a unique function of WAT. Lipolysis is also crucial for proper BAT function, providing FAs for activation of UCP-1 as well substrates for mitochondrial β-oxidation. Since desnutrin/ATGL is the major TAG lipase in adipose tissue, we postulated that ablation of this enzyme exclusively in adipose tissue would have profound effects on adipose tissue physiology. Indeed, we found that desnutrin-ASKO mice had severely blunted lipolysis in both WAT and BAT. As a result, desnutrin-ASKO mice exhibit massive TAG accumulation in both WAT and BAT. In contrast to global knockout mice of desnutrin/ATGL that exhibit severe TAG deposition in non-adipose tissues and die prematurely, desnutrin-ASKO mice exhibit normal life expectancy yet display increased TAG accumulation exclusively in adipose tissue. The impaired catabolism of TAG in desnutrin-ASKO mice leads to cold intolerance, decreased energy expenditure, diet-induced obesity and a transformation of BAT to WAT.

A novel and key finding of our paper is the demonstration that ablation of desnutrin/ATGL drastically transforms the gene expression profile of adipose tissue. UCP-1 was down-regulated in both BAT and WAT and protein levels in BAT were also decreased. In addition to UCP-1, other genes involved in mitochondrial function, BAT physiology, and FA oxidation including COXIV, ATP5B, CIDEA and CTP1B were decreased in desnutrin-ASKO BAT, making the gene expression profile more similar to that of WAT. The regulated transcription of gene networks depends on a balance between activating and repressive signals that are controlled by external factors to maintain energy homeostasis. We found that RIP140 and CTPB1, transcriptional co-repressors known to repress oxidative and thermongenic genes were upregulated in BAT. In this regard, mice lacking RIP14O are lean and resistant to diet-induced obesity due to de-repression of oxidative and thermogenic genes in WAT, resulting in BAT phenoytype in WAT (16). Our findings, raise the question of how ablation of desnutrin/ATGL could increased the expression of RIP140 and CTPB1 and transform the gene expression profile of BAT. It is conceivable, that the FAs generated via desnutrin/ATGL-mediated lipolysis could serve as ligands for nuclear hormone receptors, that control the transcription of RIP140 and CTBP1. Finally, it worth mentioning that, CTBP is activated by high cellular NADH levels (19). It is possible that NADH levels may be elevated in brown adipocytes of desnutrin-ASKO mice due to a decrease in re-esterification. In this regard, we previously found that overexpression of desnutrin/ATGL in adipose tissue of mice led in increased cylcling of FAs (6). However, further investigation will be required to confirm this hypothesis.

BAT from desnutrin-ASKO resembles WAT at both macroscopic and microscopic level. Desnutrin-ASKO BAT contained large unilocular lipid droplets, characteristic of WAT, compared to small multilocular lipid dropets found in BAT of flox/flox mice. Mitochondria from desnutrin-ASKO BAT also resembled mitochondria from WAT, in that they were less numerous with randomly oriented cristae. Recently, it has been observed that WAT and BAT are intermingled in a single fat depot of rodents and are capable of transdifferentiating into one another. This plasticity of adipocytes could be advantageous in response to changing energy demands and has been observed in conditions such as cold exposure. Notably, white-to-brown-to-white transdifferentiation is not the only example of this phenomenon in adipose tissue. During pregnancy or lactation, WAT changes to milk-secreting glands. We have demonstrated that ablation of desnutrin/ATGL is sufficient to trigger a transformation of BAT to WAT. However, we cannot exclude the possibility that this phenomenon is the result of de novo differentiation of stem cells or committed preadipocytes rather that transdifferentiation. It is interesting to note that β-adrenergic receptor deficient mice exhibit a similar phenotype in BAT presumably due to an inability to stimulated lipolysis (20). In this regard, hormone sensitive lipase (HSL) null mice display normal thermogenesis and suprisingly, WAT of HSL null mice attains BAT characteristics, including an upregulation of RIP140 and UCP-1, indicating that desnutrin/ATGL is sufficient for thermogenesis (21). Taken together, these findings underscore the importance of desnutrin/ATGL in the conversion of WAT and BAT.

Several lines of evidence indicate that desnutrin-ASKO mice have impaired thermogenesis. While normal wild type mice can withstand the cold without ill effects for 24 hours, desnutrin-ASKO mice are unable to maintain body temperature in the cold

reaching life-threatening hypothermia after only 90 min of cold exposure (22). Desnutrin-ASKO mice also have a decreased metabolic rate and are resistant to pharmacological stimulation by a β3 agonist. The impaired thermogenesis and oxygen consumption in desnutrin-ASKO mice is likely due to several factors. First, the supply of FAs from WAT lipolysis, which is increased during cold exposure and SNS activation is blunted. Therefore, brown adipocyte in desnutrin-ASKO are unable to receive sufficient FAs from white adipocytes. Futhermore, brown adipocytes from desnutrin-ASKO mice are also incapable of mobilizing their own TAG stores. As a result, insufficient amounts of FAs are available to activate UCP-1 and to provide substrate for FA oxidation. Finally, the decreased expression oxidative and thermogenic genes further impairs the thermogenic function in these mice. Interestingly we found that D2, which increases T3 levels to upregulate UCP-1 and increase thermogenesis was increased. However, our results clearly indicate that this pathway cannot compensate for lack of desnutrin/ATGL. Taken together, our findings show that desnutrin/ATGL is required for functional BAT thermogenesis and that other lipases or thermogenic pathways are unable to compensate for desnutrin/ATGL.

Inhibition of lipolysis resulted in massive TAG accumulation in both WAT and BAT. As a result other organs had to rely on their own TAG stores due to insufficient delivery of FAs from WAT, which prevented ectopic TAG storage in the liver. In this regard, desnutrin mice represent a paradoxical model, exhibiting increased adiposity yet protection from ectopic TAG storage. These findings are in contrast to total knockout mice of desnutrin/ATGL that exhibited massive TAG in multiple organs. According to the Randle hypothesis, a reciprocal relationship between glucose and FAs as an energy source exists. Due to the inability to hydrolyze TAG in adipose tissue, desnutrin-ASKO mice must rely on glucose for fuel. As a result, desnutrin-ASKO mice are protected from high-fat diet-induced insulin resistance.

In conclusion, we have shown that ablation of desnutrin/ATGL results diet induced obesity and massive TAG accumulation in WAT and BAT. However, despite increased adiposity, desnutrin-ASKO mice are protected from ectopic TAG storage and exhibit improved insulin sensitivity. More importantly, we have shown that ablation of desnutrin/ATGL, results in a remarkable transformation of BAT to WAT and impaired BAT function. It has been estimated that as little as 50g of BAT could account for 20% of daily energy expenditure(15). Therefore, it is possible that strategies designed to at targeting desnutrin/ATGL might offer promising therapeutic approaches for the treatment of obesity and related metabolic disorders.

REFERENCES

1. Duncan RE, Ahmadian M, Jaworski K, Sarkadi-Nagy E, Sul HS: Regulation of lipolysis in adipocytes. *Annu Rev Nutr* 27:79-101, 2007
2. Zimmermann R, Strauss JG, Haemmerle G, Schoiswohl G, Birner-Gruenberger R, Riederer M, Lass A, Neuberger G, Eisenhaber F, Hermetter A, Zechner R: Fat mobilization in adipose tissue is promoted by adipose triglyceride lipase. *Science* 306:1383-1386, 2004
3. Jenkins CM, Mancuso DJ, Yan W, Sims HF, Gibson B, Gross RW: Identification, cloning, expression, and purification of three novel human calcium-independent phospholipase A2 family members possessing triacylglycerol lipase and acylglycerol transacylase activities. *J Biol Chem* 279:48968-48975, 2004
4. Villena JA, Roy S, Sarkadi-Nagy E, Kim KH, Sul HS: Desnutrin, an adipocyte gene encoding a novel patatin domain-containing protein, is induced by fasting and glucocorticoids: ectopic expression of desnutrin increases triglyceride hydrolysis. *J Biol Chem* 279:47066-47075, 2004
5. Haemmerle G, Lass A, Zimmermann R, Gorkiewicz G, Meyer C, Rozman J, Heldmaier G, Maier R, Theussl C, Eder S, Kratky D, Wagner EF, Klingenspor M, Hoefler G, Zechner R: Defective lipolysis and altered energy metabolism in mice lacking adipose triglyceride lipase. *Science* 312:734-737, 2006
6. Ahmadian M, Duncan RE, Varady KA, Frasson D, Hellerstein MK, Birkenfeld AL, Samuel VT, Shulman GI, Wang Y, Kang C, Sul HS: Adipose overexpression of desnutrin promotes fatty acid use and attenuates diet-induced obesity. *Diabetes* 58:855-866, 2009
7. Ahmadian M, Wang Y, Sul HS: Lipolysis in adipocytes. *Int J Biochem Cell Biol* 42:555-559
8. Nedergaard J, Cannon B: The changed metabolic world with human brown adipose tissue: therapeutic visions. *Cell Metab* 11:268-272
9. Enerback S: Human brown adipose tissue. *Cell Metab* 11:248-252
10. Frontini A, Cinti S: Distribution and development of brown adipocytes in the murine and human adipose organ. *Cell Metab* 11:253-256
11. Gregoire FM, Smas CM, Sul HS: Understanding adipocyte differentiation. *Physiol Rev* 78:783-809, 1998
12. Smas CM SH: Pref-1, a protein containing EGF-like repeats, inhibits adipocyte differentiation. *Cell* 73:725-734, 1993
13. Seale P, Bjork B, Yang W, Kajimura S, Chin S, Kuang S, Scime A, Devarakonda S, Conroe HM, Erdjument-Bromage H, Tempst P, Rudnicki MA, Beier DR, Spiegelman BM: PRDM16 controls a brown fat/skeletal muscle switch. *Nature* 454:961-967, 2008
14. Christian M, Kiskinis E, Debevec D, Leonardsson G, White R, Parker MG: RIP140-targeted repression of gene expression in adipocytes. *Mol Cell Biol* 25:9383-9391, 2005

15. Fruhbeck G, Becerril S, Sainz N, Garrastachu P, Garcia-Velloso MJ: BAT: a new target for human obesity? *Trends Pharmacol Sci* 30:387-396, 2009
16. Leonardsson G, Steel JH, Christian M, Pocock V, Milligan S, Bell J, So PW, Medina-Gomez G, Vidal-Puig A, White R, Parker MG: Nuclear receptor corepressor RIP140 regulates fat accumulation. *Proc Natl Acad Sci U S A* 101:8437-8442, 2004
17. Cannon B, Nedergaard J: Brown adipose tissue: function and physiological significance. *Physiol Rev* 84:277-359, 2004
18. Randle PJ, Garland PB, Hales CN, Newsholme EA: The glucose fatty-acid cycle. Its role in insulin sensitivity and the metabolic disturbances of diabetes mellitus. *Lancet* 1:785-789, 1963
19. Fjeld CC, Birdsong WT, Goodman RH: Differential binding of NAD+ and NADH allows the transcriptional corepressor carboxyl-terminal binding protein to serve as a metabolic sensor. *Proc Natl Acad Sci U S A* 100:9202-9207, 2003
20. Bachman ES, Dhillon H, Zhang CY, Cinti S, Bianco AC, Kobilka BK, Lowell BB: betaAR signaling required for diet-induced thermogenesis and obesity resistance. *Science* 297:843-845, 2002
21. Strom K, Hansson O, Lucas S, Nevsten P, Fernandez C, Klint C, Moverare-Skrtic S, Sundler F, Ohlsson C, Holm C: Attainment of brown adipocyte features in white adipocytes of hormone-sensitive lipase null mice. *PLoS One* 3:e1793, 2008
22. Christoffolete MA, Linardi CC, de Jesus L, Ebina KN, Carvalho SD, Ribeiro MO, Rabelo R, Curcio C, Martins L, Kimura ET, Bianco AC: Mice with targeted disruption of the Dio2 gene have cold-induced overexpression of the uncoupling protein 1 gene but fail to increase brown adipose tissue lipogenesis and adaptive thermogenesis. *Diabetes* 53:577-584, 2004

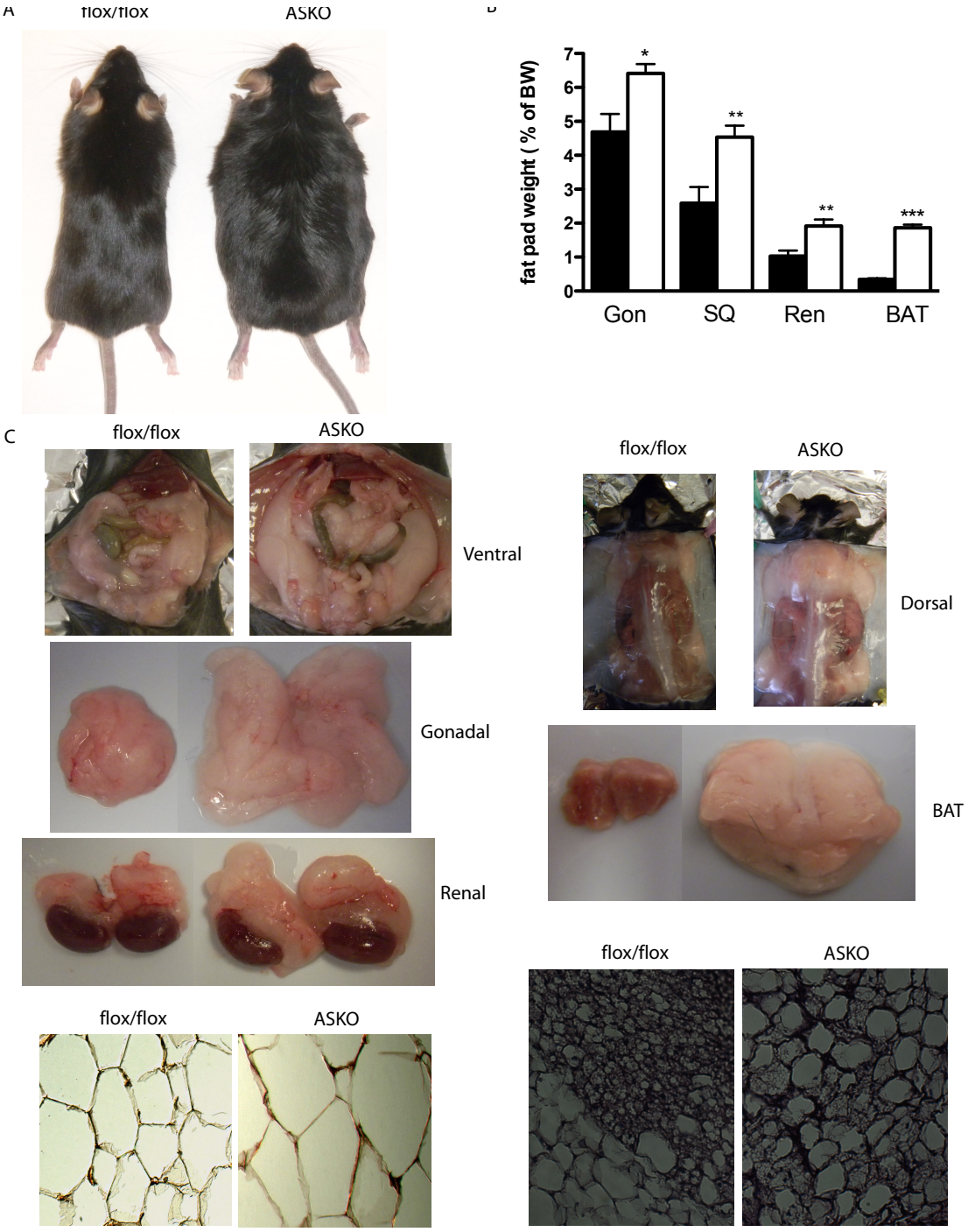

Figure III-1. Increased adiposity in desnturin-ASKO mice. A) Representative photographs of male flox/flox and desnutrin-ASKO at 16-weeks of age on a HFD (upper). Representative images of hematoxylin and eosin–stained sections of gonadal WAT from male flox/flox and desnutrin-ASKO mice at 16-weeks of age fed a HFD (lower) B) Gonadal (Gon), subcutaneous(SQ), renal (Ren) and brown adipose tissue (BAT) fat pad weight from 16 week-old HFD-fed male mice flox/flox and desnutrin-ASKO mice, expressed as a percent of body weight (n=7). C) Representative photographs of gonadal and renal fat depots (left, upper and middle) and BAT (right, upper and middle) as well as H&E-stained paraffin-embedded sections of gonadal (left, lower) and BAT (right, lower) *$P < 0.05$, **$P < 0.01$, ***$P < 0.001$

A

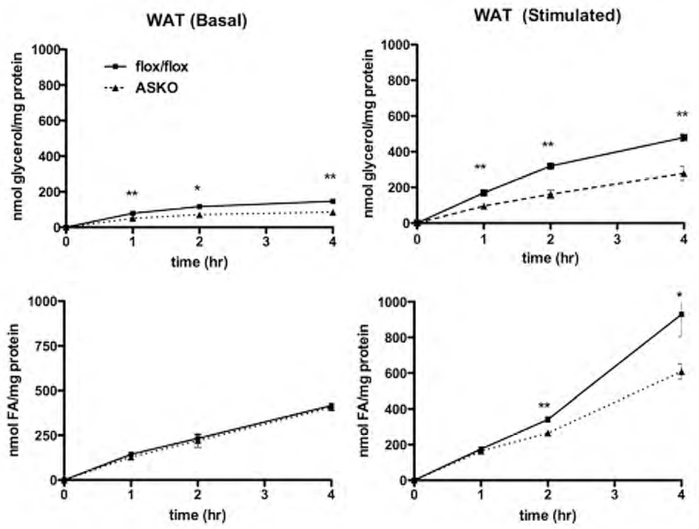

B

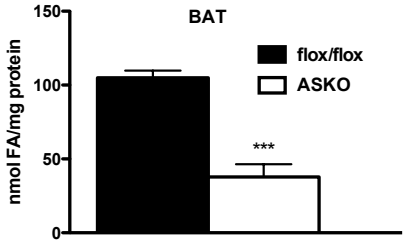

Figure III-2. Decreased lipolysis in desnutrin-ASKO mice. A) Glycerol (left) and fatty acid (right) release from 50 mg explants of fresh gonadal WAT incubated under basal conditions (upper) or stimulated with 10μM isoproterenol (lower). B) FA release after 4hrs from 40mg explants of BAT incubated under basal conditions. (n=6)*$P < 0.05$, **$P < 0.01$, ***$P < 0.001$

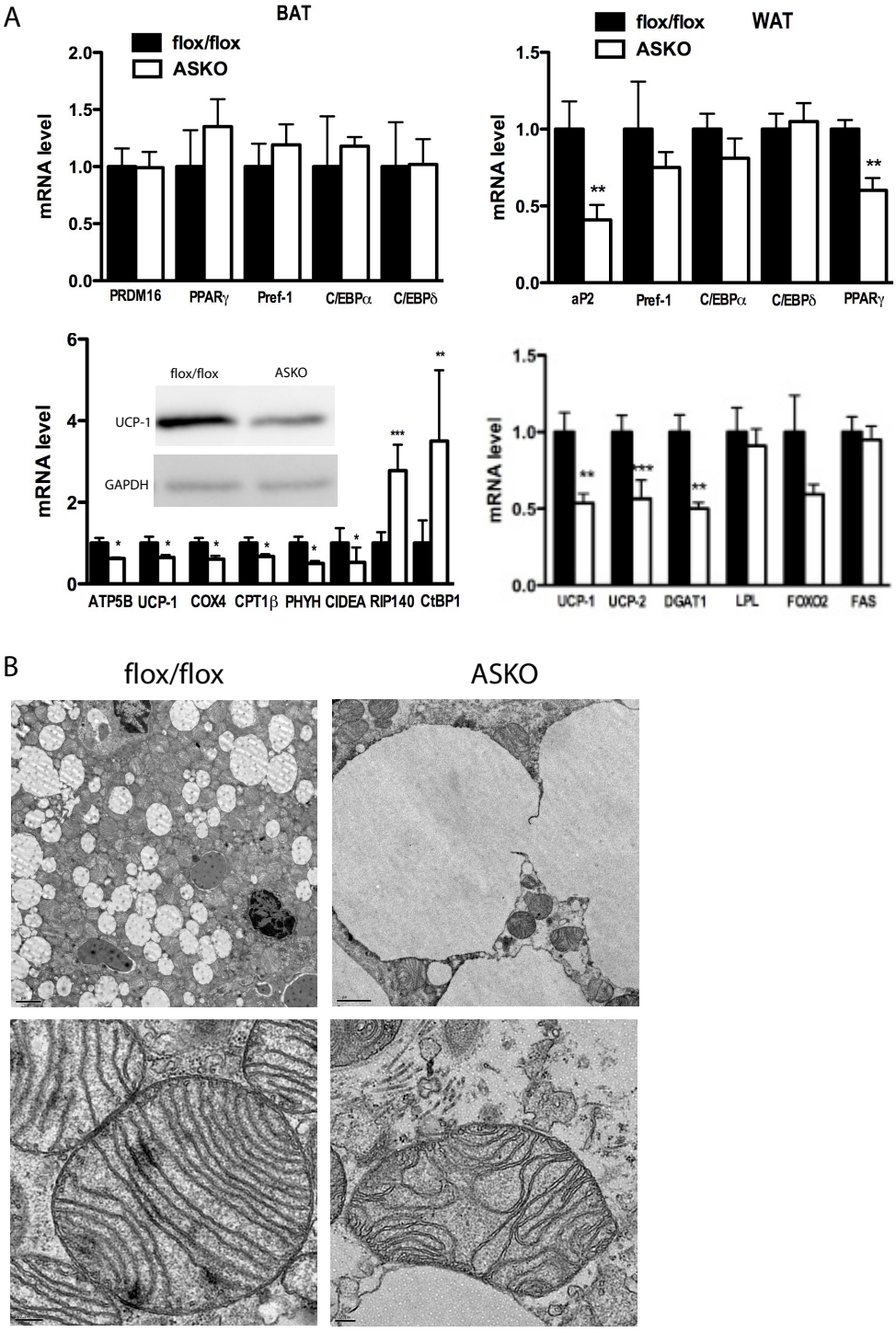

Figure III -3. Conversion of BAT to WA T. A) Gene expression profile of genes involved in differentiation or adipocyte function from BAT (left) and WAT (right) of flox/flox and desnutrin-ASKO mice as well as western blot from BAT of UCP-1 (inset, left) (n=4-10) B) Transmission electron microscopy images showing lipid droplets (upper) and mitochondria (lower) from BAT of flox/flox and desnutrin-ASKO mice. $*P < 0.05$, $**P < 0.01$, $***P < 0.00\ 1$

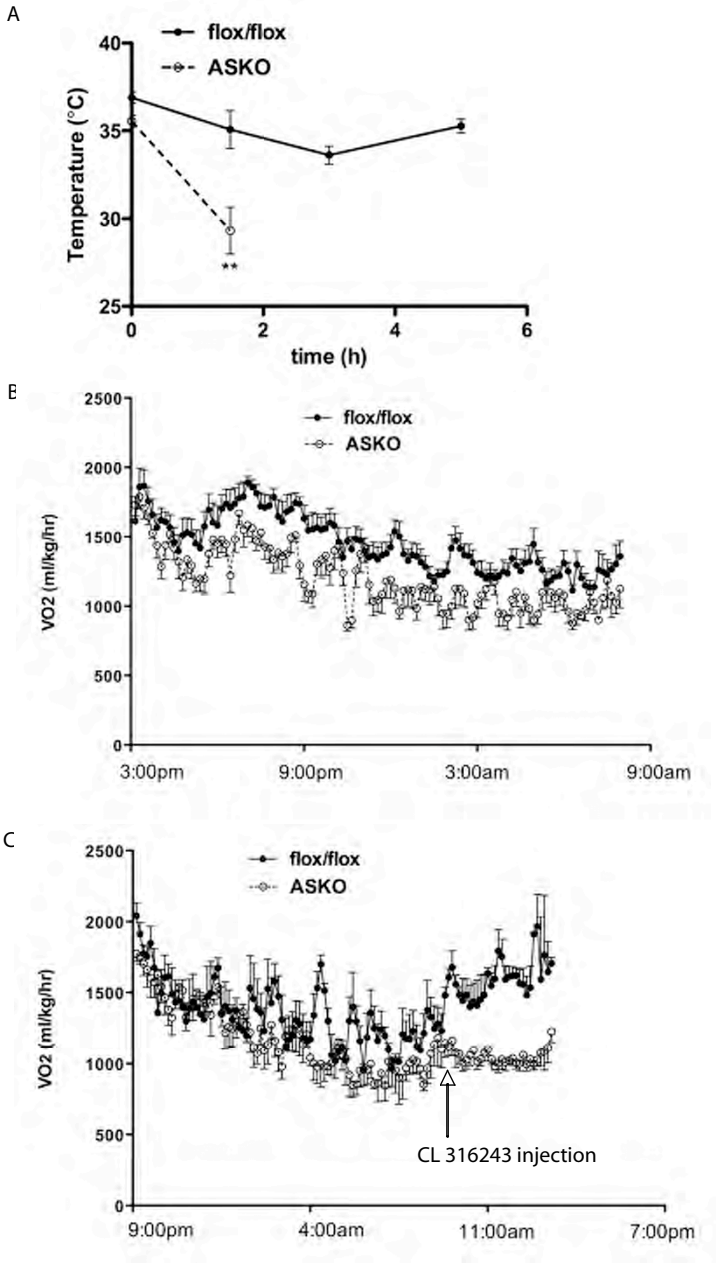

Figure III-4. Impaired thermogenesis in desnutrin-ASKO mice. A) Body temperatures of overnight-fasted flox/flox and DESNUTRIN-ASKO mice exposed to the cold. B) Oxygen consumption rate ($\dot{V}O2$) measured through indirect calorimetry C) Oxygen consumption rate ($\dot{V}O2$) measured through indirect calorimetry after intraperitoneal injection of CL316243. (n=6) $^{**}P < 0.01$

A

	flox/flox	ASKO
TG (mg/dl)	51.7 ± 6.0	45.7 ± 6.7
FFA (mmol/L)	0.54 ± 0.02	0.33 ± 0.02 (***)
Glycerol (mmol/L)	0.65 ± 0.12	0.48 ± 0.08
Insulin (ng/ml)	1.21± 0.12	0.37± 0.06 (***)

B

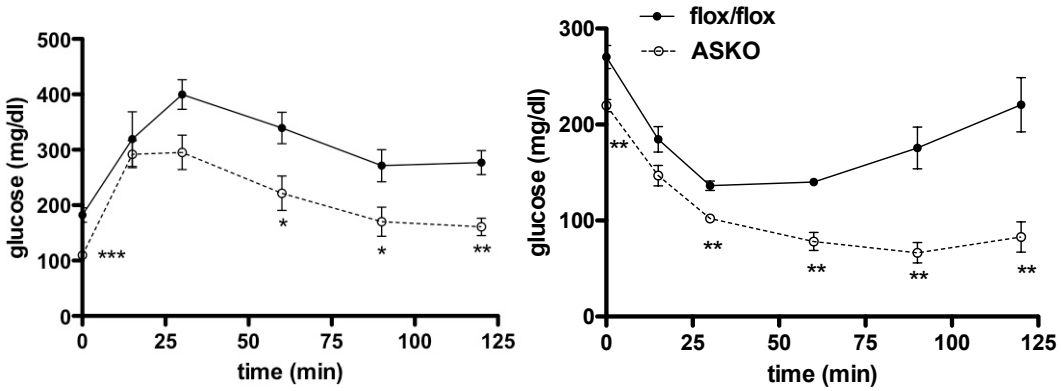

C

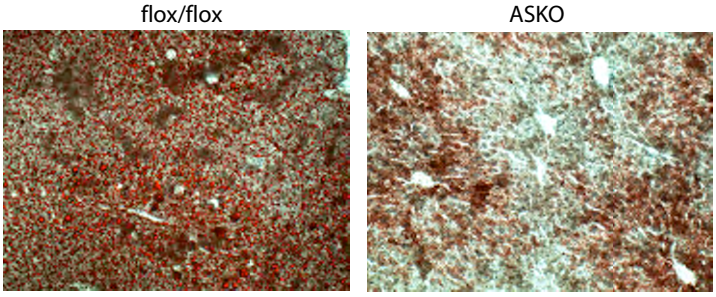

Figure III-5. **Improved insulin sensitivity in desnutrin-ASKO mice.** A**)** Serum parameters (n=6-8) B) Glucose and insulin tolerance tests (GTT and ITT) from 12-week old male mice fed a HFD C**)** Cryosections of frozen livers stained with Oil red O C) **P* < 0.05, ***P* < 0.01, ****P* < 0.001

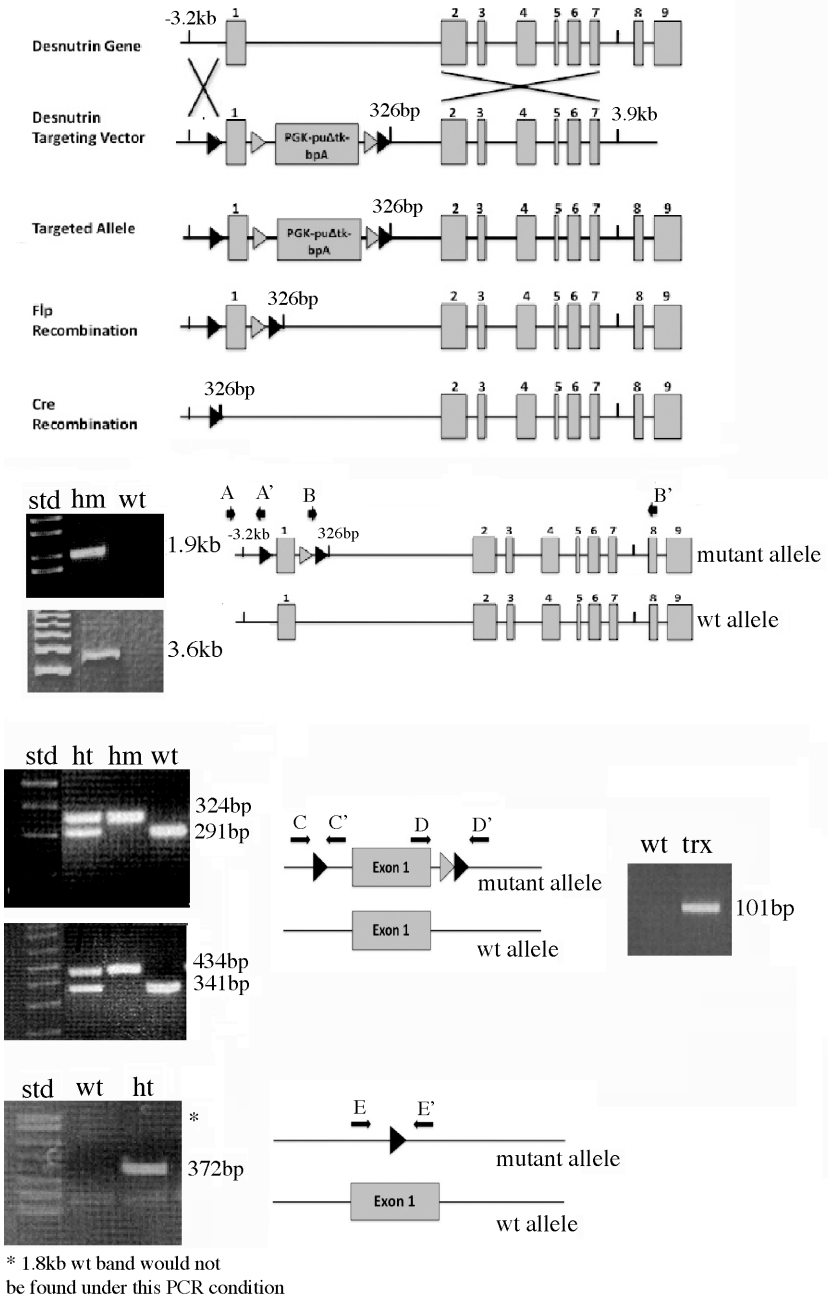

Figure III-S1 Generation of desnutrin-ASKO mice. A) Construction of targeting vector and generation of adipose tissue specific knockout mice for the desnutrin gene (desnutrin-ASKO mice) using the Flp-Cre strategy. B) PCR verification for homologous recombination, C) Flp recombination for removal of puromycin using tail DNA. After transgenic Cre insertion was verified by PCR (right), D) Verification of Cre recombination using adipose tissue DNA for removal of exon 1.

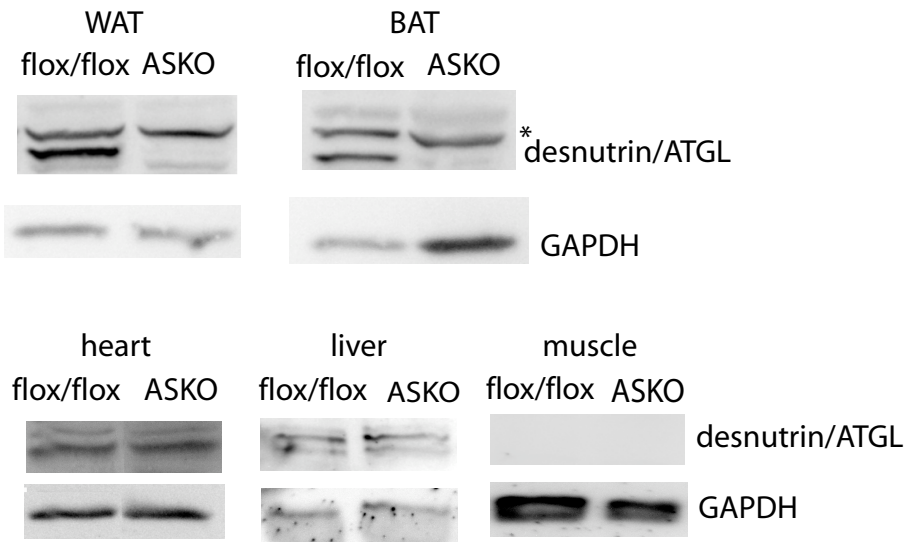

Figure III -S2 Verification of desnutrin/ATGL adipose-specific ablation. A) Western blot analysis from 40 g of lysates from WAT, BAT, heart, liver and skeletal muscle from flox/flox and desnutrin-ASKO mice, using a desnutrin-specific antibody. *non-specific

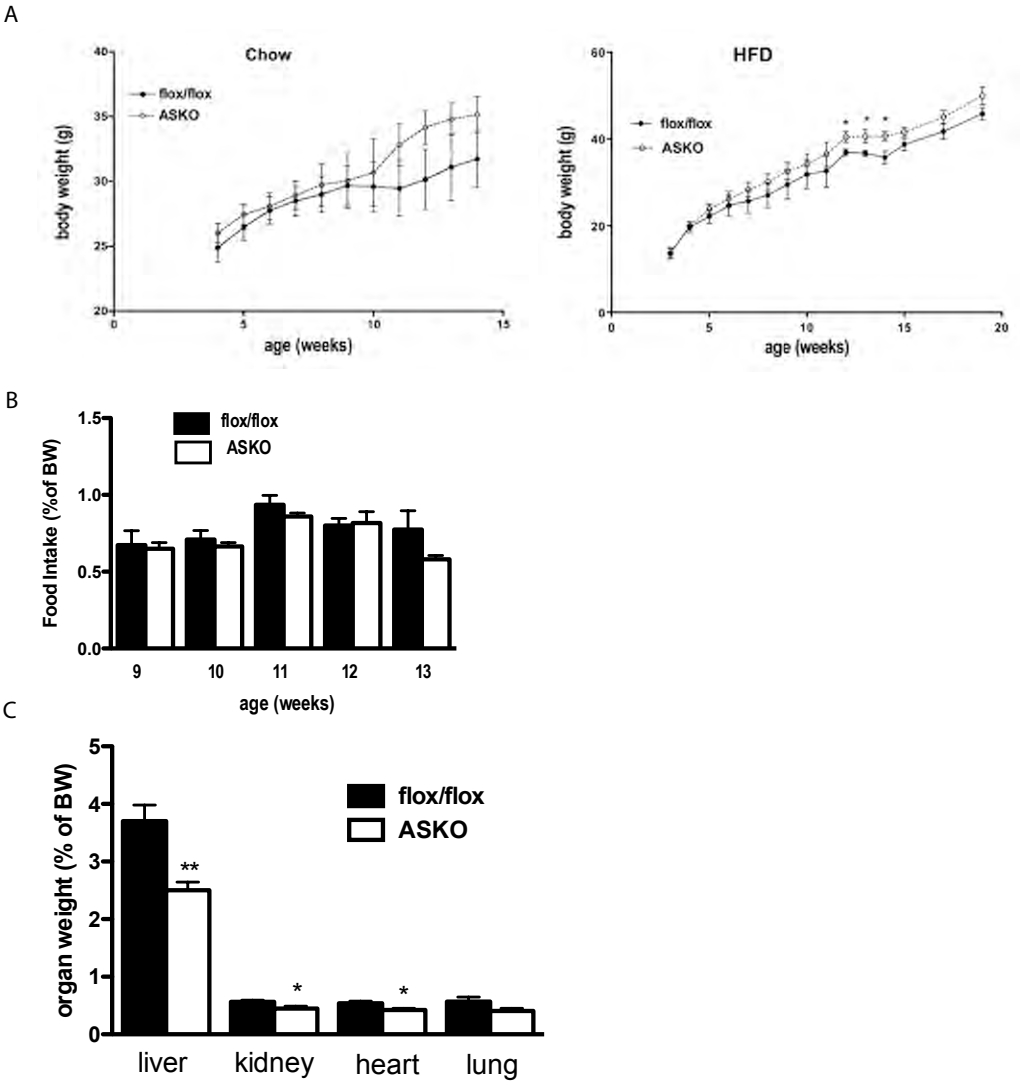

Figure III-S3. Increased body weight in desnutrin-ASKO mice despite no change in food intake. A) Body weight of male mice fed a standard chow (left) or high fat diet (HFD) (right). B) Food intake in male HFD-fed mice (n=8-14) C) Liver, kidney, heart and lung weights (upper) from 16 week-old HFD-fed male mice flox/flox and desnutrin-ASKO mice, expressed as a percent of body weight (n=7). *$P < 0.05$, **$P < 0.01$

Chapter IV: AdPLA ablation increases lipolysis and prevents obesity induced by high fat feeding or leptin deficiency

ABSTRACT

A main function of white adipose tissue is to release fatty acids from triacylglycerol for other tissues to use as an energy source. While endocrine regulation of lipolysis has been extensively studied, autocrine/paracrine regulation is not well understood. Here, we describe the role of AdPLA, the newly identified major adipocyte phospholipase A_2, in the regulation of lipolysis and adiposity. AdPLA null mice have a markedly higher rate of lipolysis, due to increased cAMP levels arising from the marked reduction in adipose PGE_2 that binds the Gαi-coupled receptor, EP3. AdPLA null mice have drastically reduced adipose tissue mass and triglyceride content, with normal adipogenesis. They also have higher energy expenditure with higher fatty acid oxidation within adipocytes. AdPLA deficient *ob/ob* mice remain hyperphagic but lean, with increased energy expenditure, yet have ectopic triglyceride storage and insulin resistance. AdPLA is a major regulator of adipocyte lipolysis and critical for the development of obesity.

INTRODUCTION

Triacylglycerol (TAG) in adipose tissue is the major energy storage form in mammals. An imbalance between energy intake and expenditure can result in excess TAG accumulation in adipose tissue, resulting in obesity (1). In morbid obesity, although controversial, increased adipocyte number (hyperplasia) may occur through adipocyte differentiation of precursor cells present in adipose tissue (2). However, obesity is largely attributed to adipocyte hypertrophy that occurs when TAG synthesis exceeds breakdown (lipolysis), resulting in elevated TAG storage (1; 3). Unlike TAG synthesis (4; 5) that occurs at high levels in other tissues, including liver for VLDL production, lipolysis for the provision of fatty acids as an energy source for use by other tissues is unique to adipocytes (6). Lipolysis in adipocytes is tightly regulated by hormones that are secreted according to nutritional status. During fasting, lipolysis is stimulated by catecholamines that increase cAMP levels, whereas, in the fed state, lipolysis is inhibited by insulin (1; 3). While regulation of lipolysis by these endocrine factors has been extensively studied, the local regulation of lipolysis in adipose tissue by autocrine/paracrine factors is not well understood.

We recently identified an adipocyte phospholipase A_2 (PLA_2) by microarray analysis that we named Adipose-specific phospholipase A_2 (AdPLA) (7) (also called PLA2G16, HRASLS3, HREV107, HREV107-3, MGC118754, H-REV107-1). AdPLA belongs to a new group of intracellular calcium-dependent PLA_2s. The PLA_2 superfamily of enzymes catalyze hydrolysis of the *sn*-2 ester bond of phospholipids (8). PLA_2s function in remodeling of membrane phospholipids by acylation/deacylation cycles (8). More importantly, since the *sn*-2 position of phospholipids is typically enriched in arachidonic acid and other unsaturated fatty acids, PLA_2s catalyze the initial rate-limiting step in the production of eicosanoids (9). Eicosanoids, including prostaglandins (PGs), are potent local mediators of signal transduction and are known to modulate many physiological systems and exert autocrine/paracrine action through binding to specific G-coupled receptors (10). Although their physiological significance is unclear, there are some reports that suggest PGs may modulate adipocyte differentiation *in vitro* (11-14). In mature adipocytes, depending on the concentrations used, some PGs have been reported to stimulate, inhibit or exert no effect on lipolysis (15; 16). Regardless, since AdPLA is highly expressed only in adipose tissue, we hypothesized that it could play an important role in adipose-specific

processes such as lipolysis through modulation of arachidonic acid provision for PG biosynthesis.

Here, we show that AdPLA is the major PLA_2 in adipose tissue, and regulates lipolysis in an autocrine/paracrine manner through PGE_2. We report that ablation of *Adpla* prevents obesity from high fat feeding or leptin deficiency by regulating lipolysis through the PGE_2/EP3/cAMP pathway.

METHODS

Cell culture. We isolated, maintained and differentiated MEF and 3T3-L1 as previously described (17).

RNA analysis. We subjected total RNA isolated with Trizol reagent (Invitrogen) to Northern blotting (Amersham) or to RT-qPCR or RT-PCR. Primers utilized with the ABI PRISM 7700 sequence fast detection system (PE Applied Biosystems) were pre-validated for efficiency of amplification that was reported to be the same for all and essentially 100%.

Western Blotting. We separated proteins by 12% SDS-PAGE, transferred to nitrocellulose and probed with primary antibodies against AdPLA, phospho-AMPKα (Thr172), AMPKα, HSL, desnutrin/Atgl, phosphoserine, IRS-1, phospho-IRS-1 (Ser307), Gapdh, or β-actin.

Lipolysis. We performed lipolysis studies in adipocytes isolated as previously described(18) from gonadal WAT, and in explants from freshly removed epididymal fat pads (~20 mg) and MEF differentiated to adipocytes. Samples were incubated in Krebs-Ringer medium buffered with bicarbonate plus HEPES with 3.5% fatty acid-free BSA and 0.1% glucose (KRB), with or without 200 nM isoproterenol (Sigma), PGE_2 (Cayman), adenosine deaminase (Calbiochem), 0.5 μM Triacsin C (Biomol) or L826266 (Merck Frosst Canada), and measured glycerol (Sigma) and fatty acid (Wako). We determined prostaglandin levels by competitive enzyme immunoassay (R&D) after solid phase extraction by SPE cartridges (C-18) (Cayman), and cAMP levels by competitive immunoassay (R&D).

Mouse maintenance. All studies received approval from the University of California at Berkeley Animal Care and Use Committee. We utilized mice on a pure C57BL/6J background, after backcrossing for 10 generations, for studies of lipolysis, energy expenditure, hyperinsulinemic-euglycemic clamping, fatty acid oxidatation, TAG clearance, and for all studies on dKO mice. In all other experiments, we compared *Adpla*–/– and wild-type littermates in a mixed genetic background (C57BL/6J and 129 SVJ), but the results were also confirmed in a C57BL/6J background. We provided either a SD or a HFD (45 kcal% fat, 35 kcal% carbohydrate and 20 kcal% protein, Research Diets) *ad libitum*. To generate *ob*/*ob* mice deficient in *Adpla*, heterozygous C57BL/6J *ob*–/+ mice (Jackson Laboratory) were bred with *Adpla*–/– mice under a C57BL/6J background resulting in heterozygotes that were interbred to produce dKO mice.

Carcass and tissue analysis. We homogenized frozen, eviscerated carcasses from 40 wk-old mice fed a HFD in water, dried the homogenates to a constant weight, and estimated lipid

content by the method of Bligh and Dyer (19).We extracted tissue neutral lipids by the method of Folch (20), isolated TAG and DAG by TLC, and quantitated lipids using Infinity reagent (Thermo Trace) after sonification in 1% Triton X-100.

Glucose and insulin tolerance tests. For GTT, we injected mice intraperitoneally with D-glucose (WT or KO, 2 mg/g BW; dKO or ob/ob mice, 0.625 mg/g BW) following an overnight fast and monitored tail blood glucose levels. For ITT, mice were injected with insulin (humulin, Eli Lily) at a level of 0.5 mU/g BW (WT and KO mice on a SD), 0.75 mU/g BW (WT and KO mice fed a HFD) or 1.75 mU/g BW (*ob/ob* and dKO) after a 5 h fast.

Hyperinsulenemic-euglycemic clamp. We implanted jugular venous catheters seven days prior to the study. After an overnight fast, we infused [3-^{3}H]glucose (Perkin Elmer) at a rate of 0.05 μCi min^{-1} for 2 hours to assess basal glucose turnover, followed by the hyperinsulinemic-euglycemic clamp for 140 min with a primed/continuous infusion of human insulin (300 pmol kg^{-1} prime (43 mU kg^{-1})) over 3 min, followed by 42 pmol kg^{-1} min^{-1} (6 mU kg^{-1} min^{-1}) infusion (Novo Nordisk, Princeton, NJ), a continuous infusion of [3-^{3}H]glucose (0.1 μCi min^{-1}), and a variable infusion of 20% dextrose to maintain euglycemia (~100–120 mg dl^{-1}). We obtained plasma samples from the tail and measured tissue-specific glucose uptake after injection of a bolus of 10 μCi of 2-deoxy-D-[1-^{14}C]glucose (Perkin Elmer) at 85 min(21). We analyzed our results as previously described (22).

Histological analysis. We embedded tissues in paraffin and stained 6 μm thick sections with hematoxylin and eosin, and determined adipocyte cell size using image J software measuring at least 300 cells from each sample.

PLA activity. We assayed supernatants of WAT for PLA activity by monitoring the liberation of [^{14}C]palmitate from 1,2-di[1-^{14}C]palmitoyl-*sn*-glycero-3-phosphocholine as previously described(23).

Indirect calorimetry and body temperature. We measured oxygen consumption (VO_2) using the Oxymax system (Columbus Instruments).

$^{2}H_2O$ Labeling and GC-MS Analysis. We extracted lipids from gonadal fat pads of mice administered $^{2}H_2O$ in drinking water for a 2-week period, trans-esterified the lipid phase by incubation with 3 N methanolic HCl and separated glycerol from fatty acid (FA)-methyl esters using the Folch technique (20). We lyophilized and derivatized the aqueous phase containing free glycerol to glycerol triacetate by incubation with acetic anhydride-pyridine (2:1). We employed a model 6890 GC with 5973 mass spectrometer (Agilent Technologies), fitted with a DB-225 fused silica column (J&W). We analyzed glycerol-triacetate under chemical ionization conditions by selected ion monitoring of mass-to-charge ratios (*m/z*) 159-161 (representing M_0–M_2) and FA-methyl esters as described elsewhere(24).
We measured fractional TAG-glycerol synthesis as described (24; 25):

$$f_{\mathrm{TAG}} = \mathrm{EM1}_{\text{TAG-glycerol}} \; / \; \mathrm{A_1}\infty_{\text{TAG-glycerol}}$$

We estimated net lipolysis from f_{TAG} synthesis and adipose mass as follows:

[f_{TAG} × (adipose mass / labeling time) – (Δadipose mass / labeling time)] /fat pad mass

Values with net lipolysis equivalent to zero were excluded from analysis.

Fatty Acid Oxidation. We determined fatty acid oxidation in isolated adipocytes as previously described (26).

Statistical Analysis. We assessed the results by Student's *t* test to compare two groups or by one-way ANOVA with Dunnett's post-hoc test for multiple comparisons and expressed them as means ± SEM. We analyzed adipocyte size distribution by Wilcoxon Signed Rank Test.

Reference Sequences. *Adpla* is located on chromosome 19 in the mouse genome. Reference sequence identifiers for mouse *Adpla* are: gene (NT_039687.7), protein (NP_644675), and mRNA (NM_139269).

RESULTS

Adpla is expressed at a high level primarily in adipose tissue

As we have shown previously (7), the 1.3 kb *Adpla* mRNA and the 18 kDa AdPLA protein are expressed in mice at a high level only in white adipose tissue (WAT) and brown adipose tissue depots (BAT) (Fig. 1a). *Adpla* is found exclusively in adipocytes and not in the stromal vascular fraction of adipose tissue that contains preadipocytes (Fig. 1a). In humans, similar to mice, *Adpla* was undetectable by RT-PCR in skeletal muscle and barely detectable in liver, but was abundantly expressed in WAT (Fig. 1a). We measured expression of all currently known intracellular PLA_2s. (7) We detected *Adpla* at approximately 10^3- to 10^5-fold higher levels (Fig. 1b), indicating that AdPLA is the major PLA_2 in adipose tissue. We investigated *Adpla* regulation in different nutritional and hormonal states. *Adpla* mRNA level in epididymal WAT was low in fasted mice but rose drastically (by 8-fold) after feeding a high carbohydrate, fat-free diet ($P < 0.01$) (Fig. 1c). *Adpla* mRNA was also low in adipose tissue of streptozotocin-diabetic mice, but similarly increased by approximately 10-fold after insulin administration. We observed substantially higher *Adpla* mRNA in WAT of genetically obese *ob/ob* mice that are hyperinsulinemic and have markedly higher adipose tissue TAG storage (Fig. 1c), and higher AdPLA protein levels in obese *ob/ob* and *db/db* mice than in lean WT mice in both the fasted and refed states (Fig. 1c). *Adpla* is therefore highly and specifically expressed in adipocytes and is upregulated by feeding/insulin and in obesity.

Adpla null mice have reduced adiposity and are resistant to diet-induced obesity

To elucidate the physiological role of AdPLA, we used gene targeting to generate *Adpla* null mice (Suppl. Fig. 1) that we compared with wild-type littermates under a mixed genetic background (C57BL/6J and 129 SVJ) as well as on a C57BL/6J background (genetic backgrounds of mice utilized in specific experiments are indicated in the Methods). Although total body weights did not differ at weaning, at 11 wks, *Adpla* null mice fed a high fat diet (HFD) began to gain weight at a slower rate than wild-type littermates (Fig. 1d). This disparity in body weight was exacerbated as mice aged such that by 64 wks of age, *Adpla* null mice fed a HFD

weighed only 39.1 ± 0.2 g (n = 3), versus wild-type littermates that weighed 73.7 ± 0.3 g (n = 3), P<0.001. The decreased weight gain was also observed in *Adpla* null mice fed a standard chow diet (SD), albeit to a lesser extent (Fig. 1d). Food intakes in *Adpla* null and wild-type mice were equivalent, despite differences in body weights (0.09 g d^{-1} g BW^{-1}, n = 6).

The lower body weight of *Adpla* null mice was largely accounted for by a reduction in WAT weight. Body composition analysis indicated that *Adpla* null mice had decreased TAG content (Suppl. Table 1). At 18 wks, *Adpla* null mice fed a HFD had substantially smaller WAT depots compared to wild-type littermates with a combined WAT depot weight that was 74% lower (Fig. 2a). This difference increased further as the mice aged. We observed the same pattern of lower body and fat pad weight in *Adpla* null mice fed a SD, and in *Adpla* null mice under a C57BL/6J background (data not shown).

By standard pathology analysis, *Adpla* null mice showed no evidence of any gross, microscopic, or functional abnormalities, aside from reduced adiposity. However, as described in later sections, upon HFD feeding we detected enlarged livers in *Adpla* null mice with increased liver TAG content (Supplementary Table 1), although liver function was largely normal (Supplementary Fig. 2). Moreover, blood cell profile and immunological parameters in serum and adipose tissue were not changed in these mice compared to wild-type (Supplementary Fig. 2), and the weights of other organs were similar between the two groups (data not shown).

Adpla null mice have smaller adipocytes rather than impaired adipocyte differentiation

A decrease in adipose tissue mass can result from a reduction in adipocyte size and/or a reduction in adipocyte number due to impaired differentiation. Evidence indicates that AdPLA deficiency did not significantly affect adipocyte differentiation. Expression levels of adipogenic transcription factors (27),(28) including CCAAT/enhancer binding protein alpha (*C/ebpa*) and peroxisome proliferator-acivated receptor gamma (*Pparg*) as well as the preadipocyte marker preadipocyte factor 1 (*Pref1*), were similar in wild-type and *Adpla* deficient WAT, as were late markers of adipocyte differentiation, including fatty acid synthase (*Fas*), diglyceride acyltransferase 1 (*Dgat1*), and adipocyte fatty acid binding protein (*aP2/aFabp*) (Fig. 2b). DNA content in the fat depots of *Adpla* null and wild-type mice also did not differ significantly (140.4 ± 22.6 μg versus 123.7 ± 14.6 μg DNA per fat pad, respectively, n = 6). We employed mouse embryonic fibroblasts (MEF) from wild-type and *Adpla* null embryos as well as 3T3-L1 cells transfected with *Adpla* or control vector. After undergoing differentiation to adipocytes in high insulin containing media, there were no differences between wild-type and *Adpla* null MEF or between *Adpla* overexpressing and control 3T3-L1 cells with regards to rounded adipocyte morphology or Oil red O staining (Fig. 2b). Expression of adipocyte markers such as *C/ebp*a, *Ppar*g, *aP2/aFabp* and *Pref1* were also similar between wild-type and *Adpla* null MEF, confirming the same degree of differentiation (Fig. 2b).

Histological analysis showed that epididymal WAT from *Adpla* null mice contained a significantly greater frequency (P < 0.05) of the smallest adipocytes and a lower frequency of the midsized and largest adipocytes (P < 0.01) (Fig. 2c). We also found drastically decreased TAG content in adipose tissue of *Adpla* null mice (Fig. 2a). *Adpla* ablation therefore causes adipocyte hypotrophy due to lower TAG accumulation and smaller adipocyte size, rather than impaired adipocyte differentiation.

Adpla ablation increases lipolysis in adipose tissue

To investigate if the drastically decreased adiposity observed in AdPLA null mice was due to increased lipolysis, we measured *in vivo* TAG metabolism over a two week period using a recently developed heavy water labeling technique (24). The fractional contribution of TAG-glycerol synthesis to adipose tissue TAG was significantly higher in *Adpla* null mice, reflecting a greater than 2-fold higher rate of replacement of preexisting TAG molecules with newly labeled TAG-glycerol, indicating increased TAG turnover (Fig. 3a). In agreement, the net *in vivo* lipolytic rate, calculated from the absolute rate of new TAG synthesis and the change in adipose tissue mass, was also 4- to 6-fold higher per gram of adipose tissue in *Adpla* null mice compared to wild-type mice (Fig. 3b). We measured [U-^{14}C]palmitate incorporation into TAG in adipose tissue explants and found similar incorporation in wildtype or AdPLA null mice, indicating comparable WAT fatty acid esterification in these animals (Fig. 3C). Therefore, we conclude that TAG hydrolysis, but not synthesis, is altered in WAT of AdPLA null mice.

To further investigate the effect of *Adpla* ablation on lipolysis, we compared basal and stimulated glycerol and fatty acid release from explants of WAT from *Adpla* null and wild-type mice (Fig. 3d). Under basal conditions, rates of glycerol and fatty acid release were significantly higher in adipose tissue from *Adpla* null mice. Furthermore, isoproterenol-stimulated lipolysis was also higher in *Adpla* deficient adipose tissue. Notably, the molar ratio of FFA to glycerol released from WAT explants was lower in AdPLA null mice (Fig. 3e). Because of the heterogeneity of cell populations within WAT explants, we also examined the effect of *Adpla* ablation on lipolysis in adipocytes differentiated from MEF that were isolated from *Adpla* null embryos. Probably due to the very high level of insulin in the media, the basal rate of lipolysis was very low in these cells and we could not detect differences in basal lipolysis between adipocytes differentiated from wild-type and *Adpla* null MEF (Fig. 3f). This finding is in agreement with the comparable lipid content in MEF differentiated adipocytes (Fig. 2b). However, isoproterenol stimulated lipolysis, measured as free fatty acid release, was significantly higher in adipocytes differentiated from *Adpla* null MEF (Fig. 3f). These results clearly indicate that lack of *Adpla* results in increased lipolysis in adipose tissue.

***Adpla* null mice have reduced total PLA activity and PGE_2 levels in adipose tissue**

PLA activity in WAT was dramatically reduced by 82% in *Adpla* null mice (from 3.71 pmol mg^{-1} min^{-1} in wild-type to only 0.66 pmol mg^{-1} min^{-1}) (Fig. 4a), while expression of other PLA_2s was unchanged. This finding establishes AdPLA as the major PLA in adipose tissue. Given the inverse relationship between PLA activity and lipolysis in *Adpla* null mice, we hypothesized that AdPLA may function in adipose tissue to regulate lipolysis locally by generating arachidonic acid for the production of PGs. We first measured levels in wild-type mice of PGs known to be found in adipose tissue. PGE_2 was present at significantly higher levels than any other PGs which were detected at levels well below effective concentrations required for binding to their cognate receptors (29) (Fig. 4b). We next determined expression levels in adipose tissue of the receptors for these PGs and found that EP3 was detected at a markedly higher level than other receptors examined including IP, DP, and EP1 (all undetectable) as well as EP2 and EP4 that were present at much lower levels (Fig. 4b). When we compared the levels of various PGs in adipose tissue from *Adpla* null and wild-type mice (Fig. 4b), we found that $PGF_2\alpha$ and 15-deoxy-$\Delta^{12,14}$-PGJ_2 that have been reported to affect adipocyte differentiation *in vitro* (13; 30; 31) were unchanged in *Adpla* deficient adipose tissue. However, PGE_2 levels were reduced to 12% of wild-type levels in *Adpla* deficient adipose tissue. PGI_2 levels were also significantly reduced. However, PGI_2 concentrations were well below those required for receptor

activation, and IP was not detected in adipose tissue. Since PGE_2 and EP3 were found in adipose tissue at the highest levels, and since PGE_2 level was the most drastically affected of the PGs in *Adpla* null adipose tissue, we postulated that the change in PGE_2 through EP3 may have been a major contributor to the observed effects.

If AdPLA regulates the production and release of PGE_2 that can bind Gαi-coupled EP3, then cAMP levels should be increased in adipose tissue of *Adpla* null mice. Indeed, we detected an approximate 2-fold increase in cAMP levels relative to wild-type (Fig. 4c) and found significantly higher phosphorylation of hormone-sensitive lipase (HSL) in the absence of a change in HSL or desnutrin/ATGL protein levels (Fig. 4d). Our results support the idea that AdPLA that is induced by feeding/insulin, inhibits lipolysis by increasing PGE_2 that, in turn, activates EP3 and thereby decreases cAMP levels. In this regard, addition of exogenous PGE_2 decreased lipolysis to wild-type levels in differentiated adipocytes derived from *Adpla* null MEF (Fig. 4e) and in WAT explants (data not shown) as well as in isolated adipocytes from *Adpla* null mice (Fig. 4f). The addition of PGE_2 also restored cAMP levels in adipocytes isolated from *Adpla* null mice (Fig. 4g). Addition of L826266, an EP3 antagonist, prevented the anti-lipolytic effect of PGE_2 in adipocytes (Fig. 4h), providing evidence that EP3 mediates the anti-lipolytic effect of PGE_2.

Adpla ablation prevents obesity in *ob/ob* mice

To test whether *Adpla* deficiency could prevent genetic obesity such as that caused by leptin deficiency, we introduced *Adpla* deficiency into *ob/ob* mice to generate double knockout (dKO) mice. On a SD, dKO mice gained drastically less weight than *ob/ob* mice (Fig. 5a,b). Striking differences in body weights were apparent by as early as 6 wks and became even more pronounced with age. Surprisingly, differences were not attributable to a reduction in food consumption since intakes were, in fact, somewhat increased in dKO mice compared to *ob/ob* mice (Fig. 5b). However, dKO mice exhibited reduced adiposity with a marked reduction in the weight of WAT depots compared to *ob/ob* mice (Fig. 5c). Other organ weights, except for the increased liver weight, were similar between the two groups of mice (data not shown). Carcass analysis showed that body and carcass weights of *Adpla* null and dKO at 40 weeks of age were less than those of either wild-type or *ob/ob* mice, while the proportion of water and lean tissue mass was increased (Fig. 5d). Percent lipid was reduced by 81% in AdPLA null and 69% in dKO mice compared to wild-type and *ob/ob* mice, respectively reflecting the drastically leaner phenotype in AdPLA deficiency.

We observed significantly higher lipolysis in dKO mice under both basal and stimulated conditions compared to *ob/ob* mice (Fig. 5e) that was accompanied by an 86% reduction in PGE_2 levels (Fig. 5f) and a 4-fold increase in cAMP levels (Fig. 5g). In *ob/ob* mice, reflecting higher *Adpla* expression, PGE_2 levels were 2.6-fold higher compared to wild-type mice. Notably, PGE_2 levels in dKO mice did not differ from *Adpla* null mice, indicating that AdPLA dominantly regulates PGE_2 levels in adipose tissue. Taken together, these results indicate that *Adpla* deficiency drastically influences PGE_2 and cAMP levels to modulate lipolysis and adiposity, even in a genetic obesity caused by leptin deficiency.

Adpla ablation causes insulin resistance and ectopic fat storage

Changes in adiposity are often associated with alterations in glucose and insulin homeostasis. *Adpla* null mice fed a SD showed an attenuated response to insulin during the insulin tolerance test (ITT), but glucose tolerance similar to wild-type mice (Supplementary Fig.

5), likely due to elevated insulin secretion (Supplementary Table 2). *Adpla* null mice fed a HFD had significantly impaired glucose clearance during glucose tolerance test (GTT) and an impaired response to insulin during ITT compared to wild-type littermates (Fig. 6a). In addition, we found that *Adpla* ablation further impaired glycemic control in *ob/ob* mice on both a SD (data not shown) and HFD, making dKO mice even more glucose and insulin intolerant than the already impaired *ob/ob* mice (Fig. 6b). In agreement with our findings from GTT and ITT, *Adpla* null mice fed a SD showed normal fasting glucose but elevated serum insulin, whereas HFD-fed mice had elevated fasting serum glucose and insulin compared to wild-type mice (Supplementary Table 2). Serum glucose and insulin levels were also elevated in dKO compared with *ob/ob* mice on either diet (Supplementary Table 2).

To discern the impact of *Adpla* ablation on peripheral and hepatic insulin action, we performed a hyperinsulinemic-euglycemic clamp. The glucose infusion rate necessary to maintain euglycemia in *Adpla* null mice was 77% lower than in wild-type mice, indicating severely blunted insulin-stimulated glucose uptake and metabolism (Fig. 6c and Supplementary Fig. 5). Compared with wild-type mice, *Adpla* null mice showed a 50% decrease in whole-body glucose uptake (Fig. 6d), and 44% and 65% decreases ($P < 0.05$) in glycolysis and glycogen synthesis, respectively, indicating decreased glucose metabolism. In addition, we found that suppression of hepatic glucose production (HGP) by insulin during the clamp was severely blunted in *Adpla* null mice (Fig. 6e), indicating hepatic insulin resistance. We found no difference in gastrocnemius 2-deoxyglucose (2-DG) uptake between wild-type and *Adpla* null mice (Fig. 6f). Notably, epididymal WAT 2-DG uptake per gram was higher, although the drastic decrease in adipose tissue mass resulted in a 72% reduction in *total* insulin stimulated glucose uptake by this tissue (Fig. 6g) that may explain lower net whole body glucose metabolism.

The livers of *Adpla* null mice were pale-tan in color and enlarged with numerous, lipid-laden vacuoles in hepatocytes (Supplementary Fig. 5). Liver DAG levels that have been associated with insulin resistance (32) were also significantly increased in *Adpla* null mice compared with wild-type mice (3.05 ± 0.46 μg mg^{-1} tissue versus 1.47 ± 0.38 μg mg^{-1} tissue, respectively, $P<0.05$). Lipid staining with Oil Red O also showed higher intramyocellular TAG content in skeletal muscle, although we found no difference in skeletal muscle DAG content (data not shown) or IRS-1 phosphorylation (Supplementary Fig. 5).

We found that circulating levels of leptin and adiponectin were decreased in *Adpla* null mice on both a SD and HFD (Supplementary Table 2). Relative expression levels of these adipokines in WAT from HFD-fed mice were also decreased (1.0 ± 0.30 versus $0.25 \pm .07$, $P < 0.01$ for leptin, and 1.0 ± 0.26 versus 0.28 ± 0.05, $P < 0.01$ for adiponectin, in wild-type and *Adpla* null mice, respectively). Circulating levels of adiponectin were lower in *ob/ob* mice compared to dKO mice (Supplementary Table 2). Adiponectin has been shown to increase fatty acid oxidation in skeletal muscle (33). We found decreased phosphorlylation of AMPK at Thr 172 and reduced expression of acyl-CoA oxidase in skeletal muscle of *Adpla* null mice, as well as lower oxidation of [U-^{14}C]-palmitate (Supplementary Fig. 5).

Despite increased lipolysis, serum non-esterified fatty acid (NEFA) levels were not higher but lower in *Adpla* null mice on both a SD and HFD (Supplementary Table 2). Serum triglycerides were also lower in *Adpla* null and dKO mice, despite pronounced steatosis and hepatic insulin resistance (Supplementary Table 1). We found increased TAG clearance in mice upon oral lipid load but no difference in serum TAG when lipoprotein lipase was first inhibited by WR1339 injection (Supplementary Fig. 4). Although its significance is unclear, lipoprotein

lipase expression was 2-fold higher in livers from *Adpla* null mice (Supplementary Fig. 4). Taken together, fatty acid uptake by the liver appears to be higher in AdPLA null mice.

Adpla null mice have increased energy expenditure and fatty acid oxidation in adipose tissue

Total oxygen consumption was higher in *Adpla* null and dKO mice compared with wild-type and *ob/ob* mice, respectively (Fig. 6h), and these differences were not attributed to changes in ambulatory activity (data not shown). We first examined BAT, but found no significant difference in the morphology or weight of interscapular BAT, nor any change in mRNA levels of genes involved in thermogenesis in BAT when mice were housed at 4ºC (data not shown). In WAT from *Adpla* null mice, however, we detected a 5.5-fold upregulation of uncoupling protein 1 (*Ucp-1*), as well as upregulation of other genes involved in oxidative metabolism including 3.2- and 5-fold increases in expression of peroxisome proliferator-activated receptor delta (*Ppar*-δ), and deiodinase 2 (*Dio*2), respectively (Fig. 6i). We determined the production of $^{14}CO_2$ from [U-^{14}C] palmitate and found that fatty acid oxidation was increased by 37% in isolated adipocytes from *Adpla* null mice compared to wild-type mice (Fig. 6j). Fatty acid oxidation was significantly lower in adipocytes from *ob/ob* mice than wild-type mice, but was restored to wild-type levels in dKO mice. As shown in Fig.3E, we observed a decrease in the molar ratio of FFA to glycerol released from WAT explant studies of *Adpla* null mice compared to wild-type mice. This change in molar ratio of fatty acid to glycerol in *Adpla* null mice indicates increased utilization of FFA within adipocytes and supports our finding of increased fatty acid oxidation in adipose tissue. These findings help to explain not only increased energy expenditure but also decreased NEFA in the circulation, despite higher lipolysis in *Adpla* null mice.

DISCUSSION

Adpla is highly expressed only in adipose tissue, where lipolysis is a major function. We postulated that, since PLA_2s catalyze the initial rate-limiting step in PG synthesis (9), AdPLA may regulate lipolysis locally by controlling the provision of arachidonic acid for the production of PGs. Since *Adpla* is induced by feeding/insulin, as well as in *ob/ob* and *db/db* models of obesity, we predicted that AdPLA likely plays an inhibitory role in lipolysis. Indeed, we found that AdPLA plays a major role in modulating adipose tissue lipolysis by regulating PGE_2 levels. As a result, ablation of *Adpla* in mice prevented obesity induced by feeding a HFD, or by leptin deficiency.

While the regulation of lipolysis by catecholamines and insulin has been extensively studied, the local regulation of lipolysis in adipose tissue by autocrine/paracrine factors remains unclear (34). We found that *Adpla* is expressed in adipocytes at a much higher level than any other known PLA_2s, and total PLA activity was greatly reduced in adipose tissue of *Adpla* null mice while expression of other known PLA_2s remained unchanged, revealing that AdPLA is the major PLA_2 in this tissue and may provide arachidonic acid for PG synthesis. Among the PGs that have previously been detected in adipose tissue, we found that PGE_2 is present at levels one to two orders of magnitude higher. Furthermore, PGE_2 levels are drastically decreased in *Adpla* null and dKO mice, providing evidence for a significant role for AdPLA in regulating PGE_2 synthesis. We found that the Gαi coupled receptor, EP3, was predominant in adipose tissue, and

a specific inhibitor of EP3 prevented the anti-lipolytic effect of PGE_2. These findings suggest that PGE_2 suppresses lipolysis by decreasing cAMP levels through EP3 activation during feeding/insulin when *Adpla* is drastically induced. Indeed, we found that cAMP levels were elevated in WAT of *Adpla* null and dKO mice, and PGE_2 treatment restored cAMP levels in *Adpla* null adipocytes to wild-type levels. In *Adpla* null WAT, HSL phosphorylation was increased, while total levels of HSL and desnutrin/ATGL were unchanged, suggesting that phosphorylation of HSL is likely an important mediator of increased lipolysis in these mice.

In vivo, lipolysis was markedly higher per gram of adipose tissue in *Adpla* null mice compared to wild-type mice. Furthermore, both basal and isoproterenol-stimulated lipolysis were increased in explants of *Adpla* deficient adipose tissue and in adipocytes isolated from *Adpla* null mice, and stimulated lipolysis was higher in adipocytes differentiated from *Adpla* null MEF. Exogenous PGE_2 rescued lipolytic rates in *Adpla* deficient adipocytes in all three model systems, showing AdPLA regulation of lipolysis in adipocytes via PGE_2 production. The cyclooxygenase inhibitors NS-398 (35) and indomethacin (36) have been shown to enhance basal and stimulated lipolysis, respectively, in adipose tissue, consistent with our present findings that AdPLA plays an important role in regulating lipolysis through production of PGE_2. Furthermore, we demonstrate that an EP3 inhibitor prevents the anti-lipolytic effects of PGE_2, consistent with our proposed model of lipolysis regulation by AdPLA through PGE_2 signaling. Due to increased phosphorylation of HSL and unsuppressed lipolysis, *Adpla* null mice have drastically decreased TAG content in adipose tissue. This indicates that suppression of lipolysis by the local PGE_2 produced by adipocytes plays a critical role in regulating adipocyte lipolysis and demonstrates a role for the AdPLA/PGE_2/EP3/cAMP signaling pathway in development of excess adipose tissue mass/TAG storage and obesity. In support of this, PGE_2 levels were found to be higher in adipose tissue of obese human patients (37). Overall, the present study shows that AdPLA plays a critical regulatory role in the adipocyte dominant function of lipolysis through PGE_2 in an autocrine/paracrine manner.

Fatty acids such as arachidonic acid that are released by the action of PLA_2s have been shown to either stimulate or inhibit adipocyte differentiation (38-40). Similarly, selective cyclooxygenase-2 inhibitors (12; 14), or prostaglandins themselves[11,13,21,22] were reported to induce or inhibit adipogenesis. $PGF_{2\alpha}$ via its FP receptor and 15-deoxy-$\Delta^{12,14}$-PGJ_2 as a PPARγ ligand, have been reported to affect *in vitro* adipocyte differentiation(13; 30). PGD_2 may generate 15-deoxy-$\Delta^{12,14}$-PGJ_2 and PGI_2, and through its IP receptor, may also affect adipocyte differentiation *in vitro*(11; 31). However, unlike PGE_2, we have found that these PGs are not detected at high enough concentrations in adipose tissue to effectively bind their receptors (29), which were also barely detectable in adipose tissue. PGs other than PGE_2, therefore, may not play a significant role. In our study, PGE_2 was the most abundant PG found in adipose tissue. However, our results clearly show that adipocyte differentiation, either *in vitro* or *in vivo*, was not affected by AdPLA.

The increased cAMP levels in WAT resulted in increased lipolysis and, consequently, decreased adipocyte size with lower TAG content in *Adpla* null and dKO mice, despite similar food intakes. TAG content in *Adpla* null mice and dKO mice was markedly lower than wild-type and *ob/ob* mice, respectively. Although increased lipolysis in *Adpla* null mice resulted in ectopic TAG accumulation in the liver and skeletal muscle, this could not fully account for the loss of TAG from adipose tissue. Indeed, oxygen consumption was increased in *Adpla* null and dKO mice. While we did not detect any changes in BAT, surprisingly, *Ucp-1*, *Dio2* and *Ppard* in WAT of *Adpla* null mice were significantly increased, suggesting higher oxidation and

thermogenesis in WAT. Ectopic expression of *Ucp-1* in WAT has been reported to cause resistance to diet-induced obesity with increased fatty acid oxidation in adipocytes (41). Consistent with this, we found significantly increased fatty acid oxidation in adipocytes from *Adpla* null and dKO mice compared with wild type and *ob/ob* mice, respectively, indicating that, at least in part, increased fatty acid utilization within adipocytes contributed to the increased energy expenditure.

Adpla null and dKO mice are extremely lean but insulin resistant, representing a lipodystrophy model. Results from hyperinsulinemic-euglycemic clamping studies indicate that insulin resistance in *Adpla* null mice is due to hepatic insulin resistance as well as reduced peripheral glucose metabolism. Interestingly, there was no difference in insulin-stimulated skeletal muscle glucose uptake between wild-type and *Adpla* null mice, but total insulin stimulated glucose-uptake was lower in WAT due to the drastic reduction in the mass of this tissue. It is interesting to note that despite severe insulin resistance and increased lipolysis in *Adpla* null mice, serum NEFA levels were lower in these mice. The molar ratio of FFA to glycerol release from adipose tissue was significantly lower in *Adpla* null mice, suggesting increased utilization of fatty acids within adipose tissue. Consistent with this finding, we observed increased fatty acid oxidation in adipose tissue. Ectopic storage of TAG in liver and skeletal muscle suggests that removal of FFA from the circulation by these tissues may potentially have been increased and therefore may also have contributed to decreased serum NEFA levels. However, it is most likely that even with the higher rate of lipolysis, the drastically reduced adipose tissue mass in *Adpla* null mice resulted, overall, in lower net FFA liberation. Indeed, other mouse models with increased lipolysis and decreased adipose tissue also reported unchanged or reduced serum NEFA (42-45).

Adpla expression in humans is also adipose-specific. Currently, little is known regarding the pathological phenotype of individuals lacking AdPLA. Database search for single nucleotide polymorphisms (SNPs) in the *Adpla* gene in humans identified one SNP (Ser48Ala) within the coding region. An additional 230 SNPs have also been detected within non-coding regions of the *Adpla* gene. It is not known whether these result in altered protein function or levels, and clinical associations for these have not been reported, most likely because the present study is the first to characterize the physiological role of AdPLA. Many questions remain regarding the effect of partial or total *Adpla* gene ablation in humans, and further research in this area will yield advances in understanding the pathology of human obesity as well as type 2 diabetes.

REFERENCES

1. Duncan RE, Ahmadian M, Jaworski K, Sarkadi-Nagy E, Sul HS: Regulation of lipolysis in adipocytes. *Annu Rev Nutr* 27:79-101, 2007
2. Gregoire FM, Smas CM, Sul HS: Understanding adipocyte differentiation. *Physiol Rev* 78:783-809, 1998
3. Jaworski K, Sarkadi-Nagy E, Duncan RE, Ahmadian M, Sul HS: Regulation of triglyceride metabolism. IV. Hormonal regulation of lipolysis in adipose tissue. *Am J Physiol Gastrointest Liver Physiol* 293:G1-4, 2007
4. Dircks L SH: Acyltransferases of de novo glycerophospholipid biosynthesis. *Progress in Lipid Research* 38:461-479, 1999
5. Yet SF LS, Hahm YT, Sul HS: Expression and identification of p90 as the murine mitochondrial glycerol-3-phosphate acyltransferase. *Journal of Biochemistry*:9486-9491, 1993
6. Vance DE, Vance JE: *Biochemistry of lipids, lipoproteins and membranes*, 2002
7. Duncan RE, Sarkadi-Nagy, E., Jaworski, K., Ahmadian, M. and Sul, H. S.: Identification and Functional Characterization of Adipose-specific Phospholipase A2 (AdPLA). *J Biol Chem* 283:25428-25436, 2008
8. Schaloske RH, Dennis EA: The phospholipase A(2) superfamily and its group numbering system. *Biochim Biophys Acta*, 2006
9. Yuan C, Rieke CJ, Rimon G, Wingerd BA, Smith WL: Partnering between monomers of cyclooxygenase-2 homodimers. *Proc Natl Acad Sci U S A* 103:6142-6147, 2006
10. Richelsen B: Release and effects of prostaglandins in adipose tissue. *Prostaglandins Leukot Essent Fatty Acids* 47:171-182, 1992
11. Aubert J, Saint-Marc P, Belmonte N, Dani C, Negrel R, Ailhaud G: Prostacyclin IP receptor up-regulates the early expression of C/EBPbeta and C/EBPdelta in preadipose cells. *Mol Cell Endocrinol* 160:149-156, 2000
12. Fajas L, Miard S, Briggs MR, Auwerx J: Selective cyclo-oxygenase-2 inhibitors impair adipocyte differentiation through inhibition of the clonal expansion phase. *J Lipid Res* 44:1652-1659, 2003
13. Forman BM, Tontonoz P, Chen J, Brun RP, Spiegelman BM, Evans RM: 15-Deoxy-delta 12, 14-prostaglandin J2 is a ligand for the adipocyte determination factor PPAR gamma. *Cell* 83:803-812, 1995
14. Yan H, Kermouni A, Abdel-Hafez M, Lau DC: Role of cyclooxygenases COX-1 and COX-2 in modulating adipogenesis in 3T3-L1 cells. *J Lipid Res* 44:424-429, 2003
15. Cohen-Luria R RG: Prostaglandin E2 can bimodally inhibit and stimulate the epididymal adipocyte adenylyl cyclase activity. *Cell signal* 4:331-335, 1992
16. Kather H, Simon B: Biphasic effects of prostaglandin E2 on the human fat cell adenylate cyclase. *J Clin Invest* 64:609-612, 1979
17. Kim KH, Lee K, Moon YS, Sul HS: A cysteine-rich adipose tissue-specific secretory factor inhibits adipocyte differentiation. *J Biol Chem* 276:11252-11256, 2001
18. Viswanadha S, Londos C: Optimized conditions for measuring lipolysis in murine primary adipocytes. *J Lipid Res* 47:1859-1864, 2006

19. Bligh EG, Dyer WJ: A rapid method of total lipid extraction and purification. *Can J Biochem Physiol* 37:911-917, 1959
20. Folch J, Lees M, Sloane Stanley GH: A simple method for the isolation and purification of total lipides from animal tissues. *J Biol Chem* 226:497-509, 1957
21. Youn JH, Buchanan TA: Fasting does not impair inuslin-stimulated glucose uptake but alters intracellular glucose metabolism in conscious rats. *Diabetes* 42:757-763, 1993
22. Samuel VT, Choi CS, Phillips TG, Romanelli AJ, Geisler JG, Bhanot S, McKay R, Monia B, Shutter JR, Lindberg RA, Shulman GI, Veniant MM: Targeting foxo1 in mice using antisense oligonucleotides improves hepatic and peripheral insulin action. *Diabetes* 55:2042-2050, 2006
23. Lucas KK, Dennis EA: Distinguishing phospholipase A2 types in biological samples by employing group-specific assays in the presence of inhibitors. *Prostaglandins Other Lipid Mediat* 77:235-248, 2005
24. Turner SM, Murphy EJ, Neese RA, Antelo F, Thomas T, Agarwal A, Go C, Hellerstein MK: Measurement of TG synthesis and turnover in vivo by 2H2O incorporation into the glycerol moiety and application of MIDA. *Am J Physiol Endocrinol Metab* 285:E790-803, 2003
25. Chen JL, Peacock E, Samady W, Turner SM, Neese RA, Hellerstein MK, Murphy EJ: Physiologic and pharmacologic factors influencing glyceroneogenic contribution to triacylglyceride glycerol measured by mass isotopomer distribution analysis. *J Biol Chem* 280:25396-25402, 2005
26. Bansode RR, Huang W, Roy SK, Mehta M, Mehta KD: Protein kinase Cbeta deficiency increases fatty acid oxidation and reduces fat storage. *J Biol Chem* 283:231-236, 2008
27. Smas CM SH: Pref-1, a protein containing EGF-like repeats, inhibits adipocyte differentiation. *Cell* 73:725-734, 1993
28. Latasa MJ GM, Moon YS, Kang C, Sul HS: Occupancy and funtion of the -150 SRE and -65 E-box in nutritional regulation of the fatty acid synthase gene in living animals. *Molecular and Cellular Biology* 23:5896-5907, 2003
29. Bell-Parikh LC, Ide T, Lawson JA, McNamara P, Reilly M, FitzGerald GA: Biosynthesis of 15-deoxy-delta12,14-PGJ2 and the ligation of PPARgamma. *J Clin Invest* 112:945-955, 2003
30. Reginato MJ, Krakow SL, Bailey ST, Lazar MA: Prostaglandins promote and block adipogenesis through opposing effects on peroxisome proliferator-activated receptor gamma. *J Biol Chem* 273:1855-1858, 1998
31. Vassaux G, Gaillard D, Ailhaud G, Negrel R: Prostacyclin is a specific effector of adipose cell differentiation. Its dual role as a cAMP- and Ca(2+)-elevating agent. *J Biol Chem* 267:11092-11097, 1992
32. Savage DB, Petersen KF, Shulman GI: Disordered lipid metabolism and the pathogenesis of insulin resistance. *Physiol Rev* 87:507-520, 2007
33. Yoon M-J, Lee G-Y, Chung J-J, Ahn Y-H, Hong S-H, Kim J-B: Adiponectin increases fatty acid oxidation in skeletal muscle cells by sequential activation of AMP-activated protein kinase, p38 mitogen-activated protein kinase, and peroxisom proliferator-activated receptor. *Diabetes* 55:2562-2570, 2006
34. Johansson SM, Yang JN, Lindgren E, Fredholm BB: Eliminating the antilipolytic adenosine A1 receptor does not lead to compensatory changes in the antilipolytic actions of PGE2 and nicotinic acid. *Acta Physiol* 190:87-96, 2007
35. Fain JN, Leffler CW, Bahouth SW: Eicosanoids as endogenous regulators of leptin release and lipolysis by mouse adipose tissue in primary culture. *J Lipid Res* 41:1689-1694, 2000

36. Girouard H, Savard R: The lack of bimodality in the effects of endogenous and exogenous prostaglandins on fat cell lipolysis in rats. *Prostaglandins Other Lipid Mediat* 56:43-52, 1998
37. Fain JN, Madan AK, Hiler ML, Cheema P, Bahouth SW: Comparison of the release of adipokines by adipose tissue, adipose tissue matrix, and adipocytes from visceral and subcutaneous abdominal adipose tissues of obese humans. *Endocrinology* 145:2273-2282, 2004
38. Gaillard D, Negrel R, Lagarde M, Ailhaud G: Requirement and role of arachidonic acid in the differentiation of pre-adipose cells. *Biochem J* 257:389-397, 1989
39. Massiera F, Saint-Marc P, Seydoux J, Murata T, Kobayashi T, Narumiya S, Guesnet P, Amri EZ, Negrel R, Ailhaud G: Arachidonic acid and prostacyclin signaling promote adipose tissue development: a human health concern? *J Lipid Res* 44:271-279, 2003
40. Petersen RK, Jorgensen C, Rustan AC, Froyland L, Muller-Decker K, Furstenberger G, Berge RK, Kristiansen K, Madsen L: Arachidonic acid-dependent inhibition of adipocyte differentiation requires PKA activity and is associated with sustained expression of cyclooxygenases. *J Lipid Res* 44:2320-2330, 2003
41. Kopecky J, Hodny Z, Rossmeisl M, Syrovy I, Kozak LP: Reduction of dietary obesity in aP2-Ucp transgenic mice: physiology and adipose tissue distribution. *Am J Physiol* 270:E768-775, 1996
42. Hertzel AV, Smith LA, Berg AH, Cline GW, Shulman GI, Scherer PE, Bernlohr DA: Lipid metabolism and adipokine levels in fatty acid-binding protein null and transgenic mice. *Am J Physiol Endocrinol Metab* 290:E814-823, 2006
43. Lucas S, Tavernier G, Tiraby C, Mairal A, Langin D: Expression of human hormone-sensitive lipase in white adipose tissue of transgenic mice increases lipase activity but does not enhance in vitro lipolysis. *J Lipid Res* 44:154-163, 2003
44. Martinez-Botas J, Anderson JB, Tessier D, Lapillonne A, Chang BH, Quast MJ, Gorenstein D, Chen KH, Chan L: Absence of perilipin results in leanness and reverses obesity in Lepr(db/db) mice. *Nat Genet* 26:474-479, 2000
45. Tansey JT, Sztalryd C, Gruia-Gray J, Roush DL, Zee JV, Gavrilova O, Reitman ML, Deng CX, Li C, Kimmel AR, Londos C: Perilipin ablation results in a lean mouse with aberrant adipocyte lipolysis, enhanced leptin production, and resistance to diet-induced obesity. *Proc Natl Acad Sci U S A* 98:6494-6499, 2001

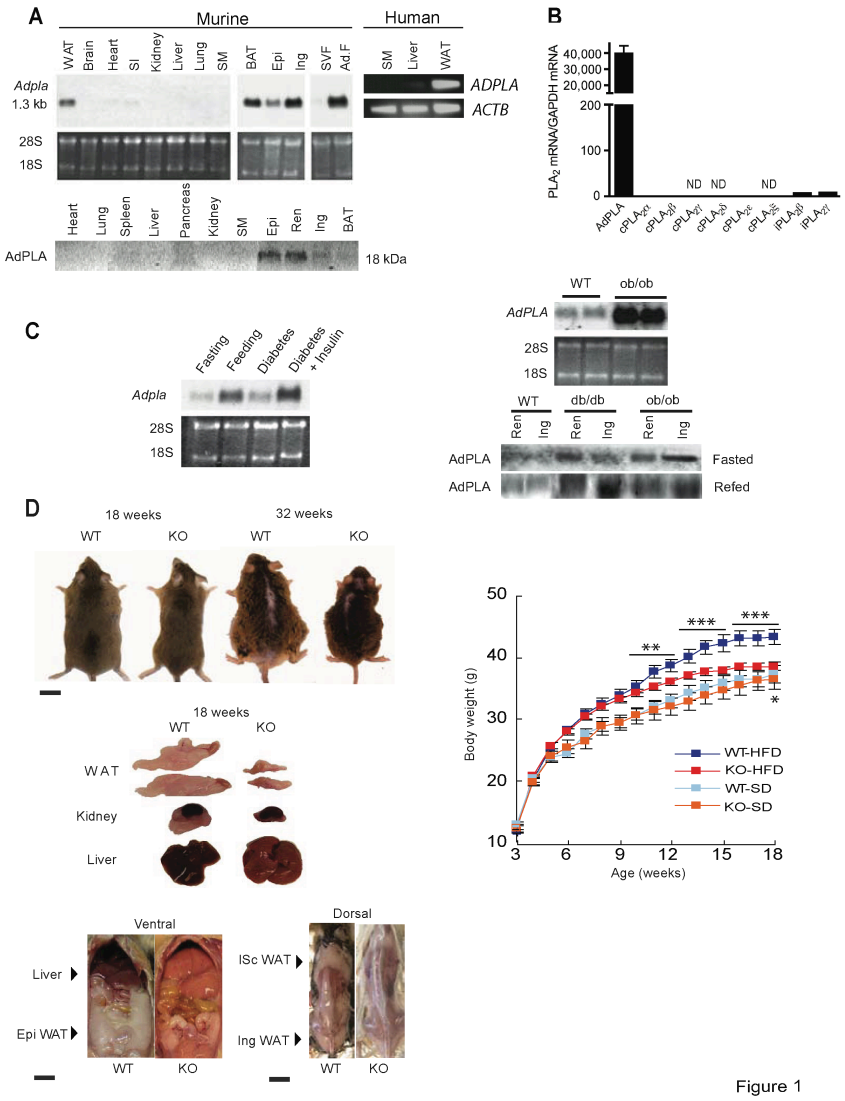

Figure 1

Figure IV-1 AdPLA tissue distribution, regulation of expression and body weights of AdPLA-null mice. (a) Top left, northern blot analysis of 10 mg of totalRNA from various mouse tissues. SI, small intestine; SM, skeletal muscle; Epi, epididymal fat; Ing, inguinal fat; SVF, stromal vascular fraction; Ad.F, adipocyte fraction. Top right, RT-PCR analysis of RNA (2.5 mg) from human SM, liver or WAT for expression of AdPLA or b-actin. Bottom, western blot analysis for AdPLA protein in various mouse tissues. 80 mg of protein was subjected to SDS-PAGE and probed with antibodies to AdPLA. Ren, renal fat. (b) Quantitative RT-PCR of RNA from wild-type (WT) renal WAT. Values for PLA2 enzymes were normalized to Gapdh mRNA and then expressed relative to cPLA2a mRNA (n =4 5). ND, not detected. (c) Top left, northern blot of AdPLA mRNA in epididymal WAT from mice fasted for 48 h, fasted and refed for 12 h or made diabetic by streptozotocin injection, with or without insulin replacement (n = 3). Samples were normalized to 18S and 28S bands. Top right, AdPLA mRNA expression in inguinal WAT from WT and ob/ob mice analyzed by northern blotting (n 1/4 3). Bottom, western blotting for AdPLA in WAT depots from WT, db/db and ob/ob mice (n 1/4 3). (d) Top left, representative photographs of male WT and AdPLA-null (KO) mice at 18 and 32 weeks of age. Scale bar, 15 mm. Right, body weights of male WT and KO on either a SD (n =11) or a HFD (n= 24-33). Bottom left, representative photographs of fat pads and organs of 18-week-old male KO and WT littermates. Isc, interscapular. Scale bar (left), 8 mm; scale bar (right), 10 mm. Results are means ± s.e.m.; **P o 0.01, ***P o 0.001 versus WT.

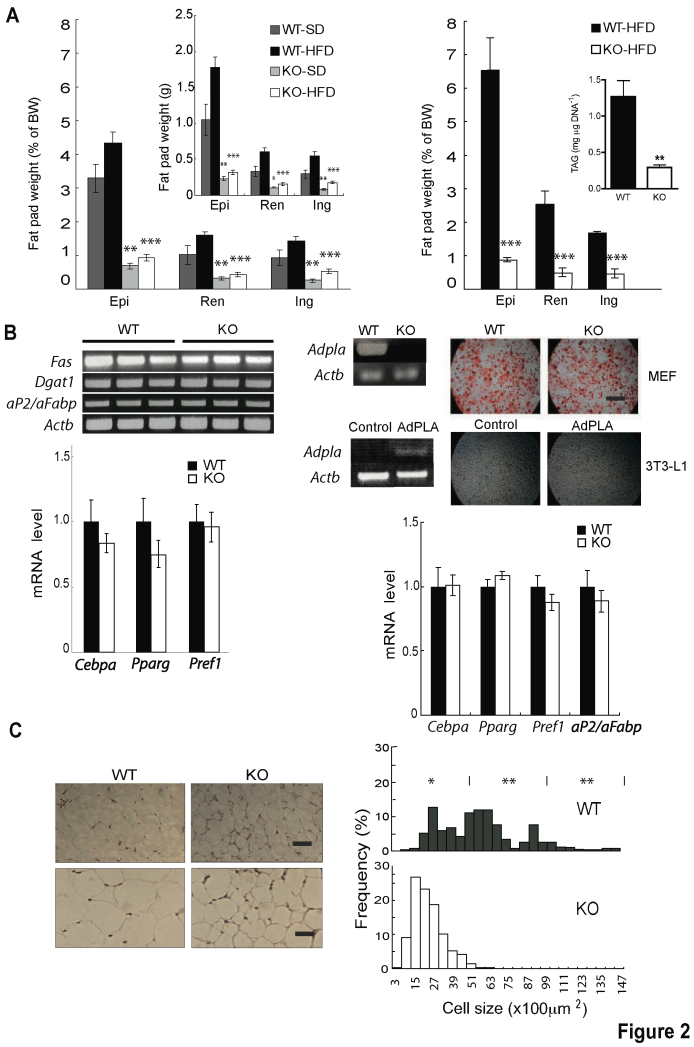

Figure 2

Figure IV-2 AdPLA ablation causes a reduction in fat pad weight, triacylglycerol (TAG) content and adipocyte size but does not affect adipocyte differentiation. (a) Left, fat pad weights as a percentage of body weight (BW) and in absolute amounts (inset) from male KO and WT littermates. Mice were fed a SD or a HFD until 18 weeks of age (n 1/4 6–16). Bottom, fat pad weights of male KO and WT littermates on a HFD at 32 weeks of age (n 1/4 8). Inset, TAG content in epididymal WAT. (b) Top left, RT-PCR for gene products involved in lipid metabolism, using RNA from epididymal WAT of male WT and KO (n 1/4 5). Bottom left, RT-qPCR for adipocyte differentiation markers, using RNA from epididymal WAT of 18 week-old male mice (n 1/4 5). Actb, b-actin. Top right, MEFs from WT and KO embryos differentiated and harvested at day 12 and stained with oil red O. 3T3-L1 cells transfected with LacZ control vector or AdPLA expression vector were also differentiated and stained for neutral lipid. AdPLA mRNA levels were determined in cells by RT-PCR using Actb mRNA as a control. Bottom right, quantitative RT-PCR of adipogenic markers using RNA from adipocytes differentiated from WT and KO MEFs (n 1/4 4). Scale bar, 6 mm. (c) Left, H&E-stained paraffin-embedded sections of epididymal WAT from 18-week-old male KO and WT mice fed a HFD. Scale bar (top), 80 mm; scale bar (bottom), 20 mm. Right, distribution of adipocyte size. Results are means ± s.e.m.; *P o 0.05, **P o 0.01, ***P o 0.001 versus WT.

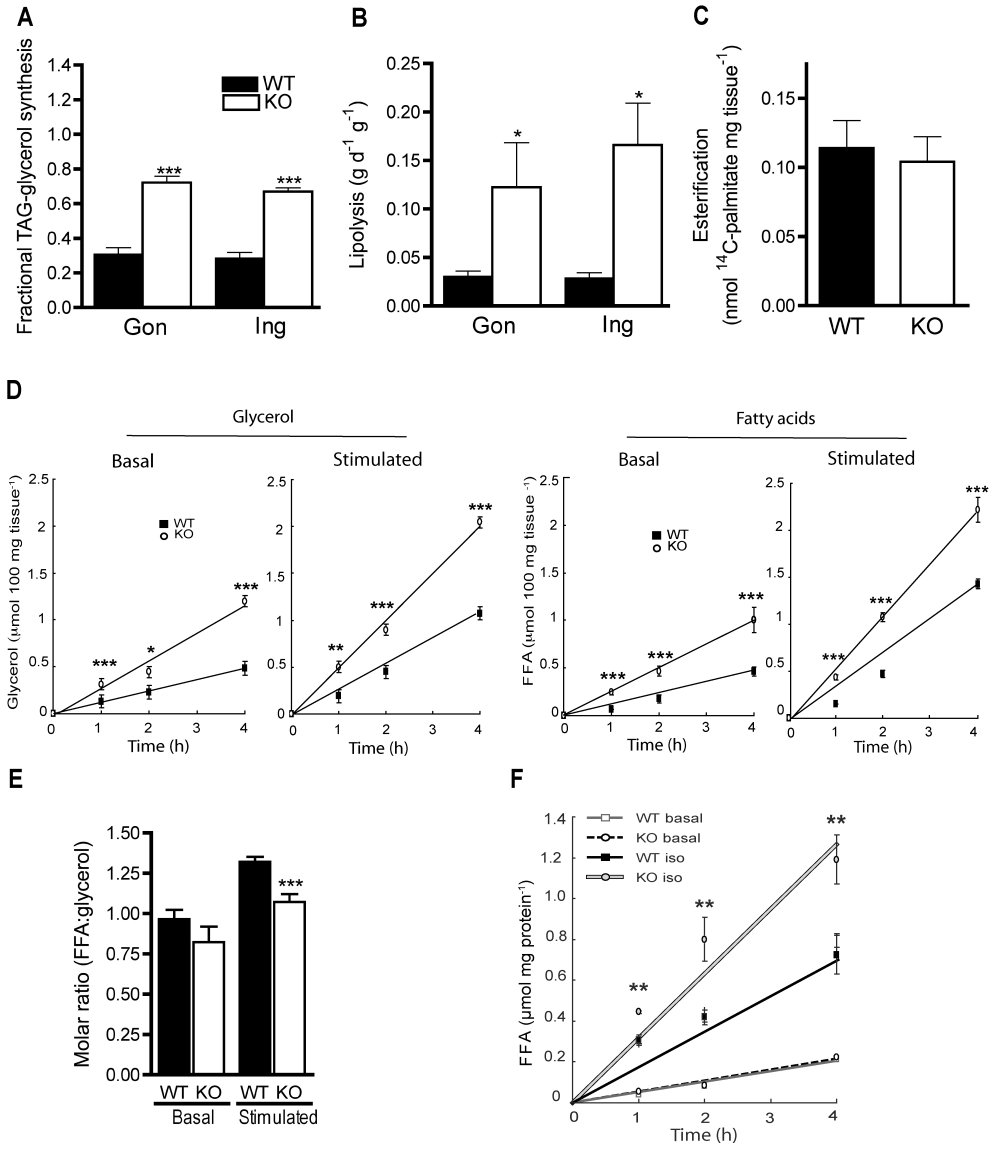

Figure 3

Figure IV-3 AdPLA ablation increases lipolysis in vivo, ex vivo and in vitro. (a) Fractional *in vivo* synthesis of triacylglycerol (TAG)-glycerol in gonadal (Gon) and inguinal (Ing) WAT of 24-week-old female mice on a HFD (n 1/4 5 or 6). (b) In vivo lipolysis in gonadal and inguinal WAT from 24-week-old female mice on a HFD measured as the change in adipose tissue TAG mass per day per gram of total adipose tissue mass (g d–1 g–1;n 1/4 3–6). (c) 14C-palmitate esterification into TAG in WAT explants. (d) Basal and stimulated (+ 100 nM isoproterenol) lipolysis, as measured by glycerol (left) and fatty acids (right) released from explants of epididymal WAT from overnight fasted 16-week-old male WT and KO mice on a HFD (n 1/4 5). (e) Molar ratio of FFA to glycerol release from WAT explants. (f) Best-fit lines of basal and stimulated lipolysis, as measured by fatty acids released from WT and KO MEFs at day 12 after differentiation into adipocytes. MEFs were incubated with or without isoproterenol (iso) at 200 nM (n 1/4 6). Results are means ± s.e.m.; *P < 0.05, **P < 0.01, ***P < 0.001.

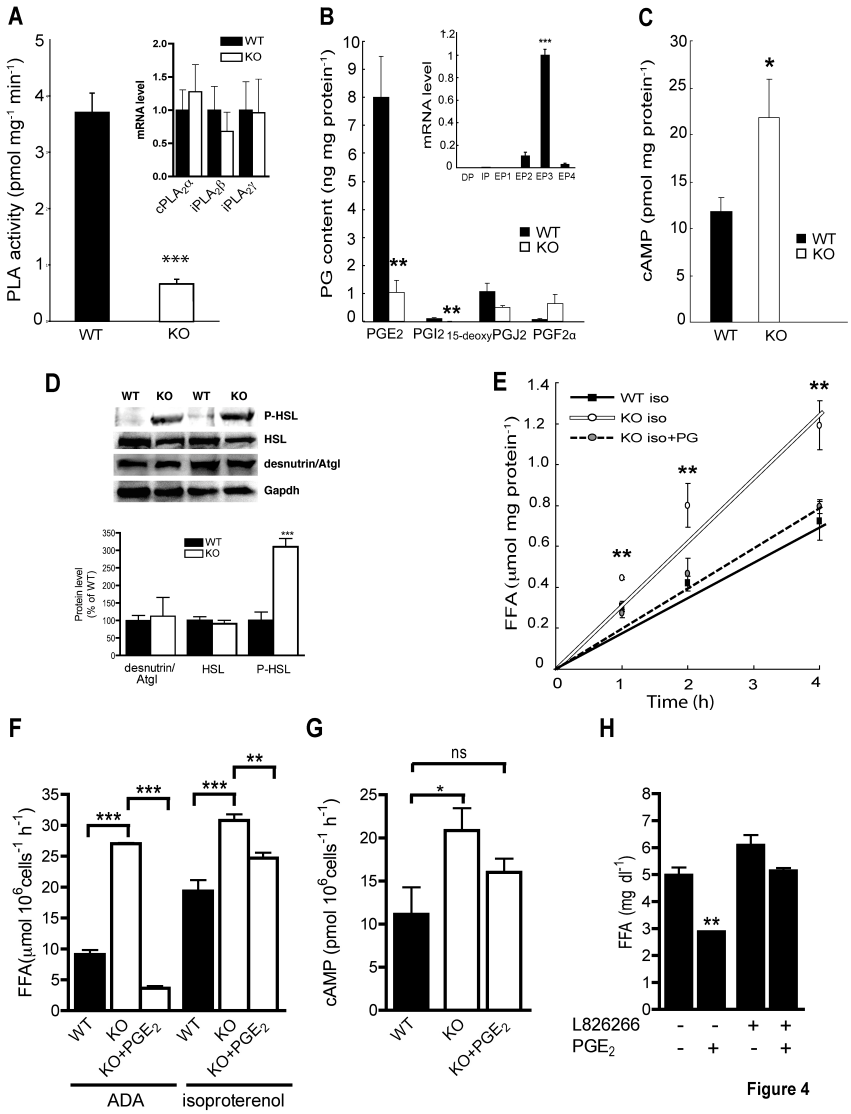

Figure 4

Figure IV-4 AdPLA deficiency increases lipolysis by decreasing PGE2 abundance and increasing cAMP levels. (a) Total phospholipase A (PLA) activity in epididymal WAT from 16-week-old male WT and KO mice fed a HFD (n =4 3). Inset, PLA2 expression in WAT. (b) Prostaglandin (PG) content in epididymal WAT of 18-week-old male WT and KO mice on a HFD (n =4 5). Inset, quantitative RT-PCR of prostaglandin receptors normalized to Actb, in WAT of WT mice (n 1/4 5). (c) cAMP abundance in epididymal WAT from male WT and KO mice on a HFD (n=4 5). (d) Immunoblot of phosphorylated HSL (P-HSL), HSL, desnutrin and Gapdh (control) (top) with relative quantification (bottom). (e) Best-fit lines of stimulated lipolysis, as measured by fatty acid release from WT and KO MEFs on day 12 after differentiation into adipocytes. MEFs were incubated with 200 nM isoproterenol and 100 nM PGE2 (PG) as indicated (n =4 6). (f) Lipolysis in isolated adipocytes from KO or WT mice incubated with 1 U ml–1 adenosine deaminase (ADA) or isoproterenol (200 nM) and treated with or without 10 nM PGE2. (g) cAMP levels in isolated adipocytes from WT or AdPLA-null mice treated with or without 10 nM PGE2. NS, not significantly different. (h) Lipolysis in isolated adipocytes treated with the EP3 antagonist L826266 (10 mM) with or without 10 nM PGE2. Results are means ± s.e.m.; *P <0.05, **P <0.01, ***P < 0.001.

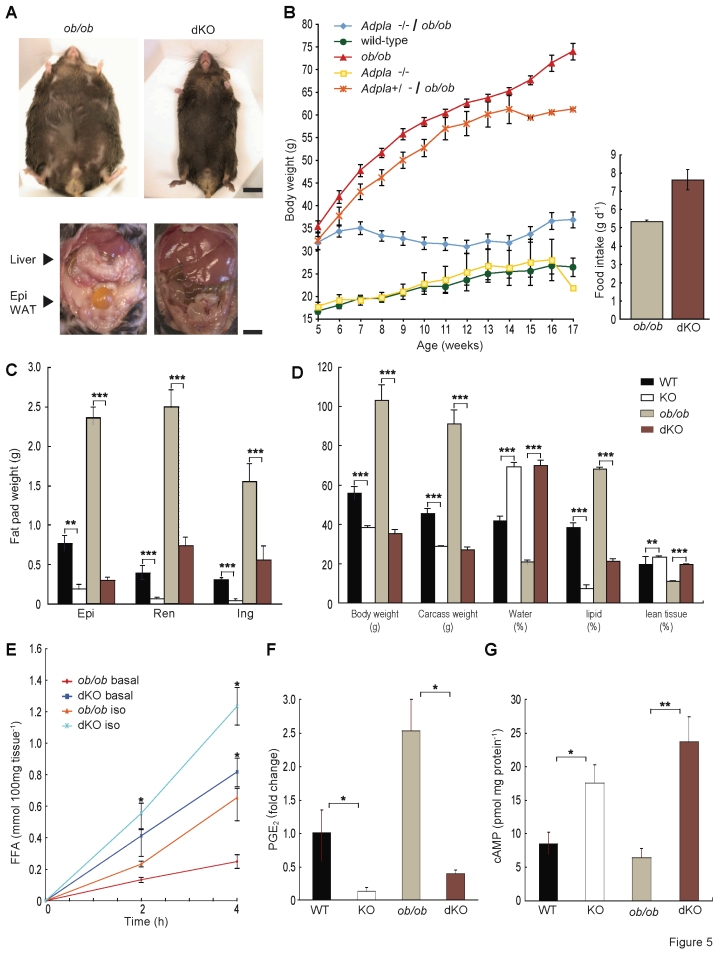

Figure 5

Figure IV-5 AdPLA deficiency prevents obesity in ob/ob leptin-deficient mice. (a) Top, representative photographs of 16-week-old male ob/ob and double-knockout mice fed a SD. Scale bar, 8 mm. Bottom, representative photographs of their livers and epididymal WAT. Scale bar, 6 mm. (b) Left, body weights of female mice on a SD. Right, food intake in 12-week-old male mice fed a SD. (c) Comparison ofweights of WAT depots from WT, KO, ob/ob and double-knockout mice. (d) Carcass analysis of 40-weekold male mice fed a HFD. (e) Basal and stimulated lipolysis measured by fatty acid release from explants of epididymal WAT in 12-week-old male ob/ob and double-knockout mice fed a HFD. (f,g) PGE2 (f) and cAMP (g) abundance in WAT of 12-week-old male WT, KO, ob/ob and doubleknockout mice fed a HFD. Results are means ± SEM; *P o 0.05, **P o 0.01, ***P o 0.001.

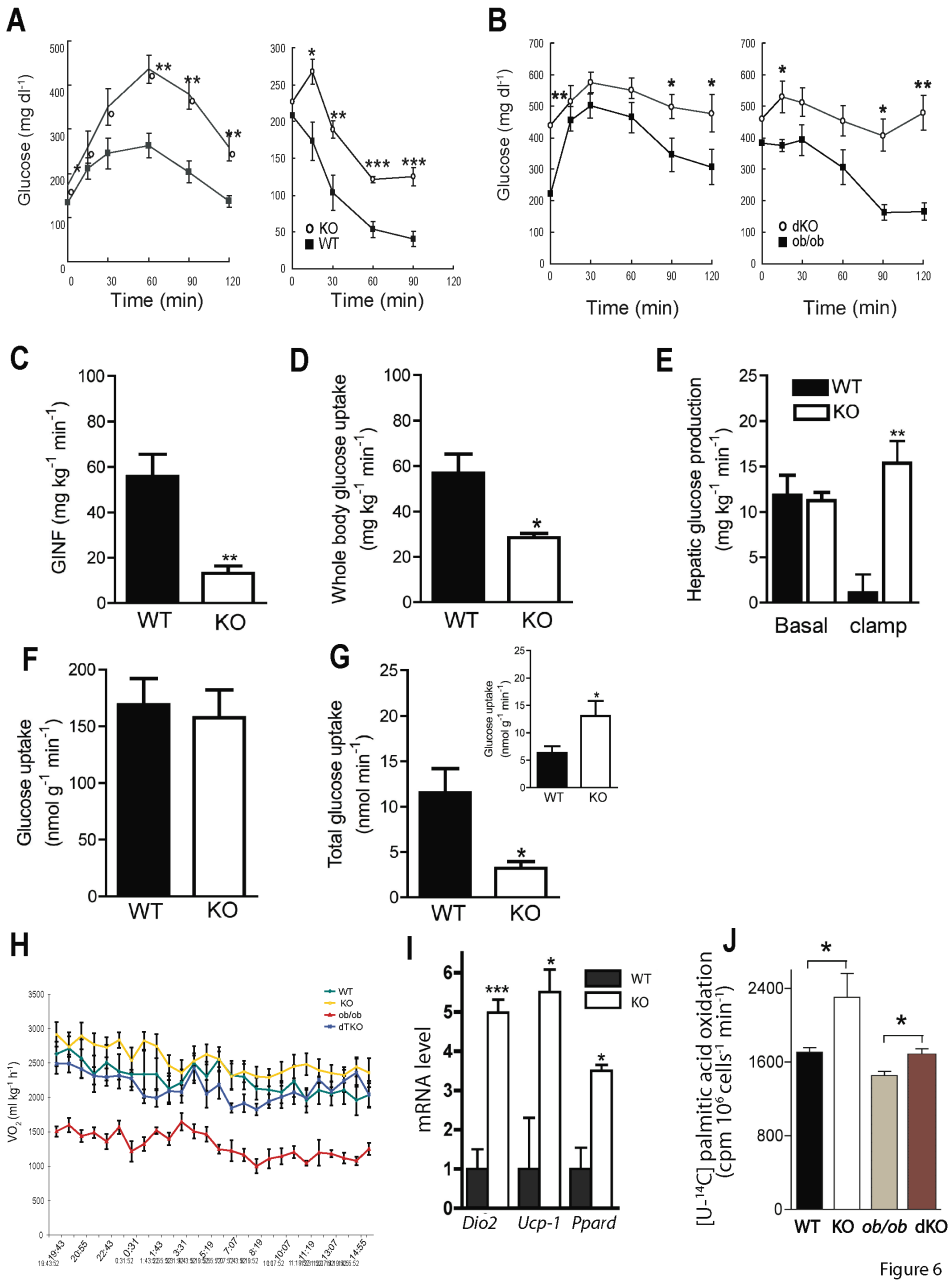

Figure 6

Figure IV-6 AdPLA deficiency impairs glycemic control, increases energy expenditure and promotes fatty acid oxidation in WAT. (a) GTT (left) and ITT (right) in 18-week-old male WT and KO mice fed a HFD (n 1/4 7). (b) GTT (left) and ITT (right) in 14-week-old male ob/ob and double-knockout mice fed a HFD (n 1/4 8 or 9). (c–g) Results from hyperinsulinemic euglycemic clamp performed in 12-week-old male WT and KO mice fed a HFD (n 1/4 4 or 5). (c) Average glucose infusion rate (GINF). (d) Whole-body glucose uptake. (e) Hepatic glucose production (HGP) under basal and clamp conditions. (f) Glucose uptake by skeletal muscle (gastrocnemius). (g) Total glucose uptake and glucose uptake per gram of tissue (inset) in epididymal WAT. (h) Oxygen consumption rate (VO2) determined via indirect calorimetry during the light (7 a.m.–7 p.m.) and dark (7 p.m.–7 a.m.) period in 18-week-old male KO and WT mice on a SD (n 1/4 3–6). (i) Quantitative RT-PCR for Ucp1, Dio2 and Ppard, using RNA from epididymal fat from 20-week-old male WT and KO mice fed a SD (n = 3-4). (j) Oxidation of [U-14C] palmitate to 14CO2 by adipocytes isolated from WT, KO, ob/ob and double-knockout mice (n =4 3). Results are means ± s.e.m.;
*P < 0.05, **P < 0.01, ***P < 0.001.

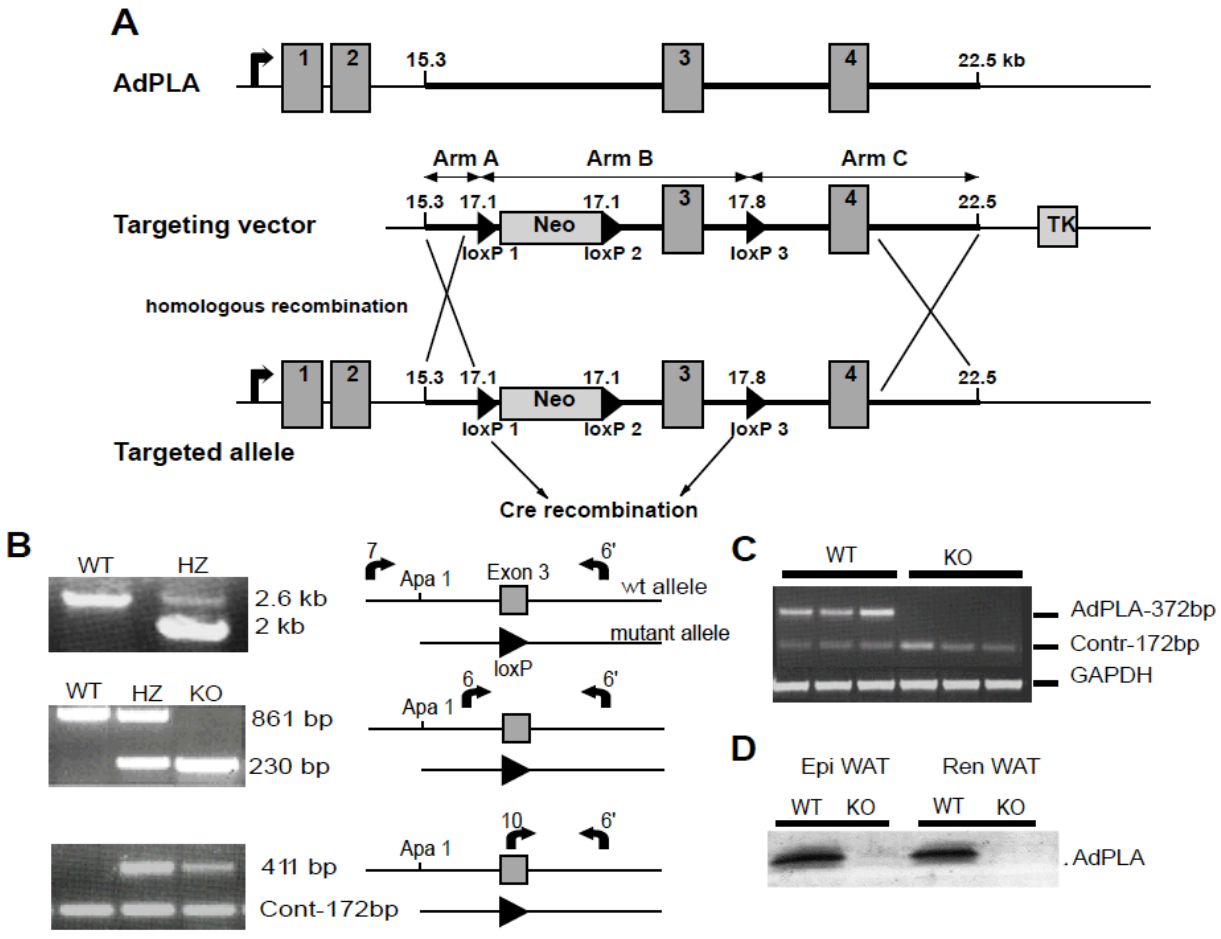

Figure IV-S1 Generation of AdPLA null mice (A) Generation of AdPLA null mice using a Cre-LoxP strategy. The AdPLA targeting vector was constructed using pEasy Flox (pEF) plasmid. A neo gene with flanking loxP sites was inserted into intron 2 and the thrid loxP site was inserted into intron 3. TK gen was inserted at the 3'end for negative selection. 1-4 designates exons. The final targeting vector was used for homologous recombination in ES cells. ES cells were cultured on gelatin-coated dishes with 1000 units/mL recombinant murine LIF (ESGRO, Chemicon).After linearization of the AdPLA-targeting vector with NotI, 50 µg DNA was electroporated into 8 x106 129/SVj E14 ES cells. G418- and ganclicovir-resistant colonies were picked and screened for homologous recombination events occurring between loxP1 and loxP3 by PCR using external forward primers upstream to the AdPLA fragment and reverse primers inside the neomycin gene. Positive colonies were identified, expanded and electroporated with pMC-Cre plasmid. G418 dying colonies were identified and screened for homologous recombination by PCR performed with aprimer pair flanking exon 3. (B) Genotyping of mice by PCR using primers spanning exon 3. WT, wild type; HZ, heterozygote; KO, knockout mice. Primer sequences in exon 32 of the mouse fatty acid synthase gene, producing a 172 bp fragment, were used as an internal control. (C) RTPCR analysis for AdPLA, using RNA form renal fat of KO and WT mice. (D) Westerblotting showing an absence of AdPLA in epididymal (epi) and renal (ren) WAT of KO mice.

A

	WT	KO	P value
Red blood cells (x10^6/mm^3)	9.46 ± 0.54	9.30 ± 0.30	0.81
platelets (x10^3/mm^3)	968 ± 60	905 ± 79	0.55
white blood cells (x10^6/mm^3)	10.5 ± 1.0	10.1 ± 1.5	0.84
neutrophil (%)	24.2 ± 2.1	26.6 ± 2.6	0.49
lymphocytes (%)	70.0 ± 2.6	66.6 ± 2.6	0.39
monocyte (%)	4.8 ± 0.6	5.8 ± 1.1	0.43
eosinophil (%)	1.0 ± 0.3	1.0 ± 0.3	1.00
basophil (%)	0	0	na

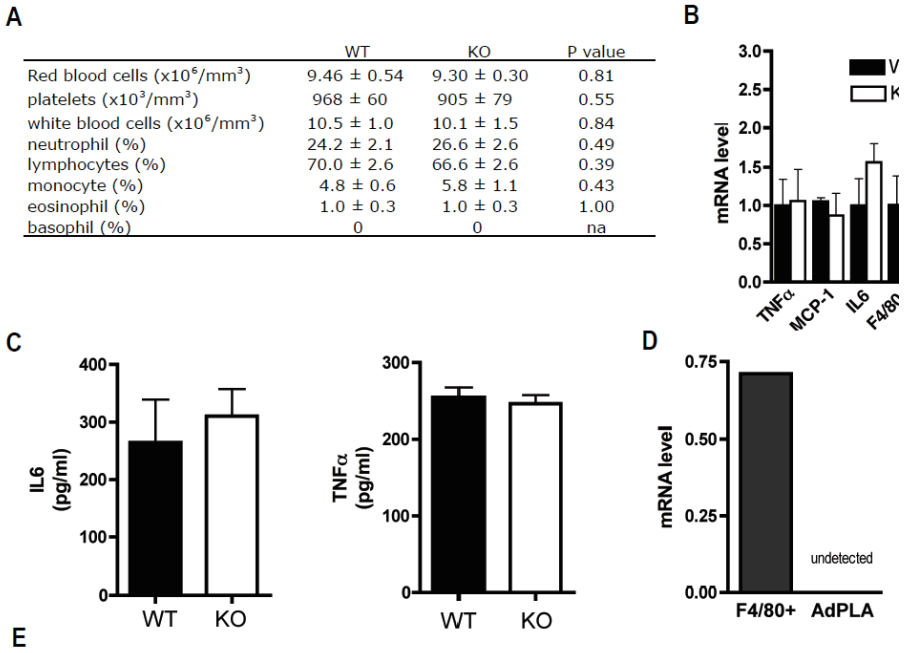

E

Blood measure	WT	KO	P value
Total bilirubin (mg/dl)	0.26 ± 0.04	0.22 ± 0.02	0.40
Aspartate Aminotransferase (U/l)[a]	223.2 ± 78.5	183 ± 56	0.69
Alanine Aminotransferase (U/l)[b]	45.2 ± 9.2	103.3 ± 17.86	0.02
Alkaline Phosphatase (U/l)	36 ± 1	50 ± 10	0.20
Albumin (g/dl)	3.84 ± 0.21	3.60 ± 0.11	0.34
Lactate dehydrogenase (U/l)	1181 ± 346	1515 ± 336	0.57
Urea Nitrogen (mg/dl)	25.4 ± 1.7	26.3 ± 1.5	0.70
Sodium (mmol/l)	150 ± 4	149.6 ± 0.5	0.92
Potassium (mmol/l)	8.60 ± 0.28	8.46 ± 0.26	0.72
Chloride (mmol/l)	83.6 ± 12.1	96.8 ± 7.9	0.39
Phosphorus (mg/dl)	8.90 ± 0.33	9.86 ± 0.67	0.24

[a]=Aspartate Aminotransferase (AST)= serum glutamic oxaloacetic transaminase (SGOT)
[b]=Alanine Aminotransferase (ALT)= serum glutamic pyruvic transaminase (SGPT)

Figure IV-S2 Inflammatory markers (A) Blood cell counts. (B) RT-qPCR analysis of levels of inflammatory cytokines and macrophage markers in adipose tissue from WT and AdPLA null (KO) mice. (C) Serum Il6 and TNF concentrations in WT and KO mice. (D) mRNA levels of F4/80+ and AdPLA in isolated peritoneal macrophages determined by RT-qPCR. (E) Hematological assessment of electrolytes, and markers of liver and renal function.

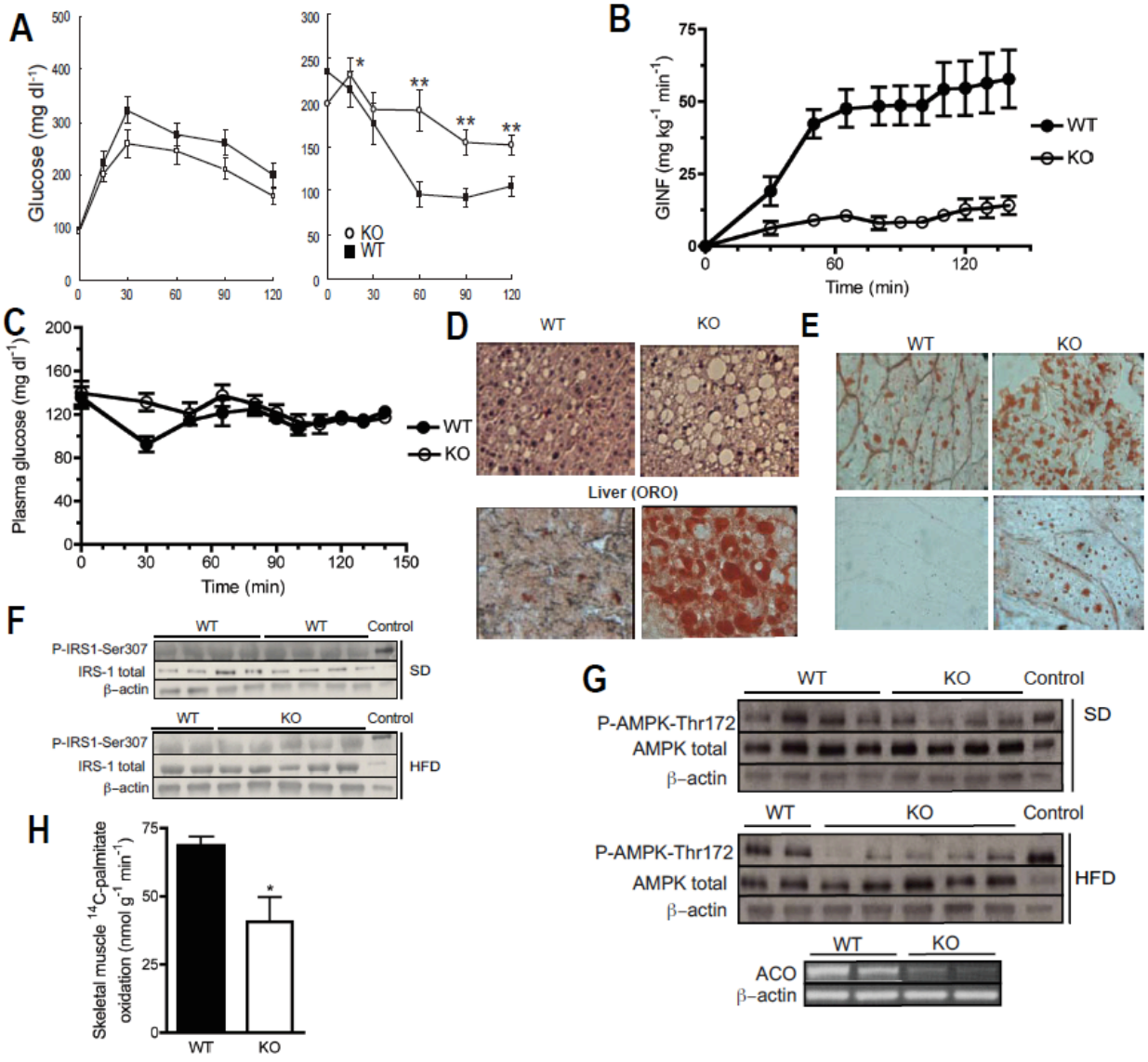

Figure IV-S3 Insulin sensitivity and skeletal muscle TAG accumulation (A) Glucose (GTT) and insulin (ITT) tolerance in 18 wk old male WT and KO mice feda SD (n=11) (B) glucose infusion rate (GINF) and (C) plasma glucose during the hyperinsulinemic euglycemic clamp study in 12 wk old maleWT and KO mice fed a HFD. (D) Top panel: Livers from16 wk old male mice fed a HFD were stained with hematoxylin and eosin (H&E). Bottom panel: cryostat sections of frozen livers from 16wk old male mice fed a HFD were stained with Oil red O. (E) Cryostat sections of frozen soleus muscles from 16 wk old male, HFD fed WT and KO mice stained with Oil red O. (F) Immunoblot analysis of total and phosphorylated IRS-1 in gastrocnemius muscle. (G)
Top panel: Immunoblot analysis of total AMPK or phosphorylated AMPK in gastrocnemius muscle from 18 wk old male WT and KO mice fed a HFD. Bottom panel: RT-PCR for acyl-CoA oxidase (ACO) using RNA from gastrocnemius skeletal muscle from 18-wk old male WT and KO mice fed a HFD. (H) Oxidation of [U-14C]-palmitate in homogenates of skeletal muscle from wild type or AdPLA null (n=4). Results are means ± SEM, *P<0.05. Results are means ± SEM, * P< 0.05, *** P<0.001.

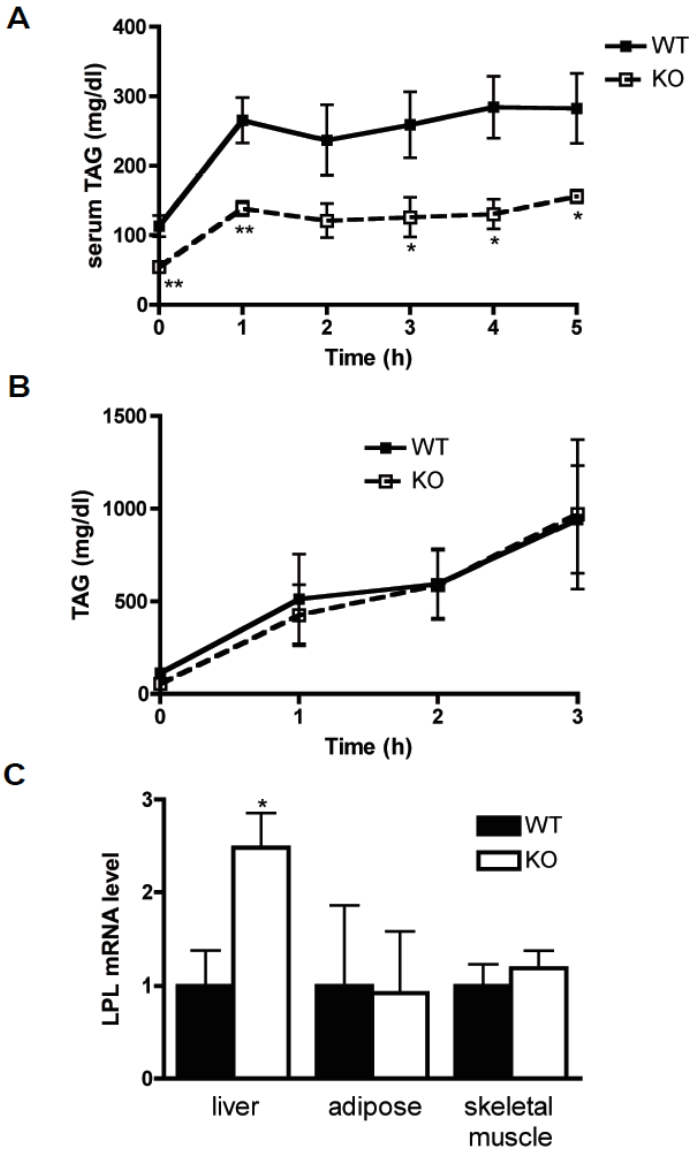

Figure IV-S4 (A) Serum TAG clearance. We followed serum TAG levels of overnight fasted mice for 5h following oral gavage with 400 l peanut oil (n=6), as described previously (Columbo et al., J. Biol. Chem. (278) 3992-3999, 2003). (B) Intestinal TAG absorbance and secretion. Serum TAG levels were measured in mice given a tail vein injection of WR1339 (to inhibit lipoprotein lipase) prior to gavage with 400 l peanut oil (n=6). (C) Lipoprotein lipase mRNA levels in the liver, adipose and skeletal muscle of WT and KO mice, normalized to GAPDH, as determined by RT-qPCR (n=3). Values are means ±SEM, **P*<0.05, ***P*<0.01.

Sequence Homology between murine and human AdPLA homologs.

Mm 1-
LAPIPEPKPGDLIEIFRPMYRHWAIYVGDGYVIHLAPPSEIAGAGAASIMSALTDKAIV
H 1-
RAPIPEPKPGDLIEIFRPFYRHWAIYVGDGYVVHLAPPSEVAGAGAASVMSALTDKAIV
Mm61-
KKELLCHVAGKDKYQVNNKHDEEYTPLPLSKIIQRAERLVGQEVLYRLTSENCEHFVNE
L
Hs61-
KKELLYDVAGSDKYQVNNKHDDKYSPLPCTKIIQRAEELVGQEVLYKLTSENCEHFVNE
L
Mm121-RYGVPRSDQVRDAVKAVGIAGVGLAALGLVGVMLSRNKKQKQ-162
Hs121-RYGVARSDQVRDVIIAASVAGMGLAAMSLIGVMFSRNKRQKQ-162

Figure IV-S5 Murine and human sequences share 83.3% homology.

	WT	KO
Body weight (g)	58.77 ± 3.41	38.33 ± 1.02***
Carcass weight (g)	47.73 ± 2.63	28.90 ± 0.31***
Water (%)	43.81 ± 2.25	69.28 ± 2.18***
Lipid (%)	40.41 ± 2.30	7.35 ± 1.77***
Lean Tissue (%)	15.78 ± 3.97	23.37 ± 0.64***
Liver weight (g)	1.50 ± 0.23	3.87 ± 0.35**
Liver TAG content (mg/g)	16.80 ± 1.04	55.00 ± 4.77***

Figure IV-S6 Body composition Body composition data for male WT and KO mice age 36 wks fed a HFD (n=6).